NASA TECHNICAL NOTE

NASA TN D-3437

NASA TN D-3437

INVESTIGATION OF A SEMISPAN TILT-WING VTOL MODEL TO DETERMINE GROUND EFFECT ON FULL-SPAN FLAPS USED FOR YAW CONTROL IN HOVERING

by Kalman J. Grunwald

Langley Research Center
Langley Station, Hampton, Va.

NATIONAL AERONAUTICS AND SPACE ADMINISTRATION • WASHINGTON, D. C. • JUNE 1966

NASA TN D-3437

INVESTIGATION OF A SEMISPAN TILT-WING VTOL MODEL TO DETERMINE GROUND EFFECT ON FULL-SPAN FLAPS USED FOR YAW CONTROL IN HOVERING

By Kalman J. Grunwald

Langley Research Center
Langley Station, Hampton, Va.

NATIONAL AERONAUTICS AND SPACE ADMINISTRATION

For sale by the Clearinghouse for Federal Scientific and Technical Information
Springfield, Virginia 22151 – Price $3.00

INVESTIGATION OF A SEMISPAN TILT-WING VTOL MODEL TO DETERMINE GROUND EFFECT ON FULL-SPAN FLAPS USED FOR YAW CONTROL IN HOVERING

By Kalman J. Grunwald
Langley Research Center

SUMMARY

A hovering force-test investigation on a semispan tilt-wing VTOL model was conducted to determine the ground effect on plain, single-slotted, and double-slotted full-span flaps used differentially as ailerons for yaw control. Although yawing effectiveness losses were experienced with all flap configurations near the ground, the slotted-flap configurations were considerably more effective in ground effect than the plain-flap configuration.

INTRODUCTION

Most of the present-generation propeller-driven tilt-wing VTOL aircraft are designed to use full-span flaps for the purpose of reducing the maximum wing-tilt angle required during transition and for providing greater efficiency (less power required) in the STOL mode.

In the hovering mode with the wing effectively tilted 90^{o} to the ground and the propeller wash blowing over the flaps, the flaps could be used to provide needed yaw control if deflected differentially as ailerons. The hovering yaw control out of ground effect produced in this manner can generally be estimated from the propeller thrust and the amount of turning effectiveness expected from the flaps. However, as the ground is approached, yawing effectiveness decreases. This loss in effectiveness has been detected and measured in other wind-tunnel tests (refs. 1 and 2) and in flight work on the VZ-2 aircraft (ref. 3). However, no detailed investigation indicating the most desirable flap configuration has been made.

The purpose of the present static-force-test investigation is to study this loss in yawing effectiveness as the ground is approached with a semispan, powered tilt-wing flap model. In particular, this investigation covers the effects of flap-chord-to-propeller-diameter ratio and the flap configuration – specifically the possible advantages of slotted flaps over plain flaps.

SYMBOLS

A three-view drawing of the model indicating the positive sense of forces, moments, and angles as well as the center-of-moment location is presented in figure 1. Measurements for this investigation were made in the U.S. Customary System of Units. Equivalent values are indicated herein in the International System (SI) in the interest of promoting the use of this system in future NASA reports.

A_p propeller disk area, sq ft (m^2)

b' wing semispan, $b/2$, ft (m)

b wing full span, ft (m)

b_a' aileron semispan, $b_a/2$, ft (m)

b_a aileron full span, ft (m)

$\bar{c}$ wing mean aerodynamic chord, ft (m)

c_f flap chord, ft (m)

D propeller diameter, ft (m)

F_L lift force, lb (N)

F_X longitudinal force, lb (N)

h height of model above ground (measured from trailing edge of flap at $\delta_f = 0^o$), ft (m)

M_X root bending moment (roll plane, fig. 1), ft-lb (N-m)

M_Y pitching moment (fig. 1), ft-lb (N-m)

M_Z root bending moment (yaw plane, fig. 1), ft-lb (N-m)

$\frac{\partial M_Z/Tb}{\partial \delta f_o}$ ratio of slope of bending-moment curve to flap-deflection curves, taken through 0^o from $\pm 20^o$, $\frac{\text{ft-lb}}{\text{deg}}$ $\left(\frac{\text{N-m}}{\text{deg}}\right)$

$\Delta M_{Z_1} = \frac{\partial M_Z/Tb}{\partial \delta f_o}$

q_s local slipstream dynamic pressure, lb/sq ft (N/m2)

R radius, in. (m)

T' semispan thrust, T/2, lb (N)

T full-span thrust, lb (N)

x,y,z distance along principal axes, ft (m)

$x/\bar{c}, y_l/\bar{c}, y_u/\bar{c}$ wing and flap ordinates in percent M.A.C.

$\Delta \delta_f$ incremental flap deflection, deg

δ_f flap deflection, deg

δ_{f_o} flap deflection at 0^o taken from $\pm 20^o$, deg

δ_v vane deflection, deg

θ turning angle, deg

Subscripts:

max maximum

u upper

l lower

MODEL AND EQUIPMENT

Photographs of the model are shown in figures 2 and 3. Figure 4 is a three-view drawing of the model with pertinent dimensions shown. The basic wing employed an NACA 4415 airfoil section (which was used previously in ref. 4). The wing consisted of a steel spar with a wood covering and had a detachable rear section into which various types of flaps could be mounted. The three plain-flap configurations are presented in

figure 5 (a 15-percent-chord flap, a 25-percent-chord flap, and a 37.5-percent-chord flap). The flaps were constructed to deflect through a range of angles from 70° to -70° in increments of 10°. The 40-percent-chord single-slotted-flap configuration is presented in figure 6. This configuration was tested with full-span flaps and with "cutouts" to simulate possible engine nacelle locations. The nacelle cutouts were 4 inches (10.2 cm) wide and were located directly behind the existing model nacelles. In both these configurations the flaps could be deflected 60° to -60° in increments of 10°. The two double-slotted-flap configurations are shown in figure 7. The smaller double-slotted flap employed a 14-percent-chord vane and a 22-percent-chord flap. The larger flap used the same 14-percent-chord vane and a 44-percent-chord flap. Each of these flap systems could be varied through a range of angles from 60° to -60° in increments of 10°.

In order to provide symmetry, the model was mounted on a reflection plane as shown in figures 1 and 2. The 2-foot-diameter (0.61-m) fiber-glass propellers were located in the same position with respect to the model throughout the tests. A 7- by 12-foot (2.14-m × 3.66-m) wood groundboard, as shown in figure 2, was placed behind the model to simulate the ground. The board could be moved to any desired height or removed to simulate the out-of-ground-effect condition. The distance from the model to the wall was 16 feet (4.88 m) ($h/D = 8$). The test room was large enough to allow the air to be considered free air; therefore, $h/D = \infty$ was used for the test condition.

Flow surveys were made by the use of a tuft grid located on the center line of the outboard propeller (fig. 2). A camera mounted on the ceiling of the room photographed the tuft grid. The tuft grid consisted of 2-inch (5.08-cm) long tufts 3 inches (7.62 cm) apart. The grid was 8 feet (2.4 m) wide and each wire spacing in the aft direction was 3 inches (7.62 cm). Wires were removed as the groundboard was moved closer to the wing.

Slipstream dynamic-pressure measurements were made at several spanwise stations at locations above and below the wing surface by the use of the pressure rake as pictured in figure 8. Force measurements taken from the wing were determined from a floor-mounted strain-gage balance. The propeller loads were measured from strain gages mounted in the engine nacelles. All the force data were recorded on strip-chart recorders.

TESTS

The test procedure used was to vary the flap deflection through its complete range of deflections with the groundboard at a fixed position. When a complete range of flap deflections was tested, the groundboard was moved to another position.

The three plain-flap configurations were tested at ratios of groundboard height to propeller diameter h/D of ∞, 3.00, 2.50, 2.00, 1.50, 1.00, 0.75, 0.50, 0.38, and 0.25. The propellers operated at a near-constant rotatational speed of 6000 rpm. The propeller rotation for the three plain-flap configurations was to the left as viewed from behind the model.

The single- and double-slotted-flap configurations were tested at ratios of groundboard height to propeller diameter of ∞, 1.75, 1.25, 1.00, 0.75, 0.50, 0.375, and 0.25. Rotational speed was set constant at 6000 rpm. However, the propeller rotation was opposite of that tested for the plain flaps; that is – rotation was to the right as viewed from behind the model. The propeller available at the time of the tests dictated the mode of rotation. Previous work has indicated that the direction of rotation appears to have only negligible effects on slipstream turning in the hovering mode.

During the tests the tuft grid described in the preceding section was photographed at each height and flap deflection in order to record the airflow at each condition as the model was moved toward the ground. Tests were also conducted with the total-pressure rake at different span locations of the plain wing in the undeflected condition. These tests were also made at a number of ground heights.

PRESENTATION OF RESULTS

Each figure presenting the basic force data is plotted in parts (a) and (b), in a manner similar to that used in past investigations. Parts (a) present the ratio of lift force to thrust, the turning effectiveness, the turning angle, and the ratio of pitching moment to thrust times propeller diameter. Parts (b) present the moments about the roll and yaw axis. All basic data are presented as a function of flap deflection with the exception of turning effectiveness.

The following table is presented for the convenience of the reader:

DISCUSSION

Ground Effect on Basic Data

The basic force and moment data for each configuration are presented in two parts. The first part represents conditions of ground height ranging from out of ground effect $h/D = \infty$ to 1 propeller diameter above the ground $h/D = 1.0$. (See figs. 9, 11, 13, 15, 17, 19, and 21.) In this height range only small changes in any of the forces and moments occur with change in ground height when compared with out-of-ground-effect conditions. However, observations of the data in the second part of the figures for each configuration at the lower ground heights $h/D = 0.75$ to 0.25 (figs. 10, 12, 14, 16, 18, and 20) show increasingly larger changes in the aerodynamic forces and moments when compared with the out-of-ground-effect condition.

Control Effectiveness Out of Ground Effect

Slipstream-deflection characteristics.- Differential deflection of the ailerons on a tilt-wing configuration in hovering produces a yawing moment by the action of the ailerons in deflecting the slipstream, forward on one wing and rearward on the other. The slipstream-deflection characteristics of the flap systems (used as ailerons) used in the present investigation are compared with the results of previous investigations (as summarized in ref. 5) in figure 23.

Effect of aileron chord and type.- The effects of aileron chord and a comparison of plain and slotted ailerons are presented in figures 24 and 25, respectively. Increasing the chord of plain ailerons increases their effectiveness in producing yawing moments as would be expected (fig. 24). The use of slotted flaps as ailerons (fig. 25) greatly increases the yawing moment that can be attained at the larger positive deflections (20° to 60° and above). Moreover, the lift loss, at moment values that can be achieved by both plain and slotted ailerons, is significantly lower for the slotted configurations. These improvements in control effectiveness and reduction in lift loss at positive deflections are due to the flow through the slots delaying flow separation on the aileron. At negative deflection,

however, the slotted ailerons are less effective than the plain ailerons because of the poor undersurface contour at negative deflections (trailing edge up). As a result, the total control moment that would be produced on a complete configuration is only slightly greater than that for plain ailerons (fig. 26).

Available flap sections were used for the slotted ailerons in this investigation. It is possible that some improvement in effectiveness at negative deflection could be achieved by altering the lower surface contour of the slotted configuration to approximate at least the contour of the plain flaps at negative deflections.

It should be noted that, with the ailerons set at the nominal zero deflection, a yawing moment was sometimes measured and is shown in the basic data. This moment arises from the deflection of the slipstream due to the wing-flap camber. On a full-span configuration, this moment would be canceled by a similar deflection of the slipstream on the opposite wing. In order to compensate for this effect and to provide a more direct comparison of configurations, the data have been plotted, in figures 24 to 28, against the flap deflection measured for zero moment out of ground effect.

Effects of Ground Proximity

The yaw control effectiveness of the configurations which were compared out of ground effect in figures 24 and 25 are compared in ground effect (h/D = 0.25) in figures 27 and 28. At this very low height, a control reversal is experienced with the plain ailerons at small positive deflections (fig. 27). The flow through the slots on the slotted ailerons alleviates the flow separation which causes this control reversal on the plain ailerons and greatly improves the moment available at positive deflections. The comparison of control effectiveness for the plain, single-slotted, and double-slotted flaps in and out of ground presented in figure 29 shows that the losses due to ground effect are considerably smaller with the slotted configurations.

The variations of control effectiveness with height above the ground for the various aileron configurations are shown in figure 30 in terms of the control moment per degree of aileron deflection taken near zero deflection. In general, significant losses in ground effect occur at heights of the trailing edge of the wing above the ground less than 1 propeller diameter; at very low heights the basic curves for the variation of moment with deflection are nonlinear near zero deflection as shown in the basic data and in figure 27. There are, therefore, two slopes near zero deflection as shown by the dashed curves and as illustrated by the inserted sketches in figure 30.

The ratios of the control effectiveness in ground effect to the effectiveness out of ground effect are presented in figures 31 and 32. The values out of ground effect were taken as the level of effectiveness at a height of 1.5 to 2.0 propeller diameters where the curves of figure 30 have reached a constant value. This value does not always agree with

the value at $h/D = \infty$ (groundboard removed) and the reason for this disagreement is not understood but may be associated with the change in recirculation of flow within the room in which the tests were conducted. As shown in figure 31, the effect of the ground on the percentage reduction in control effectiveness is independent of the aileron chord for the plain aileron. The effectiveness of slots in reducing the losses in effectiveness due to ground effect is again shown in figure 32.

Effects of Aileron Cutouts

For some configurations it may be desirable, from the point of view of structural or heating considerations, to leave a part of the aileron immediately behind the engine exhaust undeflected. The single-slotted aileron configuration was tested with and without such cutouts to investigate their effect on control effectiveness. These cutouts reduce the slipstream-deflection capability of the wing as shown in figure 23 and, as a result, the control effectiveness is reduced both in and out of ground effect (figs. 31 and 33).

Comparison of Present Results With Previous Investigations

Some control moments and control effectiveness data in hovering from other investigations of two- and four-propeller tilt-wing models and a two-propeller full-scale aircraft are also available for comparison (refs. 1, 2, and 3, and unpublished data). These model configurations employed conventional unslotted partial-span ailerons for yaw control in hovering. The VZ-2 aircraft (ref. 3) employed essentially full-span ailerons.

A summary of the control effectiveness $\left(\frac{\partial M_Z/Tb}{\partial \delta f_o}\right)$ out of ground effect as a function of the ratio of flap chord to propeller diameter (c_f/D) is made in figure 34 from references 1 and 3, unpublished data, and the data from the present investigation. The ratio of aileron semispan to wing semispan (b_a'/b') is based on full span with no allowance for a fuselage. All the reference investigations had fuselages that used about 10 percent of the span; for example, the VZ-2 (ref. 3) used full-span ailerons and the fuselage accounted for the other 12 percent of span.

Another summary comparison showing the ratio of the control effectiveness throughout the ground-height range to the maximum effectiveness is presented in figure 35 for references 1 and 2, unpublished data (all unslotted aileron configurations), and the plain flap data from figure 31. As can be seen, the reference data follow the same general pattern as the plain-flap data of the present investigation. The pattern indicates only small losses in control effectiveness at values of h/D above 1 and rapidly increasing losses as h/D decreases.

Factors Affecting Aileron Effectiveness in Ground Effect

In an effort to gain a better understanding of the reasons for the loss in aileron effectiveness near the ground, flow surveys were made with a tuft grid in the plane of the outboard propeller center line (fig. 2) and by a rake of total pressure tubes (fig. 8).

Photographs of the tuft grids are presented in figures 36 and 37 and the results of pressure surveys are presented in figures 38, 39, and 40.

Tuft survey.- A schematic representation of the flow as derived from the photographs of the tuft grid is presented in figure 41 for the purpose of discussing the flow changes as the ground is approached. The same effect can be seen in the tuft surveys (figs. 36 and 37).

In the out-of-the-ground-effect conditions (fig. 41(a)), the slipstream is turned in the desired direction by the flap. If the model is brought all the way into contact with the ground (fig. 41(c)), the presence of the ground splits the slipstream. The part going "under" the wing is directed in the same direction that the flap would normally try to deflect it, but that part going "over" the wing is directed in the opposite direction. In this condition, the flap has little opportunity to influence the deflection of the slipstream and loses its effectiveness.

At the intermediate heights (figs. 41(b)) an intermediate condition exists and the ability of the flap to deflect the air coming over the wing as it would out of ground effect is dependent upon its ability to maintain attached flow on the flaps in the presence of the adverse pressure gradient created by the proximity of the ground. Apparently, it is the flow through the slots of the slotted configurations that delays separation on these flaps and thus minimizes their loss in effectiveness when compared with the unslotted-flap configuration in ground effect.

Pressure survey.- The pressure surveys were made through a range of ground heights for the plain wing configuration $\left(\delta_f = 0^o\right)$ at a number of spanwise stations to investigate the effect of the ground on the slipstream total-pressure distribution. The plane of the pressure probes was located at the 73-percent-chord station and was arranged as shown in figure 8.

The slipstream dynamic-pressure variation at each span station resulting from a change in ground position can be seen in figure 38. Data comparing only the out-of-ground-effect condition ($h/D = \infty$) and the condition nearest to the ground ($h/D = 0.25$) are presented in figures 39 and 40 (isometric projection). Large changes in the flow pattern at spanwise location $\frac{y}{b/2} = 0.236$ to 0.672 can be noted in figure 38. The cause of these large changes at only these two stations is not understood; however, it is interesting to note that both of these stations are located equal distances inboard of the inboard and

outboard propeller center lines and also that the propeller rotation is downward at these stations.

CONCLUDING REMARKS

In general, for all configurations, ground effects were not encountered at a height of the wing trailing edge of more than 1 propeller diameter above the ground. Below a height of 1 propeller diameter, control effectiveness decreased as the ground was approached.

The single- and double-slotted-flap configurations were considerably more effective in ground effect than the plain flap. This result is due to the flow through slots alleviating the ground-induced separation.

Langley Research Center,
National Aeronautics and Space Administration,
Langley Station, Hampton, Va., February 18, 1966.

REFERENCES

1. Tosti, Louis P.: Force-Test Investigation of the Stability and Control Characteristics of a 1/8-Scale Model of a Tilt-Wing Vertical-Take-Off-and-Landing Airplane. NASA TN D-44, 1960.

2. Newsom, William A., Jr.; and Kirby, Robert H.: Flight Investigation of Stability and Control Characteristics of a 1/9-Scale Model of a Four-Propeller Tilt-Wing V/STOL Transport. NASA TN D-2443, 1964.

3. Pegg, Robert J.; Kelley, Henry L.; and Reeder, John P.: Flight Investigation of the VZ-2 Tilt-Wing Aircraft With Full-Span Flap. NASA TN D-2680, 1965.

4. Hayes, William C., Jr.; Kuhn, Richard E.; and Sherman, Irving R.: Effects of Propeller Position and Overlap on the Slipstream Deflection Characteristics of a Wing-Propeller Configuration Equipped With a Sliding and Fowler Flap. NACA TN 4404, 1958.

5. Kuhn, Richard E.: Semiempirical Procedure for Estimating Lift and Drag Characteristics of Propeller-Wing-Flap Configurations for Vertical- and Short-Take-Off-and-Landing Airplanes. NASA MEMO 1-16-59L, 1959.

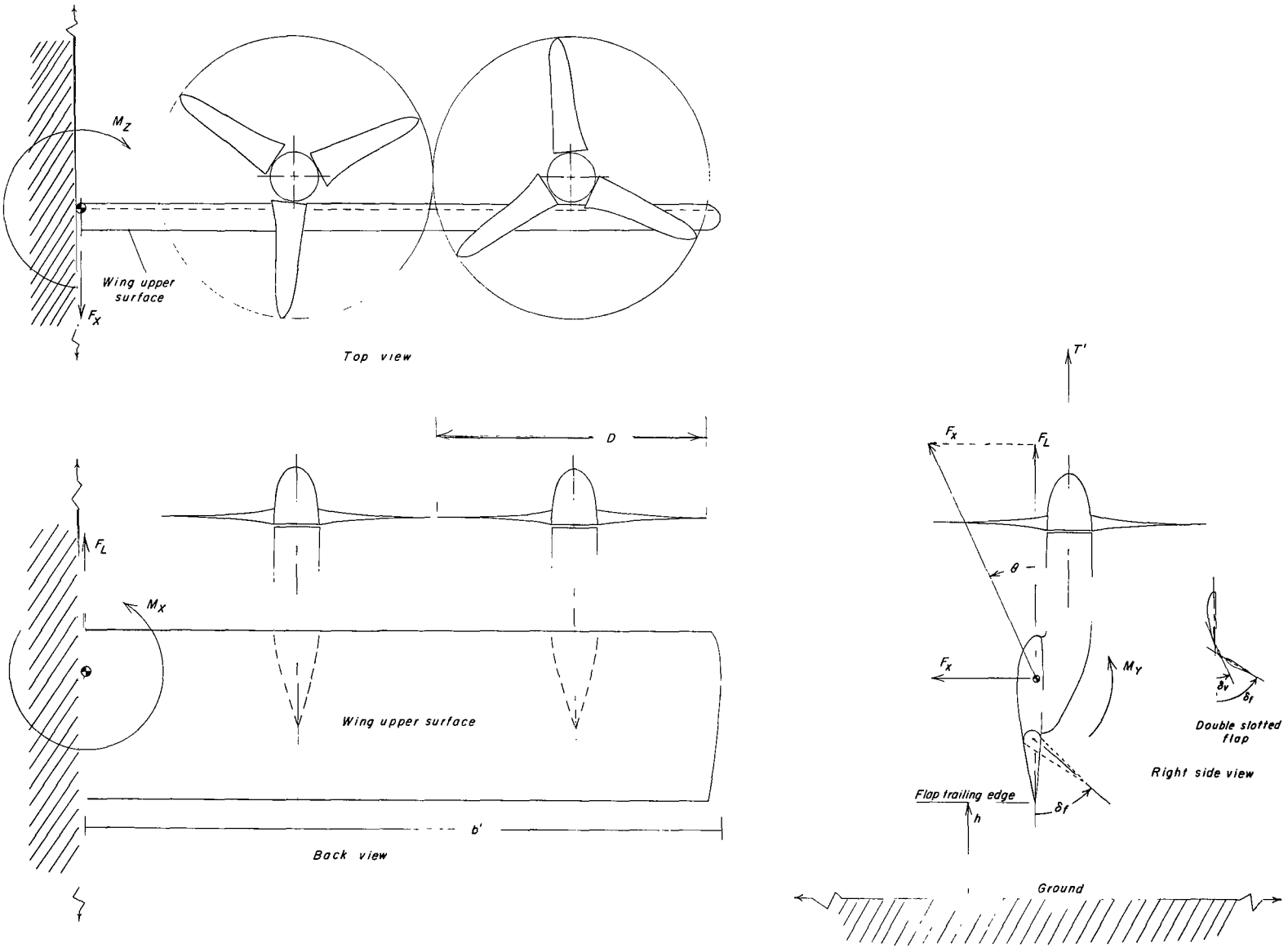

Figure 1.- Three-view drawing of model.

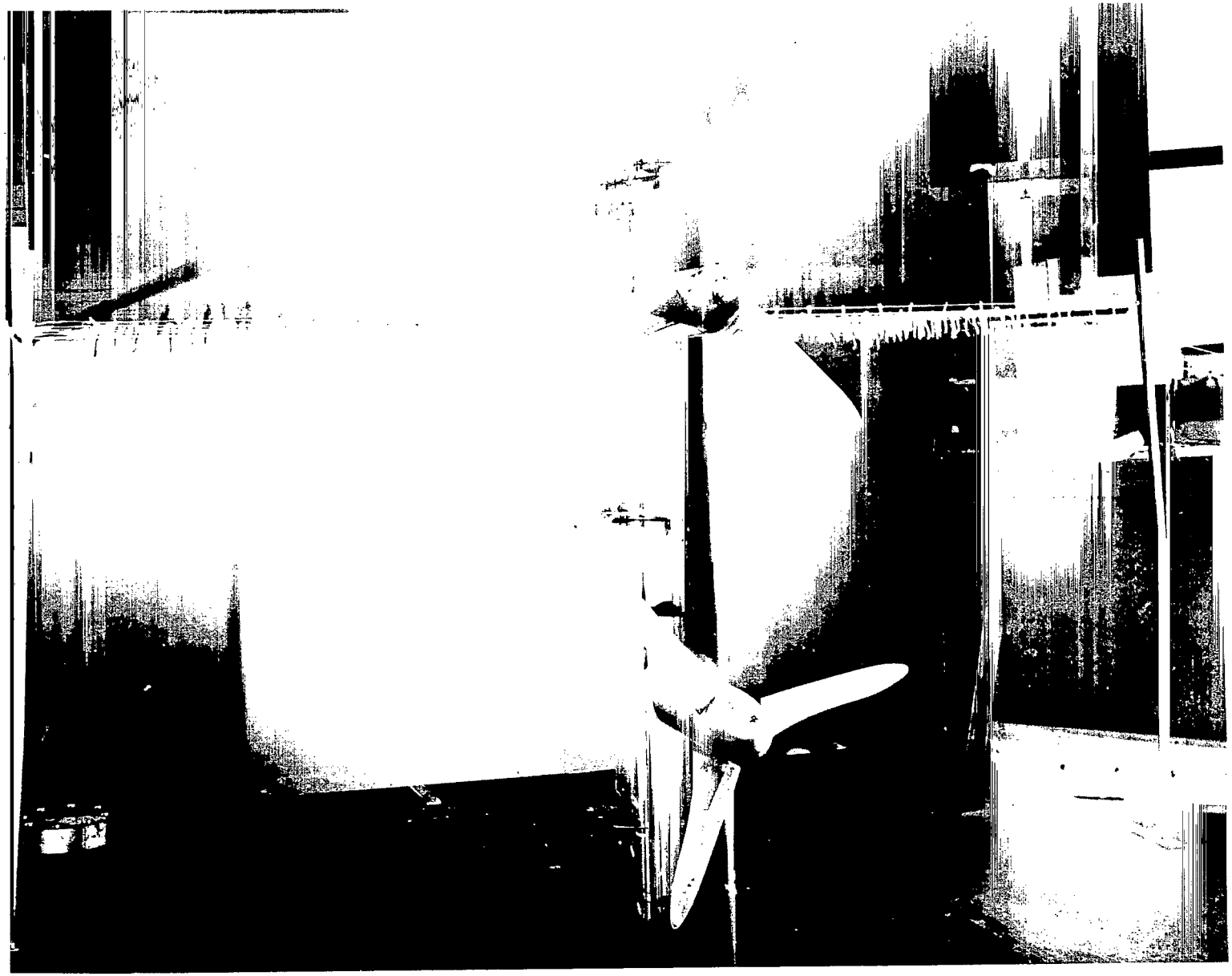

Figure 2.- Front view of model in static test facility. (VTOL model pictured in hovering mode; groundboard in background.) L-62-8354

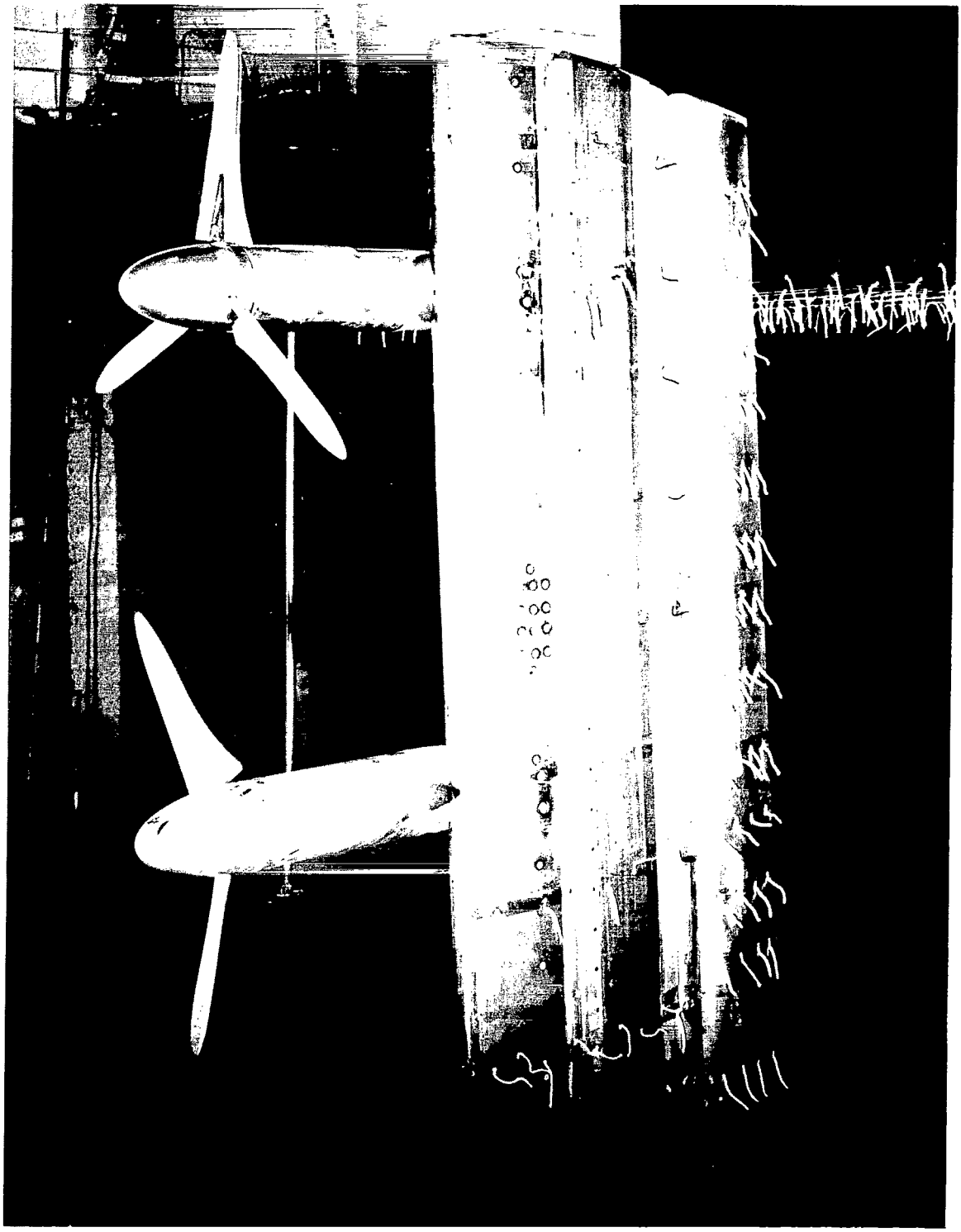

Figure 3.- Three-quarter view of model in static test facility. L-62-8352

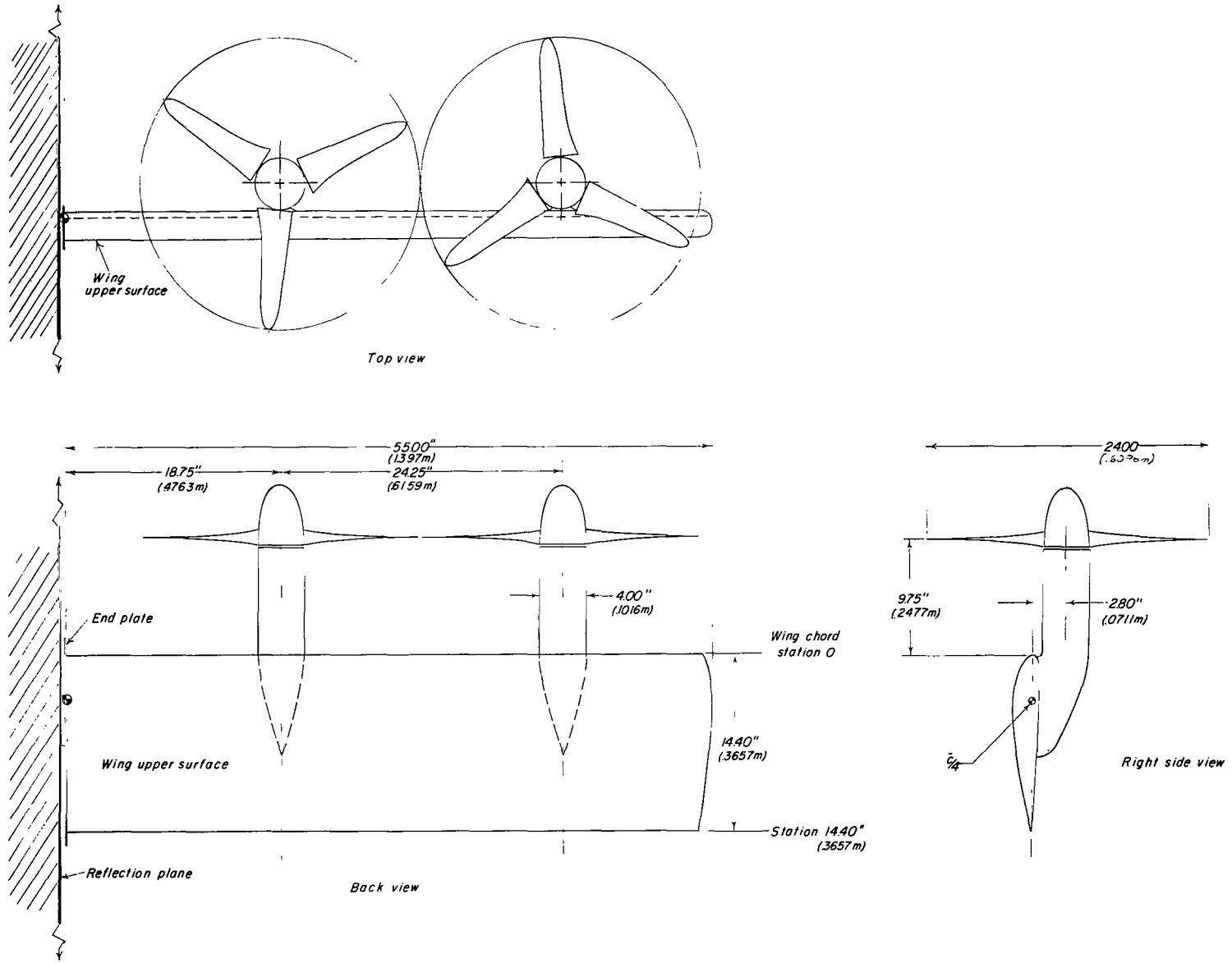

Figure 4.- Three-view drawing of basic model showing pertinent dimensions. Dimensions are presented first in inches and parenthetically in meters.

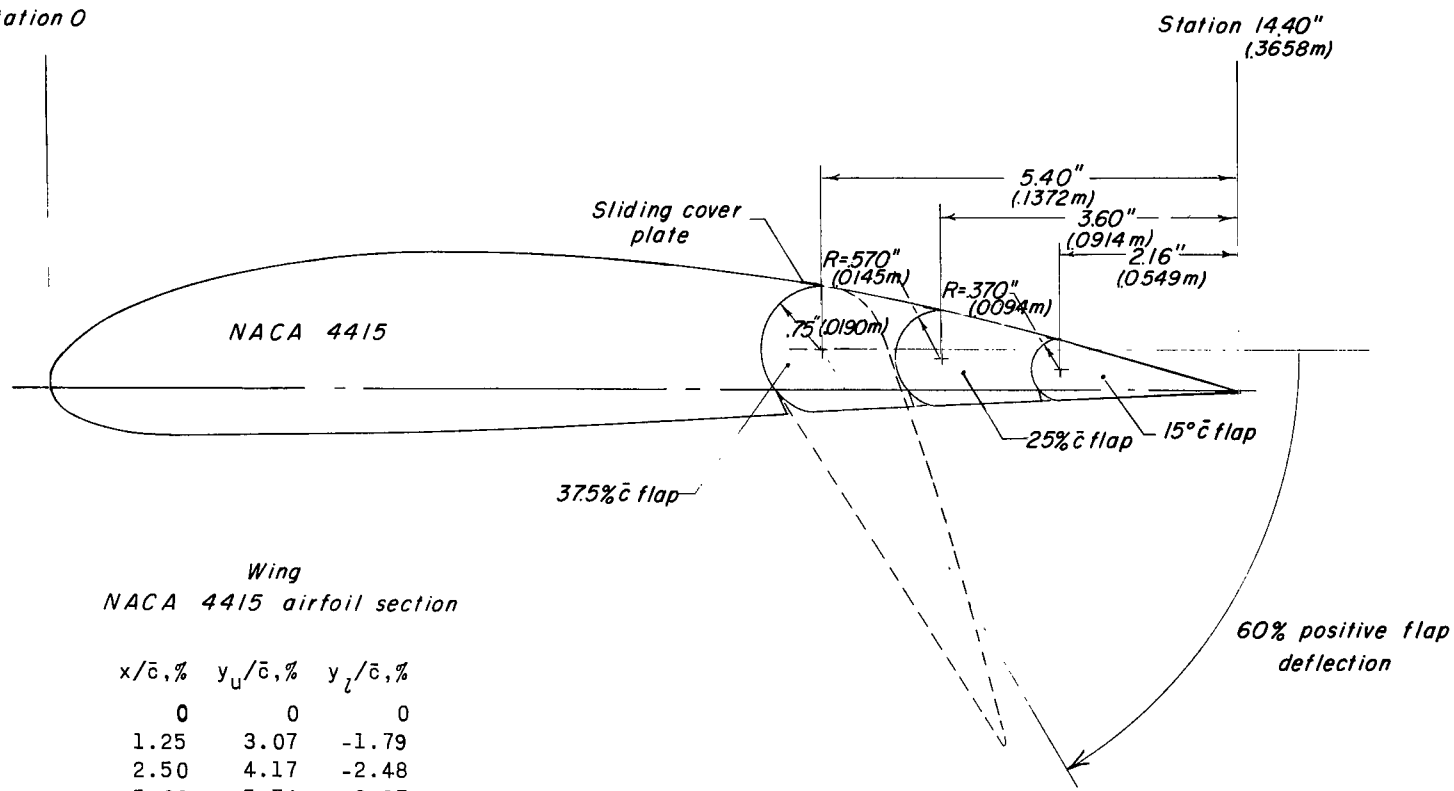

Wing
NACA 4415 airfoil section

$x/\bar{c}$,%	$y_u/\bar{c}$,%	$y_l/\bar{c}$,%
0	0	0
1.25	3.07	-1.79
2.50	4.17	-2.48
5.00	5.74	-3.27
7.50	6.91	-3.71
10.00	7.84	-3.98
15.00	9.27	-4.18
20.00	10.25	-4.15
25.00	10.92	-3.98
30.00	11.25	-3.75
40.00	11.25	-3.25
50.00	10.53	-2.72
60.00	9.30	-2.14
70.00	7.63	-1.55
80.00	5.55	-1.03
90.00	3.08	- .56
95.00	1.67	- .36
100.00	.16	- .16

Figure 5.- Wing ordinates and drawing of wing section of three plain-flap configurations. Dimensions are given first in inches and parenthetically in meters.

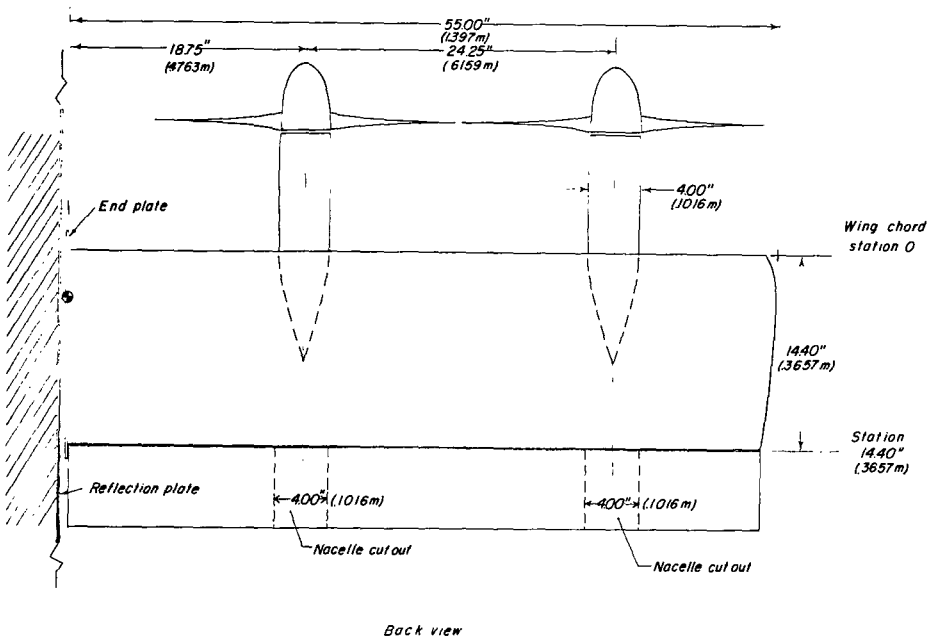

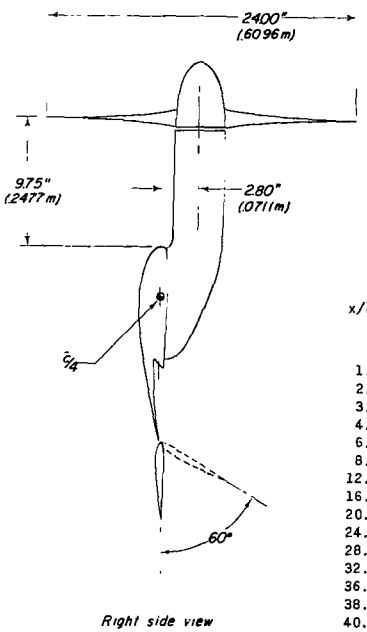

Single slotted flap
40% chord

x/c̄,%	$y_u/\bar{c}$,%	$y_l/\bar{c}$,%
0	1.40	1.40
.50	2.18	.77
1.00	2.60	.59
2.00	3.16	.37
3.00	3.54	.25
4.00	3.84	.16
6.00	4.27	.06
8.00	4.54	.01
12.00	4.68	0
16.00	4.56	0
20.00	4.21	0
24.00	3.66	0
28.00	2.94	0
32.00	2.09	0
36.00	1.12	0
38.00	.60	0
40.00	.05	0

Figure 6.- Flap ordinates and drawing of single-slotted-flap configurations indicating nacelle cutouts. Dimensions are given first in inches and parenthetically in meters.

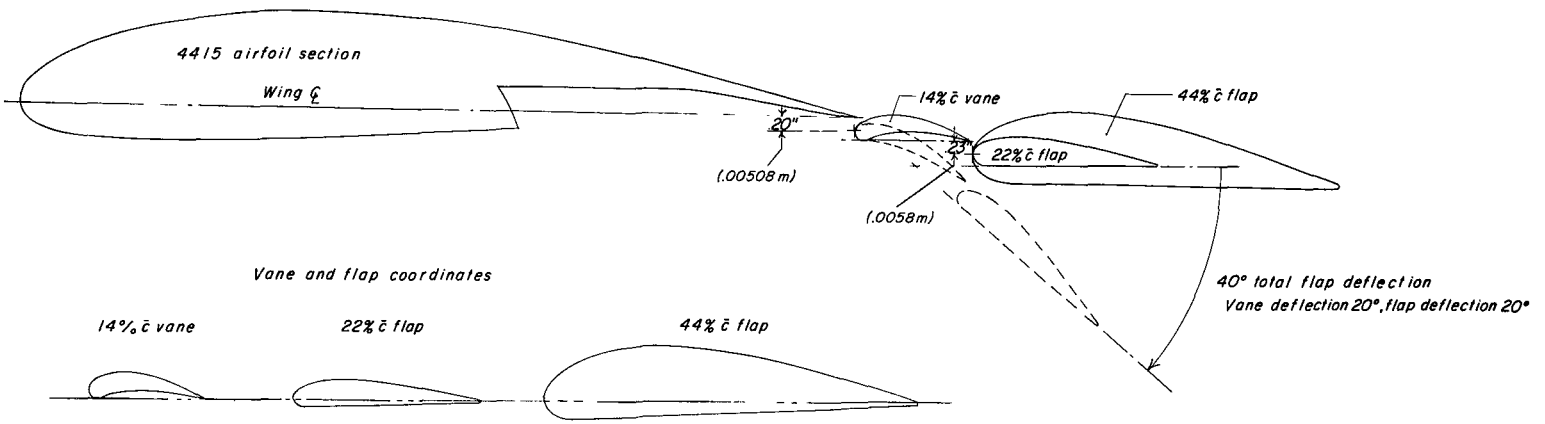

Vane and flap coordinates

14% c̄ vane

x/c̄, %	$Y_u/\bar{c}$, %	$Y_l/\bar{c}$, %
0	0.97	0.97
0.35	1.81	.42
.69	2.08	.14
1.04	2.22	0
1.39	2.36	0
2.08	2.64	.42
2.78	2.64	.56
4.17	2.78	.83
5.56	2.64	1.11
6.94	2.50	1.18
8.33	2.22	.97
9.72	1.81	.83
11.11	1.39	.56
12.50	.83	.21
13.89	0	0

22% c̄ flap

x/c̄, %	$Y_u/\bar{c}$, %	$Y_l/\bar{c}$, %
0	0	0
0.56	0.78	-0.83
1.11	1.22	-1.00
1.67	1.54	-1.06
2.22	1.76	-1.06
4.44	2.22	- .96
6.67	2.24	- .84
8.89	2.17	- .72
11.11	2.00	- .53
13.33	1.78	- .53
15.56	1.47	- .44
17.78	1.04	- .37
20.00	.56	- .28
22.22	0	- .18

44% c̄ flap

x/c̄, %	$Y_u/\bar{c}$, %	$Y_l/\bar{c}$, %
0	0	0
0.56	1.78	-1.22
1.11	2.49	-1.56
1.67	3.11	-1.82
2.22	3.56	-1.94
3.33	4.33	-2.08
5.56	5.40	-2.04
11.11	6.56	-1.72
13.89	6.67	-1.57
16.67	6.51	-1.41
20.00	6.26	-1.24
22.22	6.00	-1.14
24.44	5.60	-1.06
27.78	4.83	- .90
33.33	3.42	- .63
38.89	1.85	- .40
44.44	.18	- .18

Figure 7.- Ordinates for vane and flaps and drawing of two double-slotted-flap configurations. Dimensions are given first in inches and parenthetically in meters.

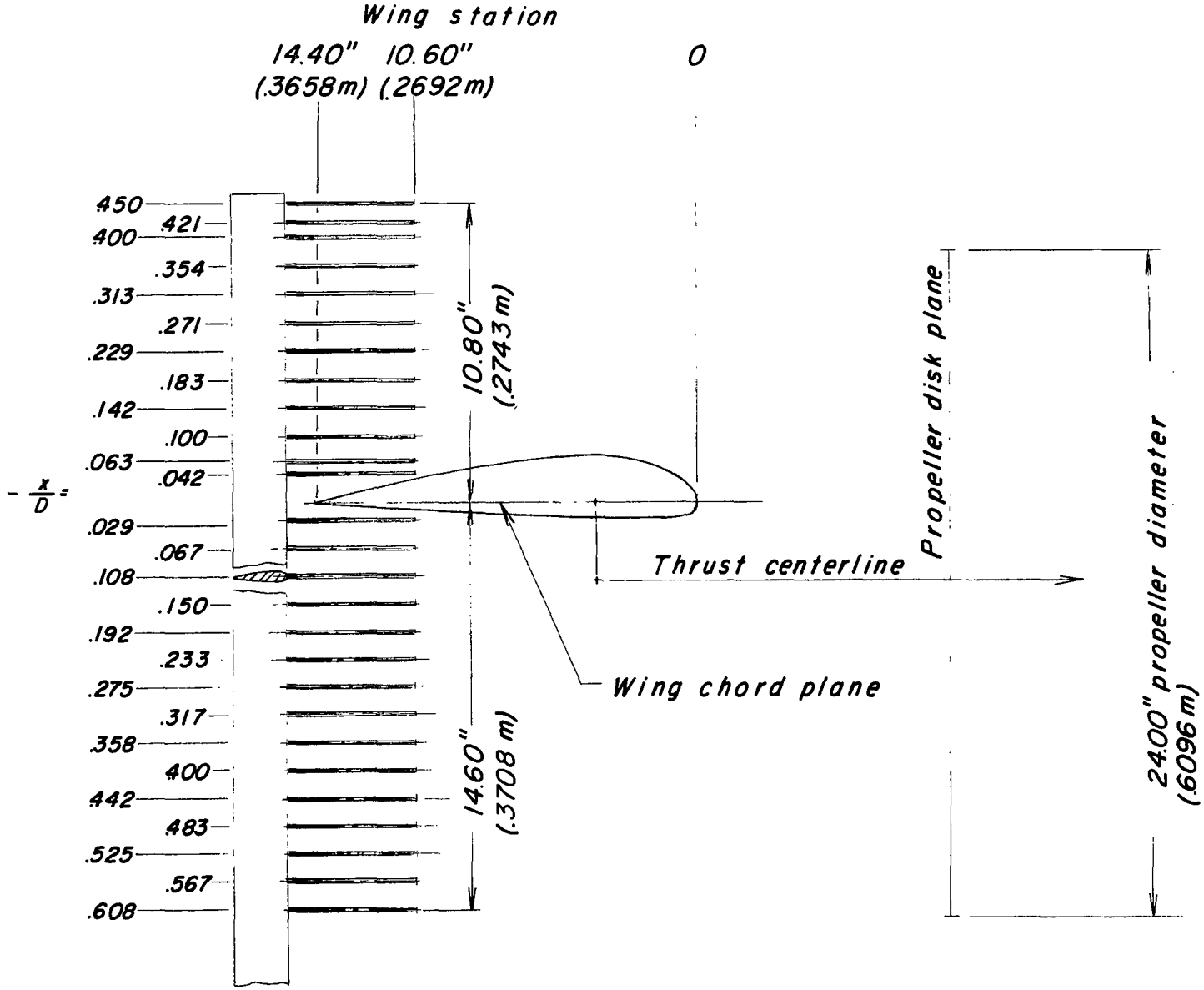

Figure 8.- Drawing of pressure-probe locations used for slipstream pressure evaluation.

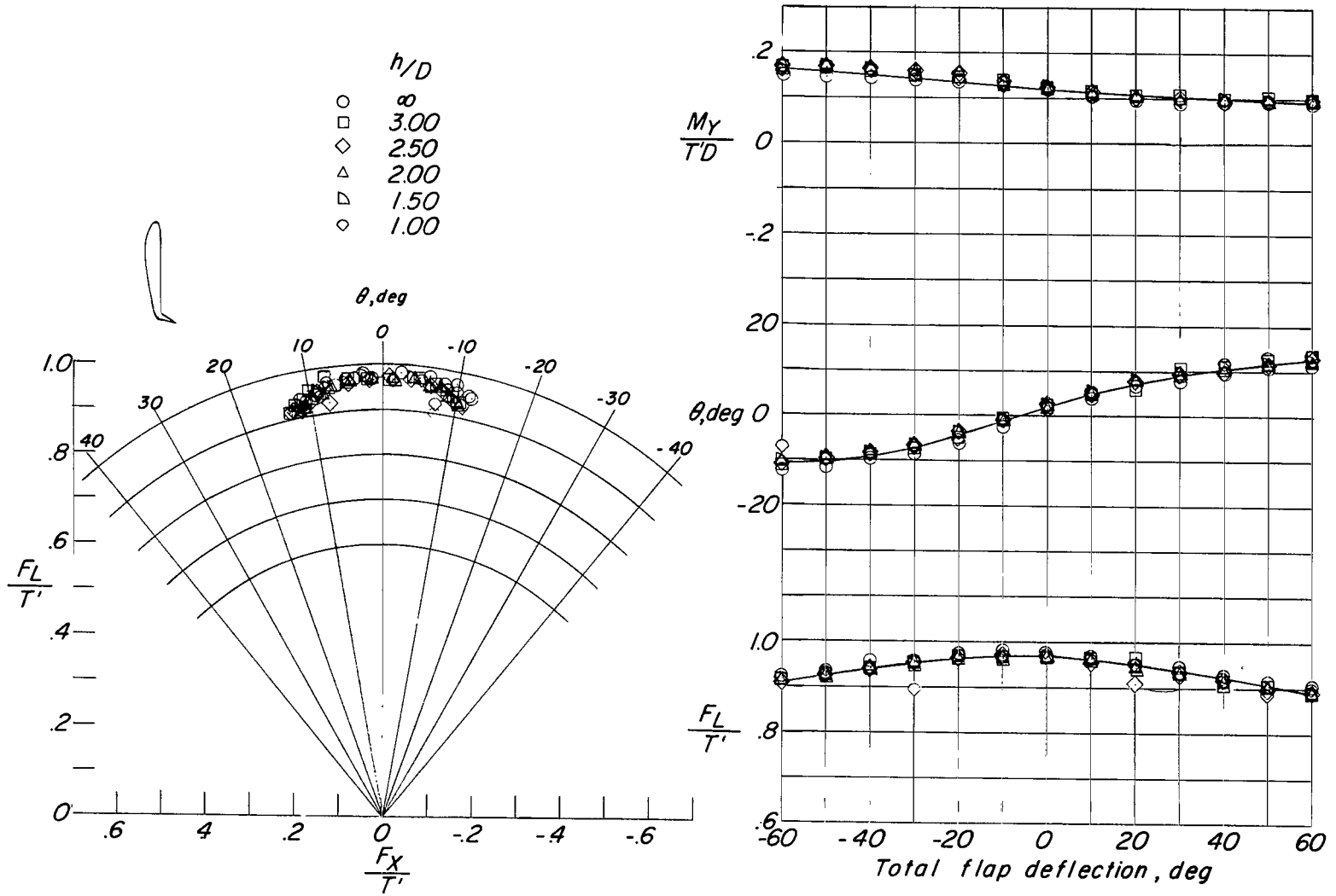

(a) Turning effectiveness, pitching moment, and lift-thrust ratio.

Figure 9.- Ground effect on hovering-flight characteristics for tilt-wing 15-percent-chord plain-flap configuration. h/D = ∞ to 1.00.

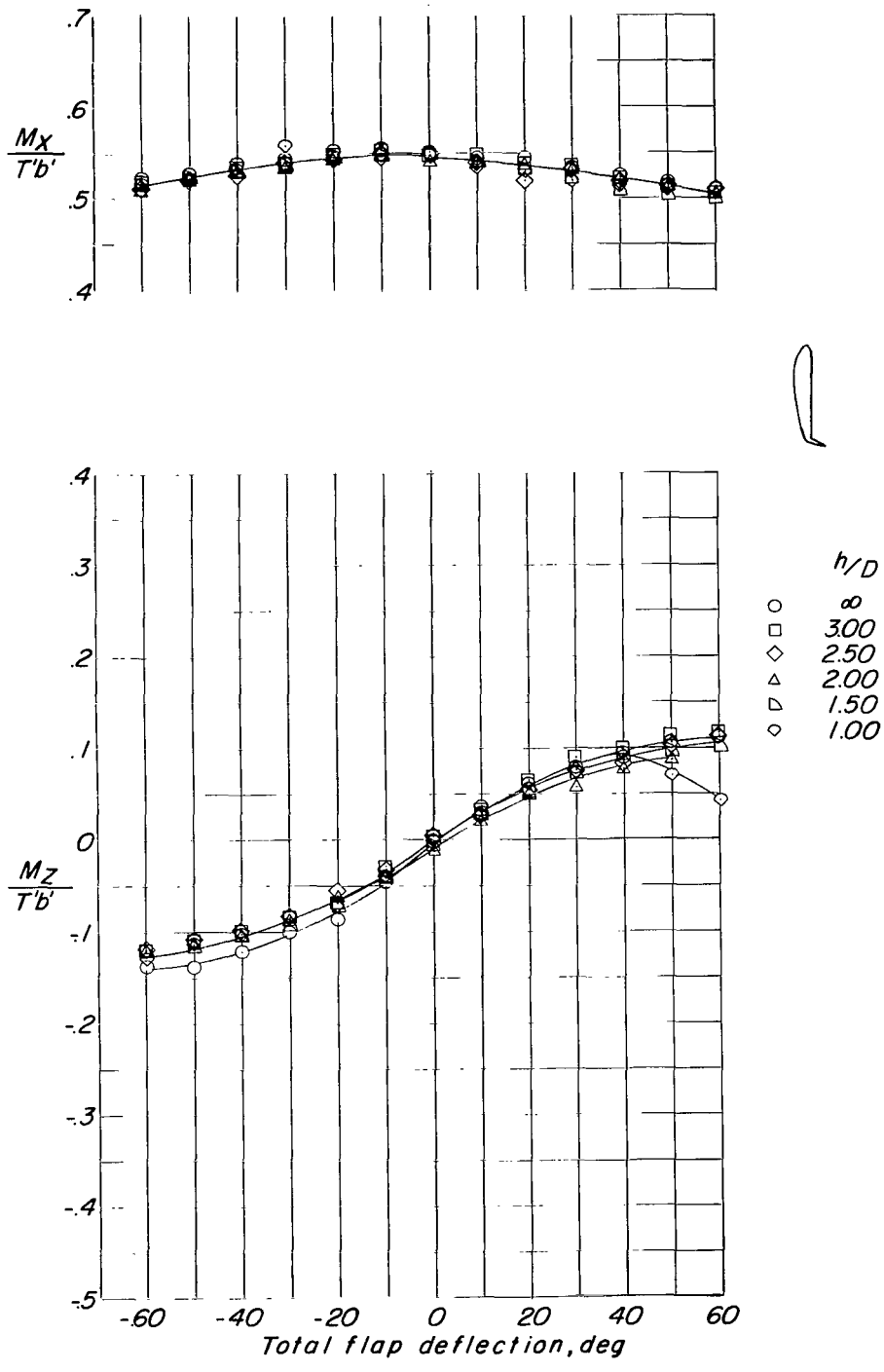

(b) Root bending moments.

Figure 9.- Concluded.

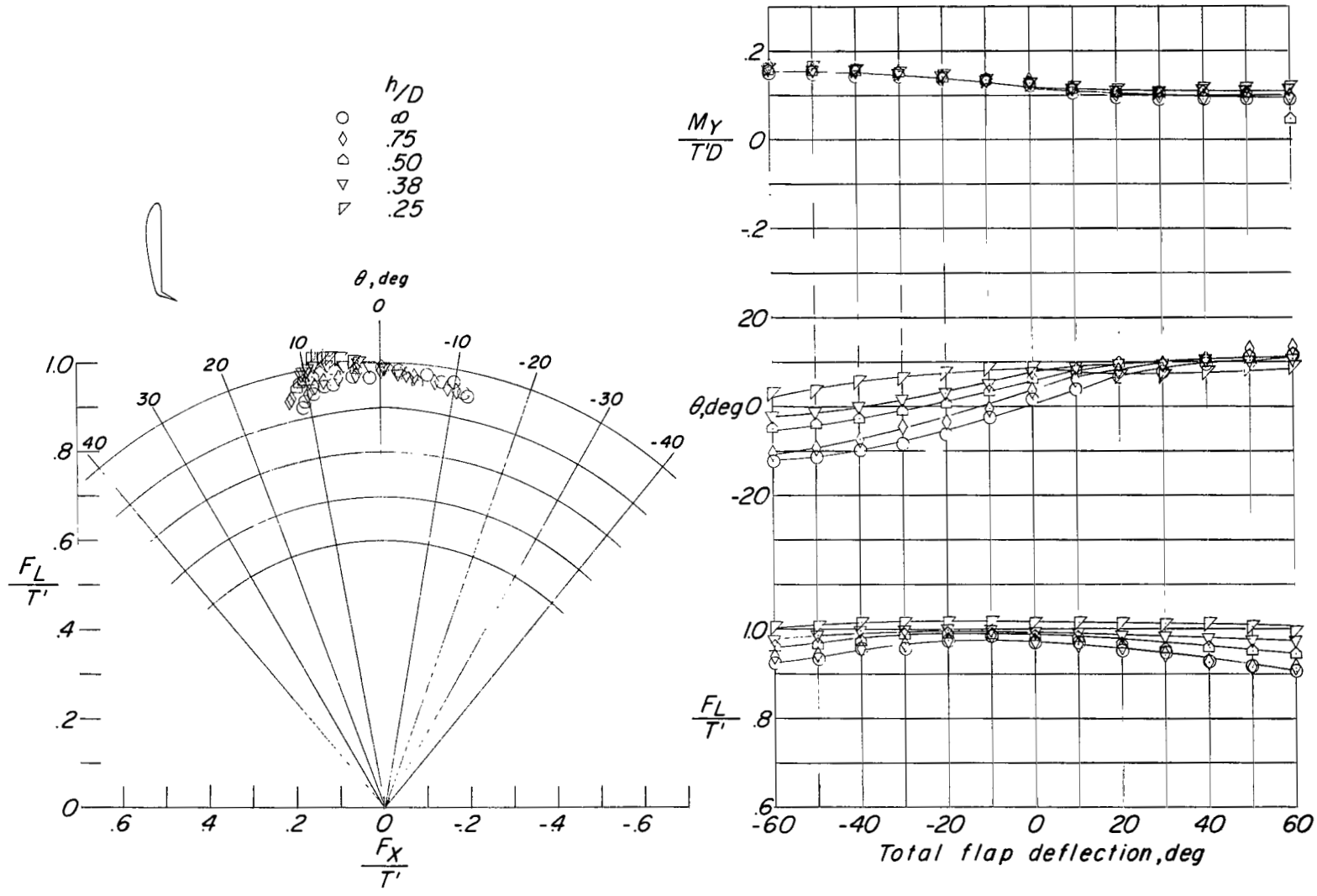

(a) Turning effectiveness, pitching moment, and lift-thrust ratio.

Figure 10.- Ground effect on hovering-flight characteristics for tilt-wing 15-percent-chord plain-flap configuration. h/D = 0.75 to 0.25.

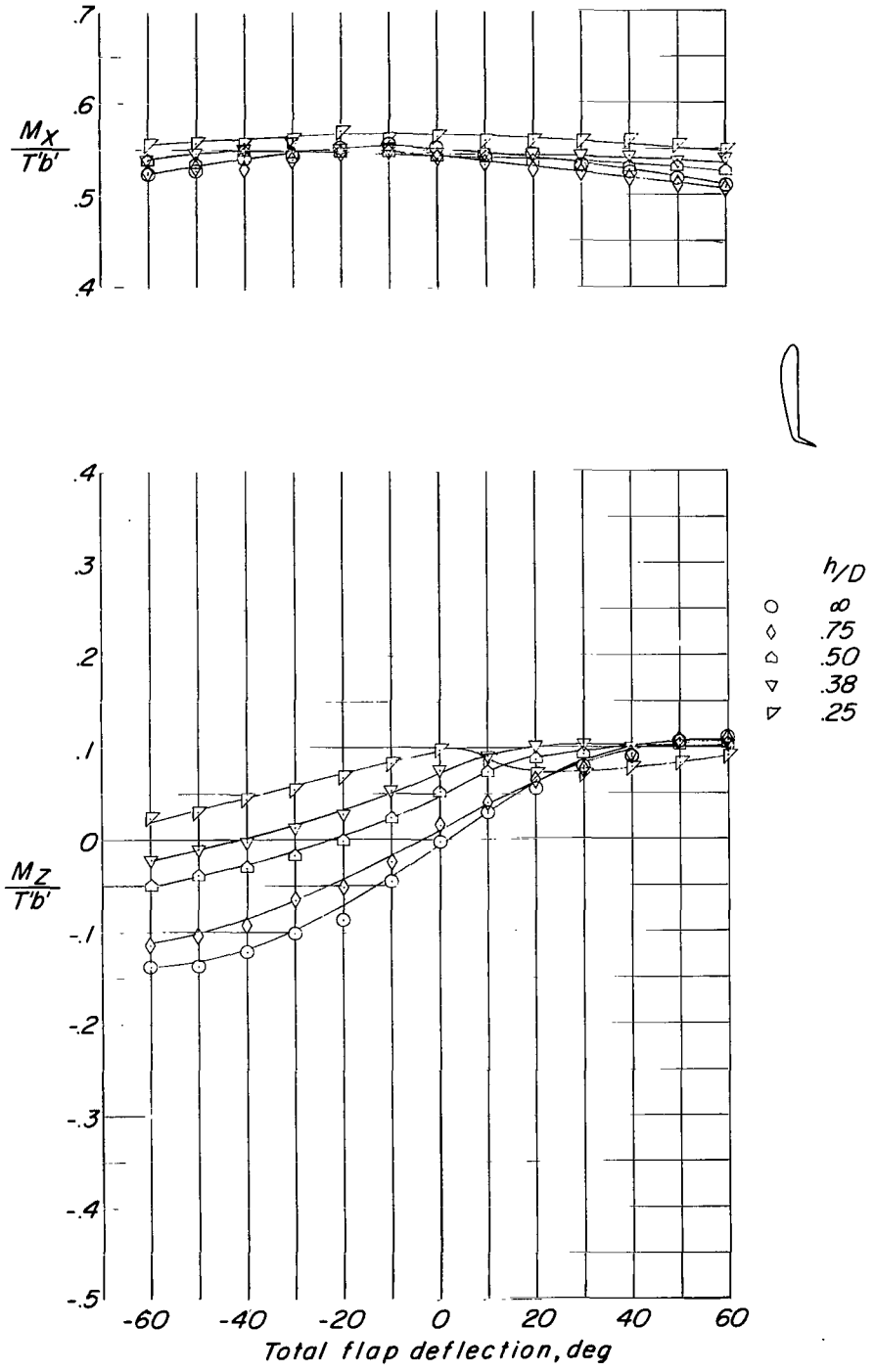

(b) Root bending moments.

Figure 10.- Concluded.

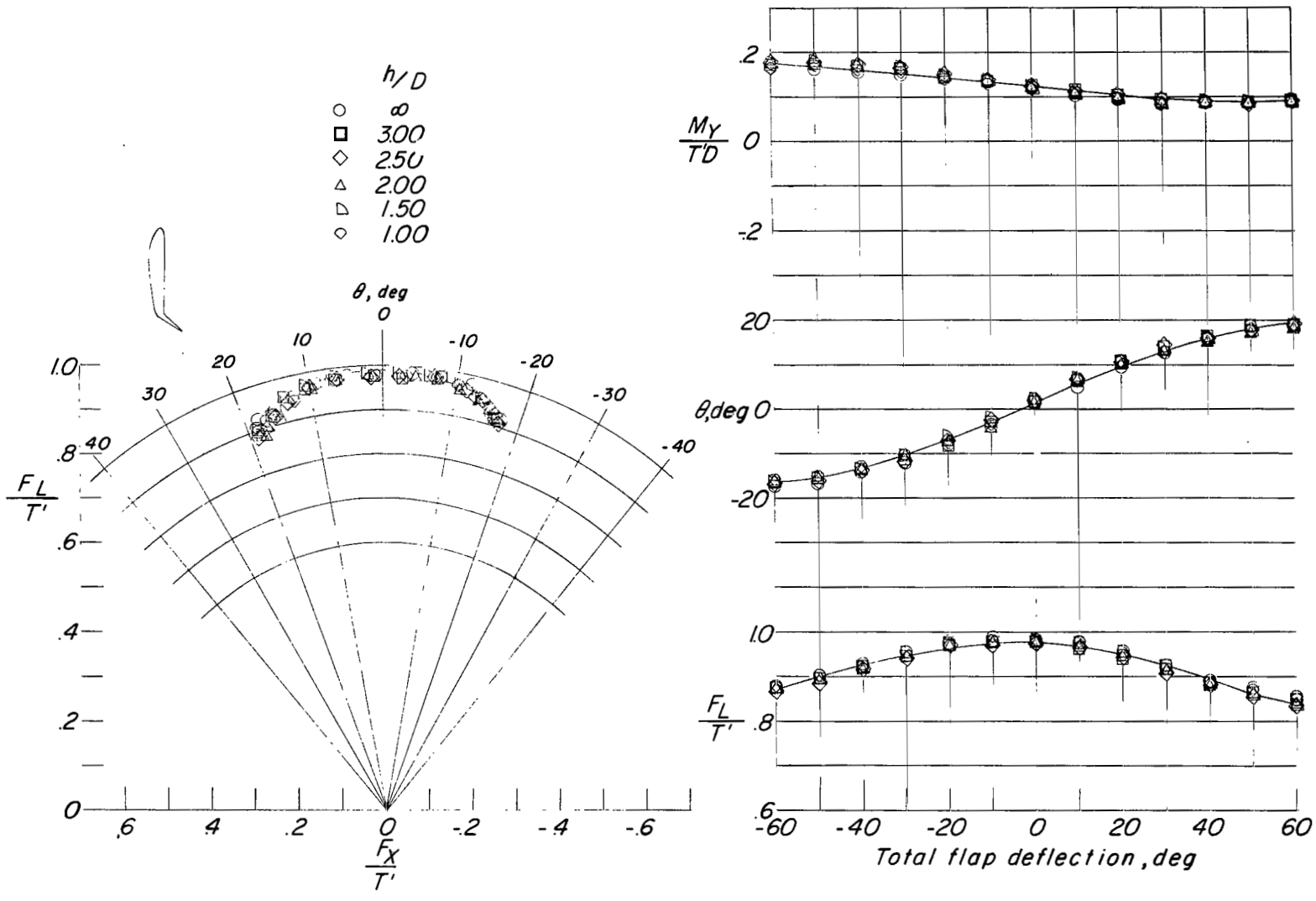

(a) Turning effectiveness, pitching moment, and lift-thrust ratio.

Figure 11.- Ground effect on hovering-flight characteristics for tilt-wing 25-percent-chord plain-flap configuration. h/D = ∞ to 1.00.

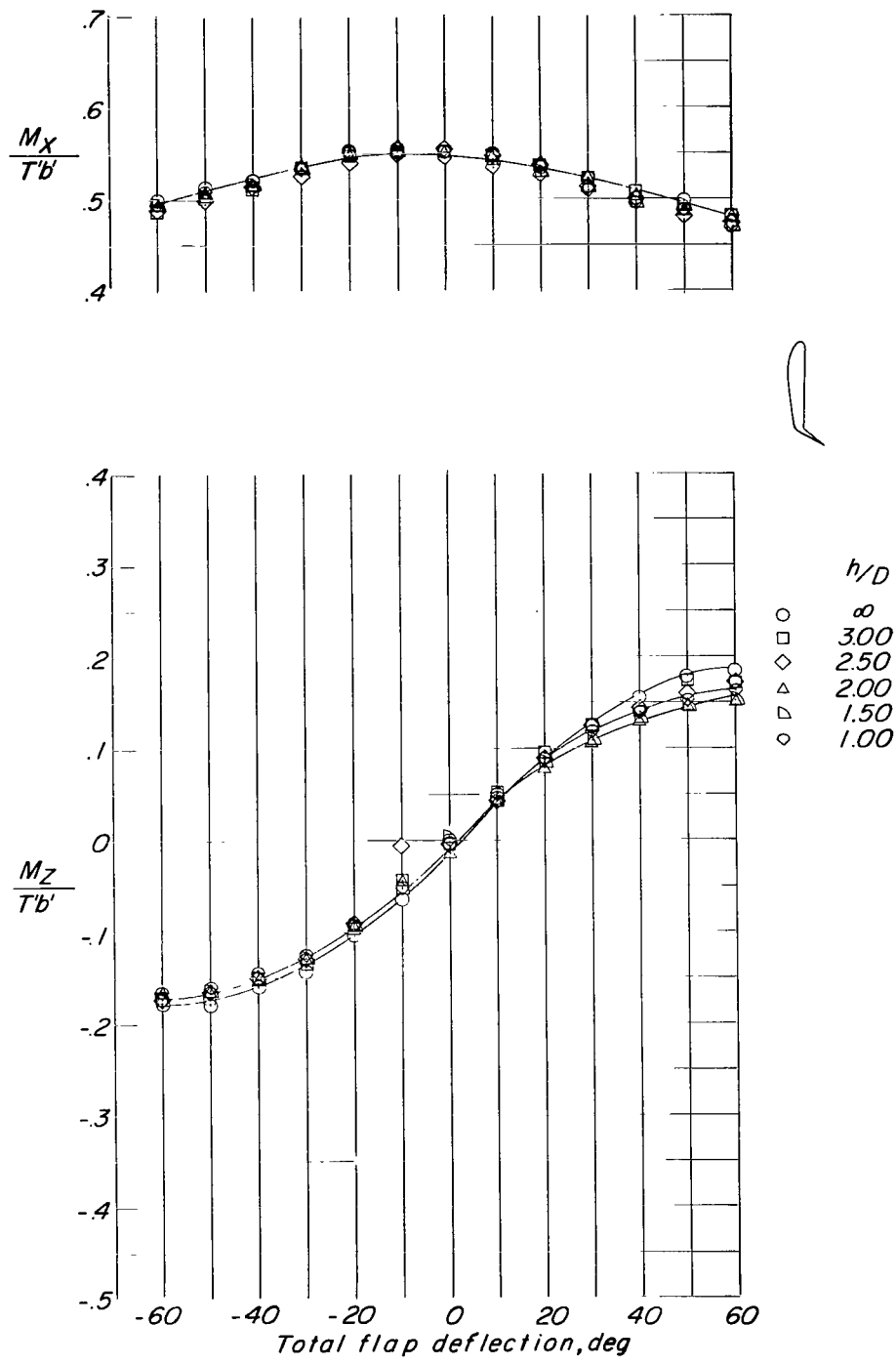

(b) Root bending moments.

Figure 11.- Concluded.

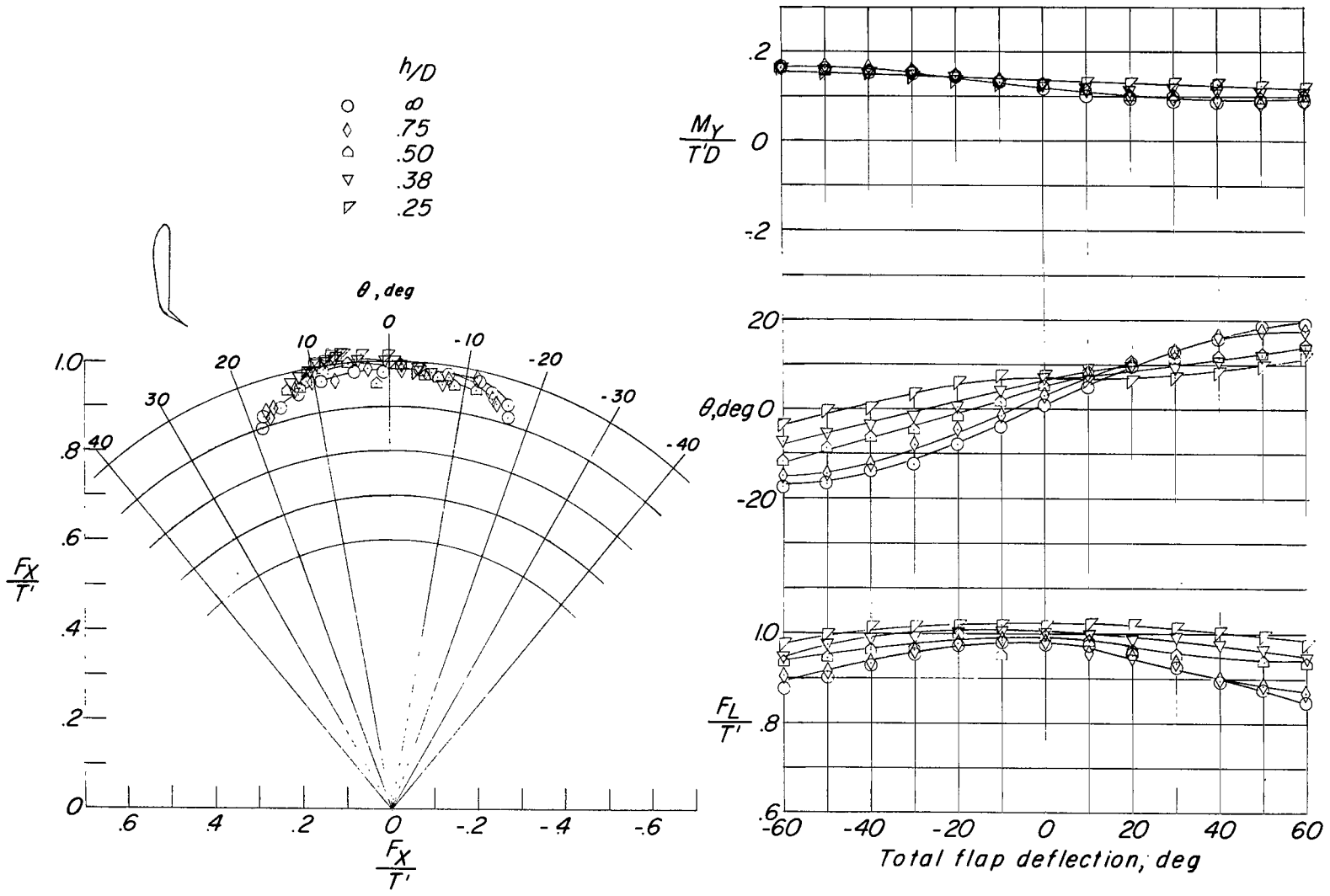

(a) Turning effectiveness, pitching moment, and lift-thrust ratio.

Figure 12.- Ground effect on hovering-flight characteristics for tilt-wing 25-percent-chord plain-flap configuration. h/D = 0.75 to 0.25.

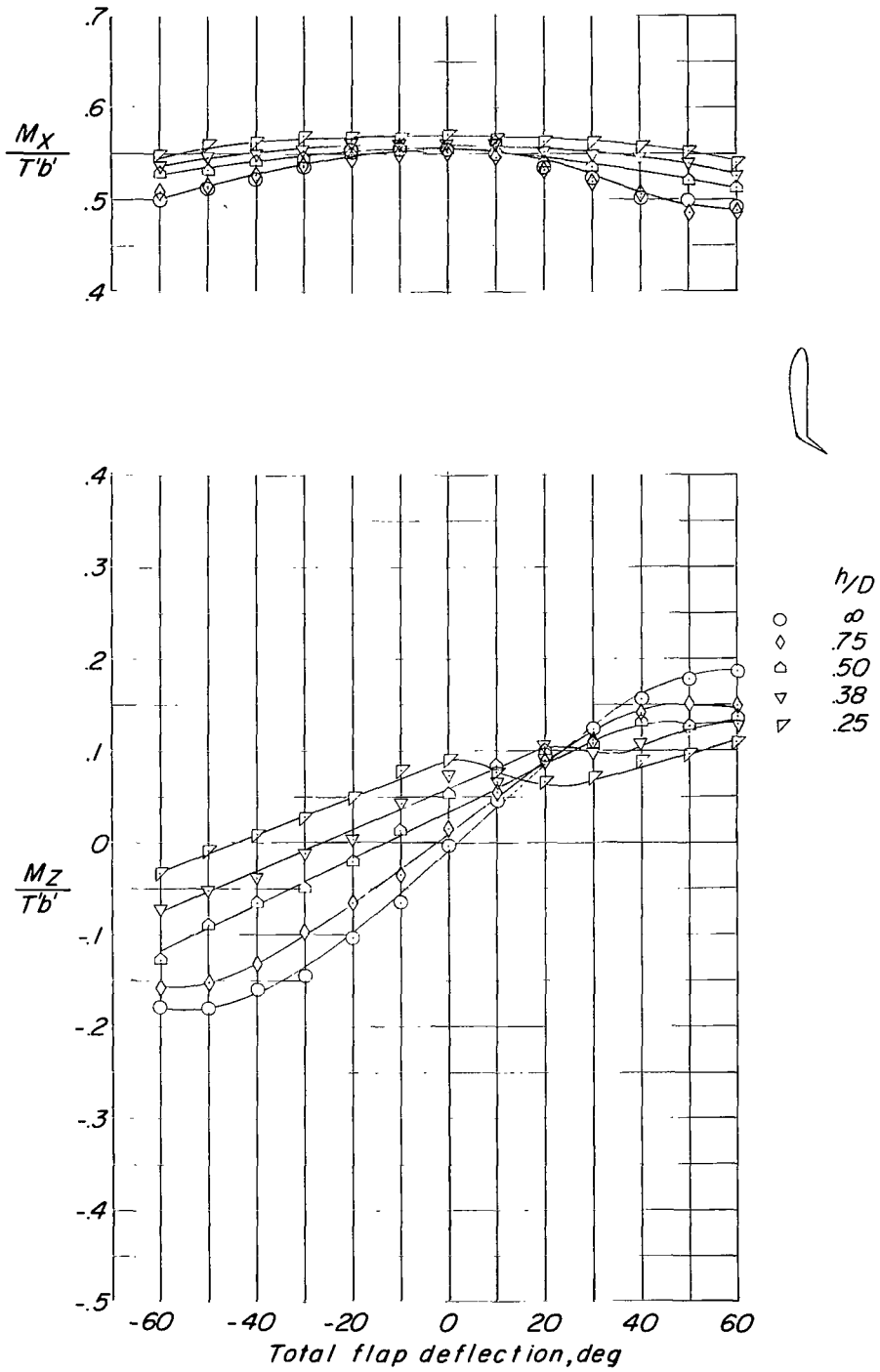

(b) Root bending moments.

Figure 12.- Concluded.

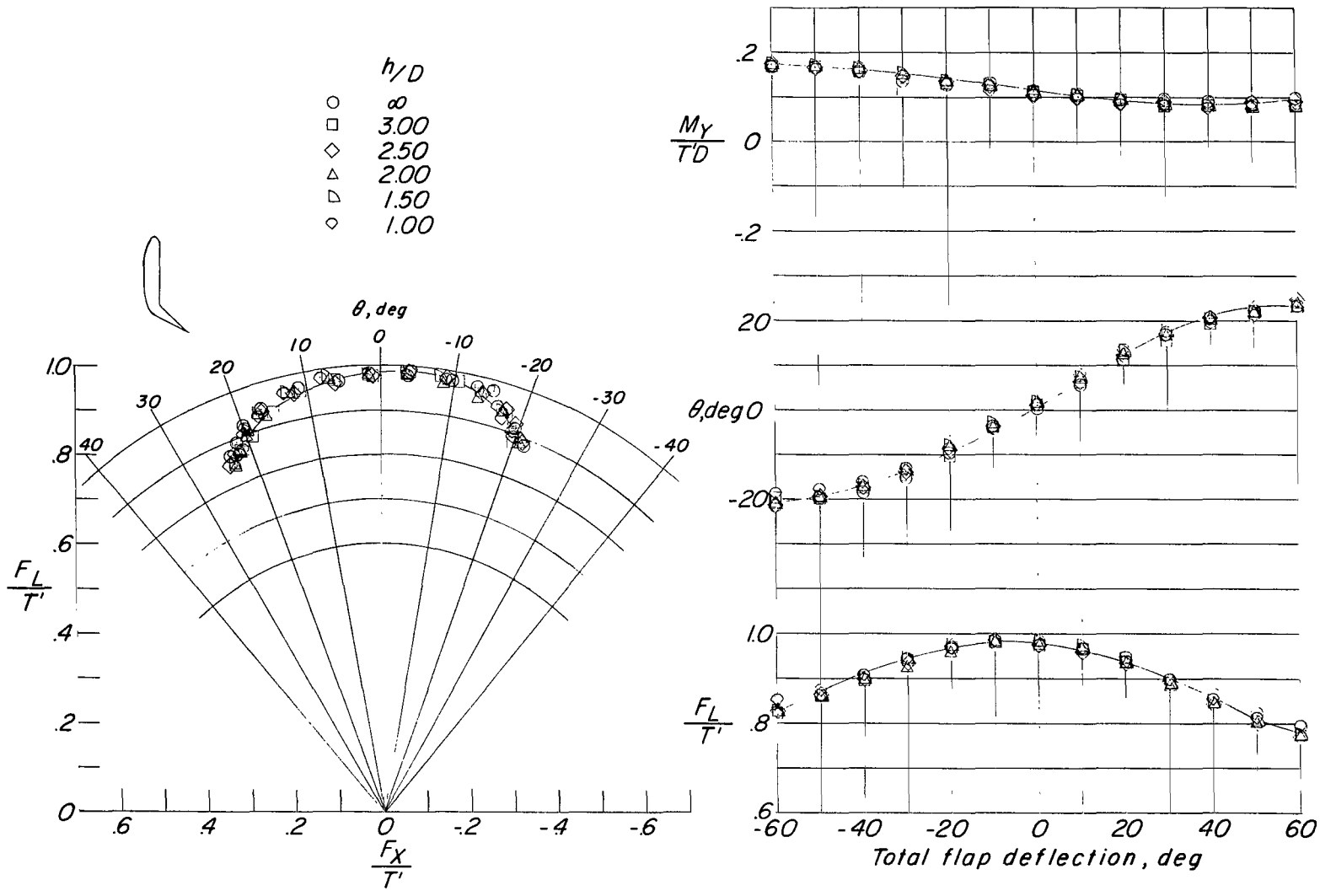

(a) Turning effectiveness, pitching moment, and lift-thrust ratio.

Figure 13.- Ground effect on hovering-flight characteristics for tilt-wing 37.5-percent-chord plain-flap configuration. h/D = ∞ to 1.00.

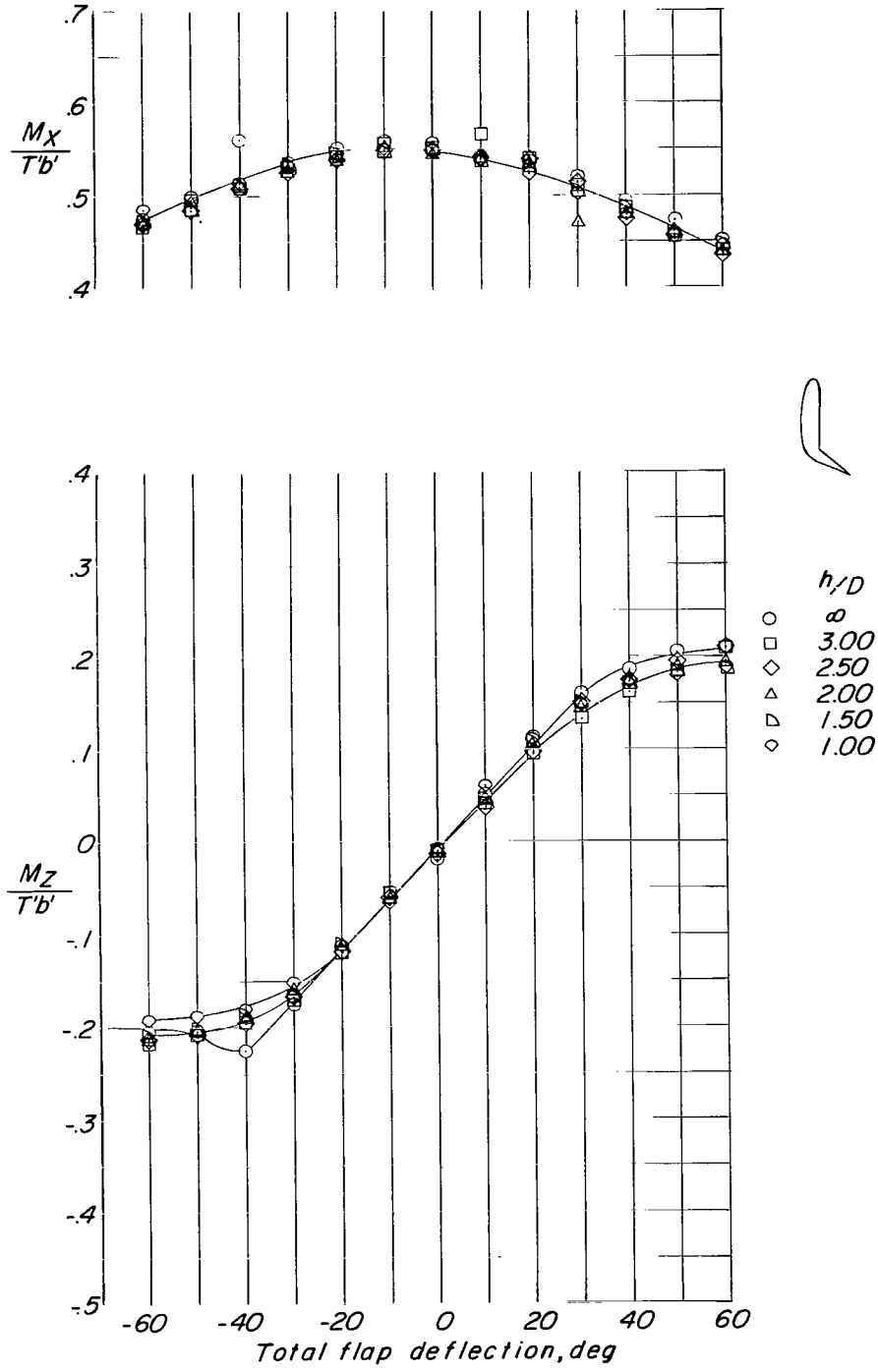

(b) Root bending moments.

Figure 13.- Concluded.

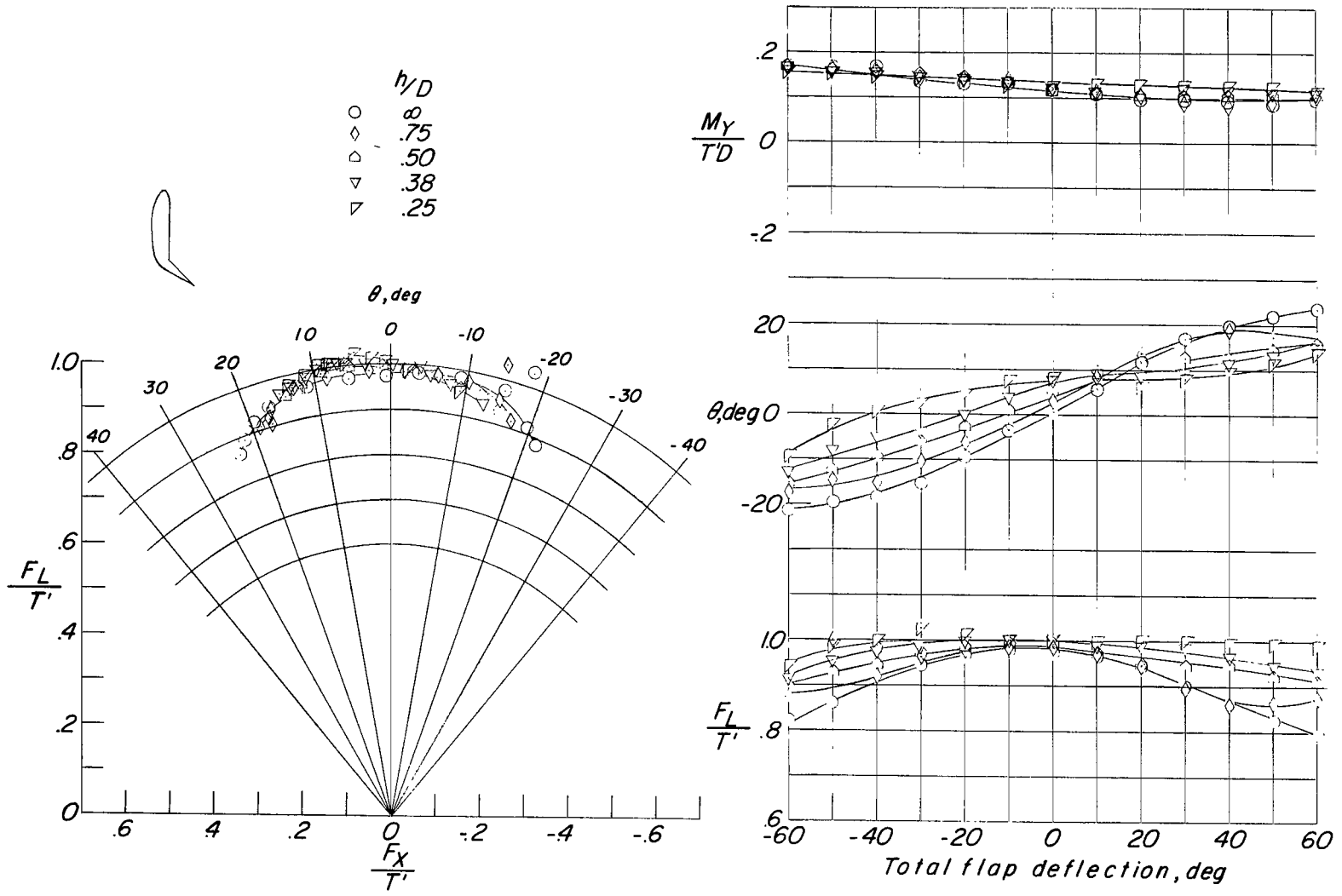

(a) Turning effectiveness, pitching moment, and lift-thrust ratio.

Figure 14.- Ground effect on hovering-flight characteristics for tilt-wing 37.5-percent-chord plain-flap configuration. h/D = 0.75 to 0.25.

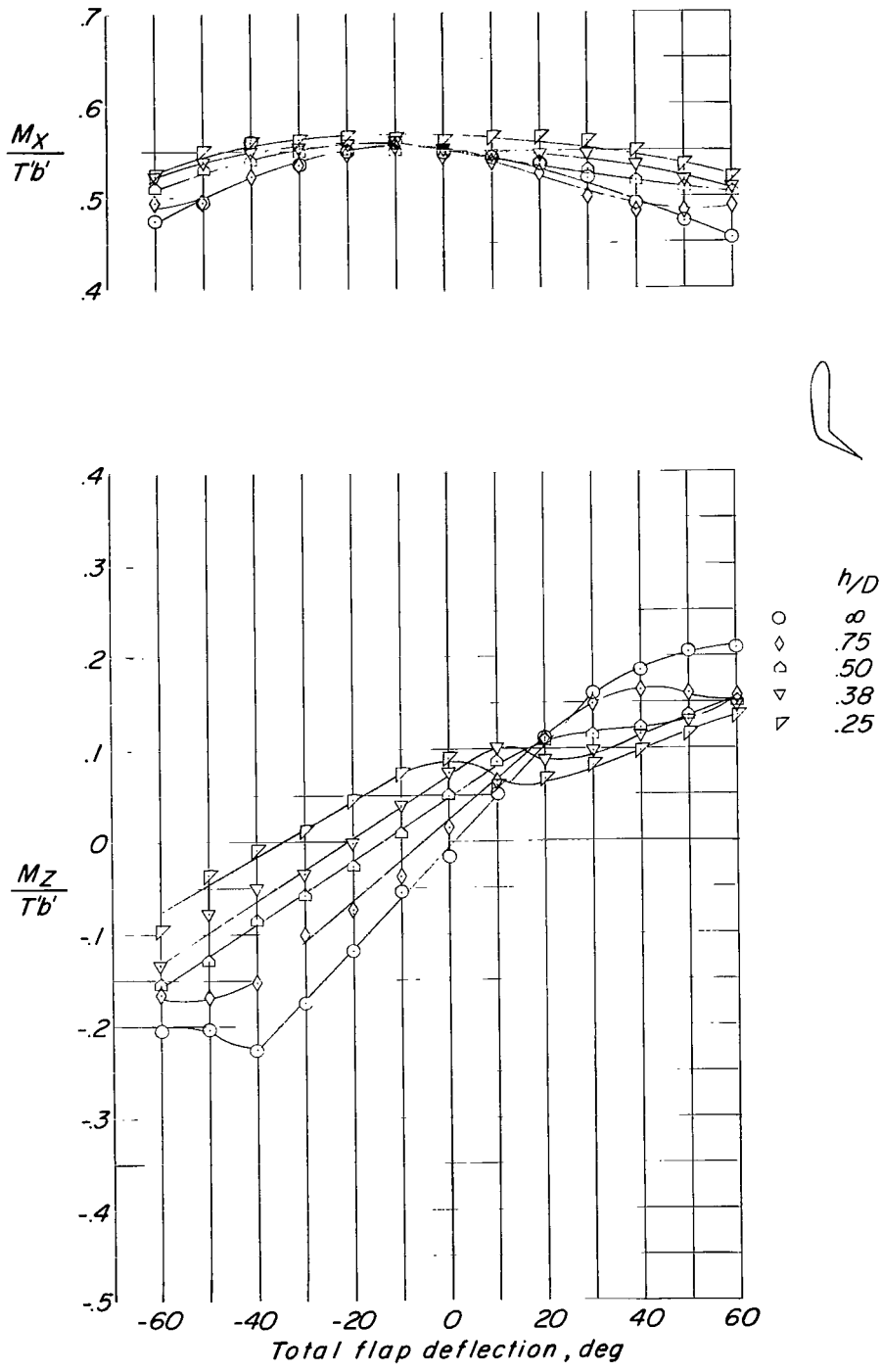

(b) Root bending moments.

Figure 14.- Concluded.

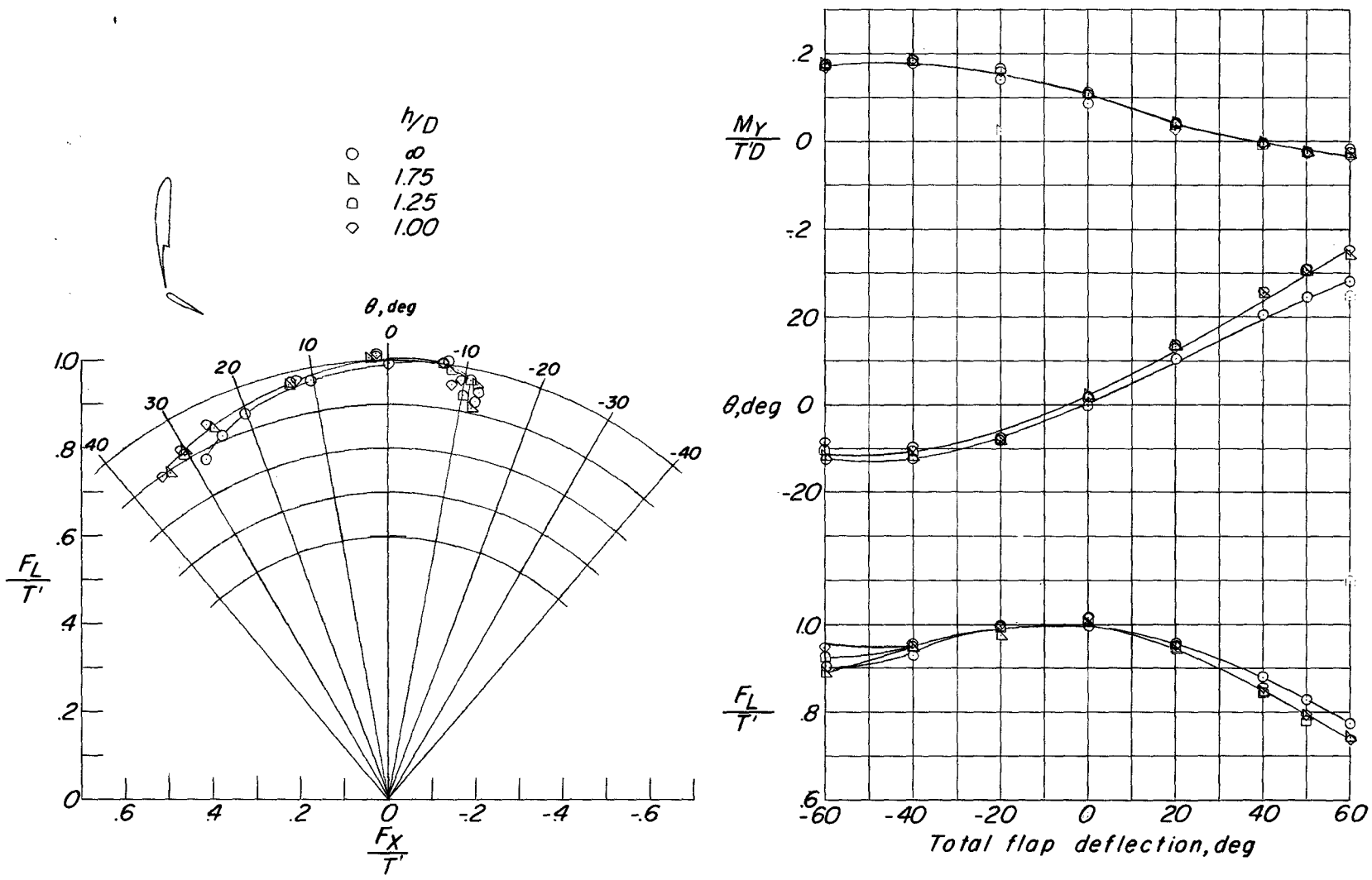

(a) Turning effectiveness, pitching moment, and lift-thrust ratio.

Figure 15.- Ground effect on hovering-flight characteristics for tilt-wing single-slotted 40-percent-chord flap configuration. h/D = ∞ to 1.00.

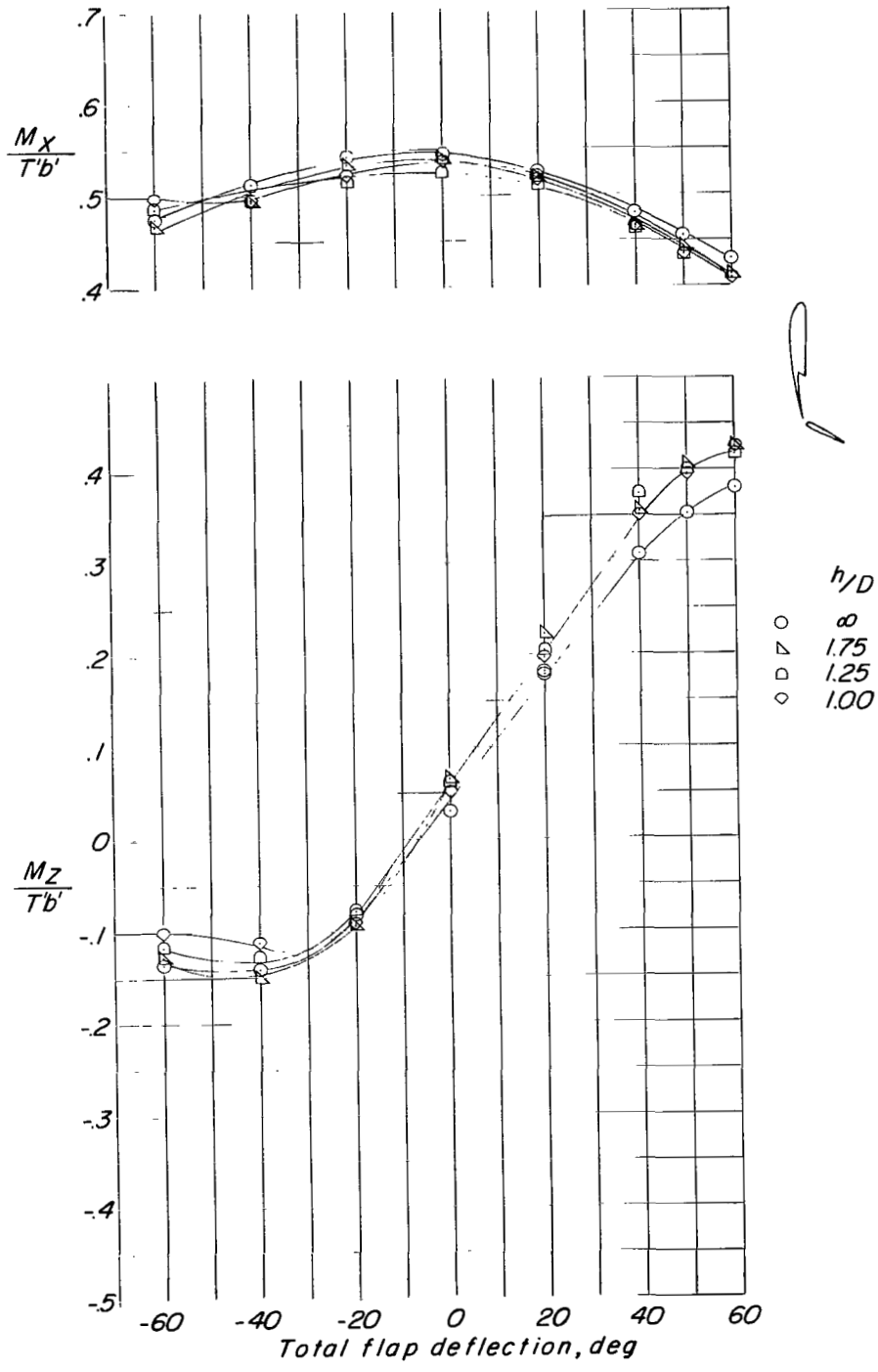

(b) Root bending moments.

Figure 15.- Concluded.

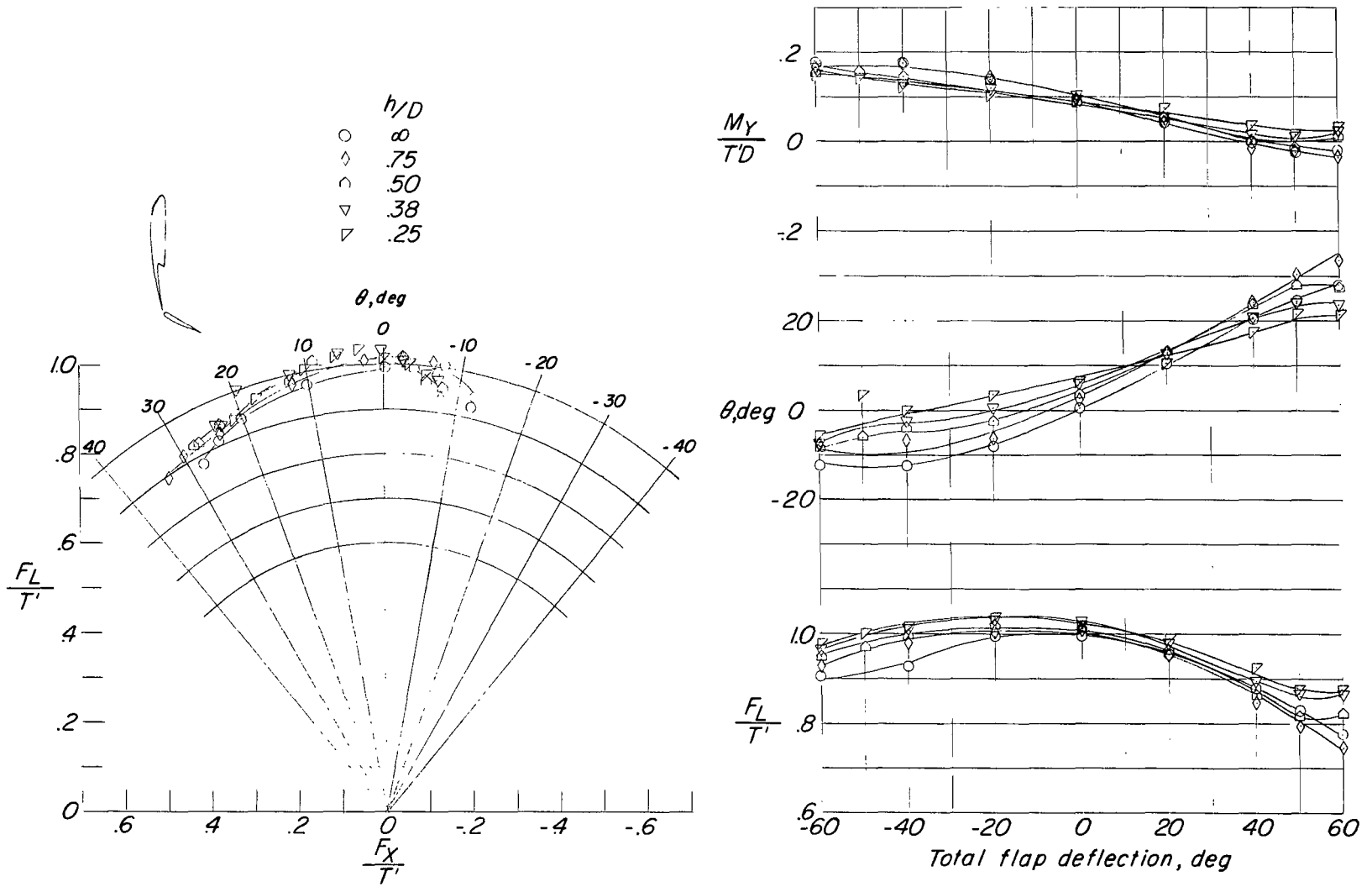

(a) Turning effectiveness, pitching moment, and lift-thrust ratio.

Figure 16.- Ground effect on hovering-flight characteristics for tilt-wing single-slotted 40-percent-chord flap configuration. h/D = 0.75 to 0.25.

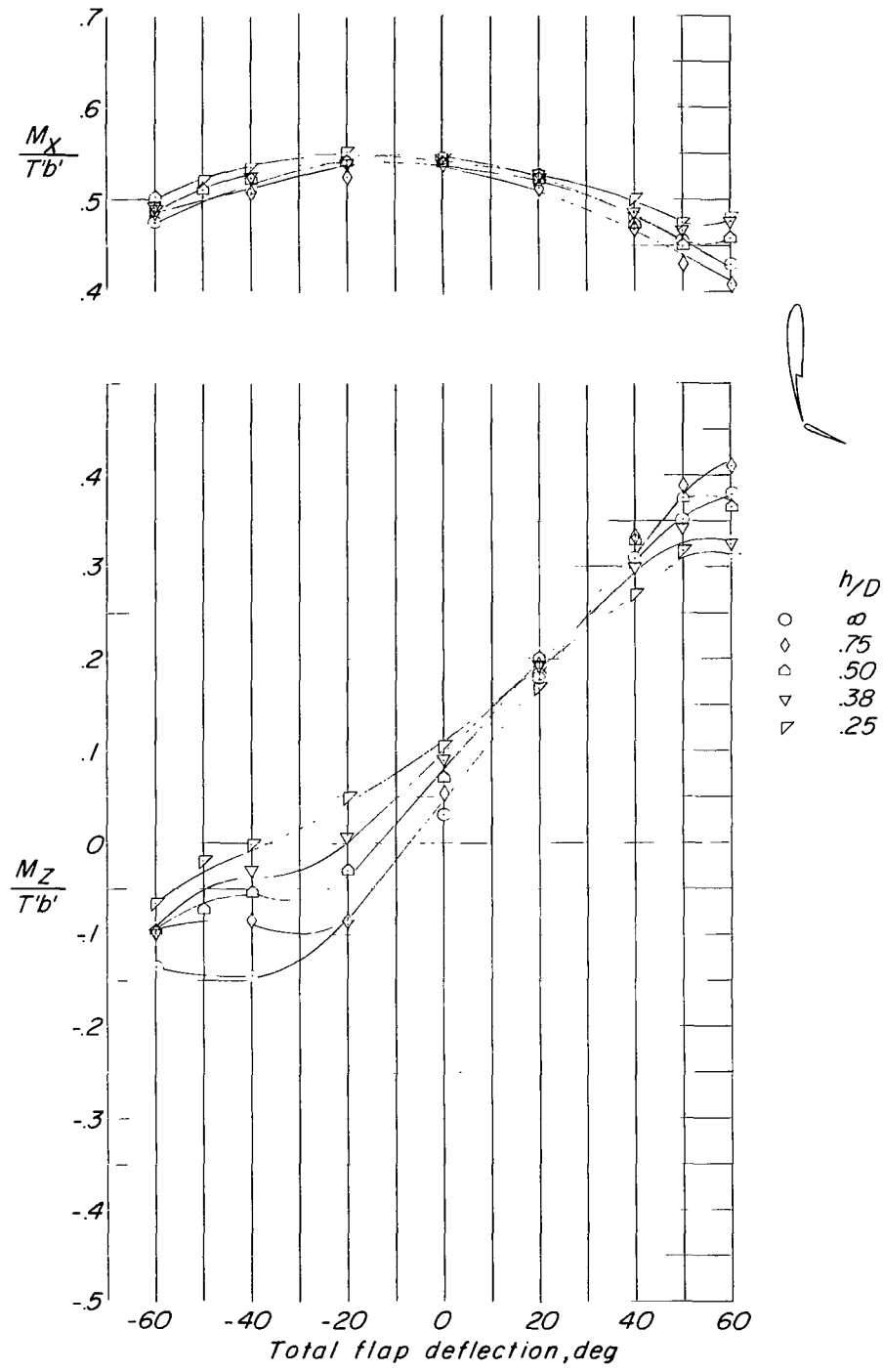

(b) Root bending moments.

Figure 16.- Concluded.

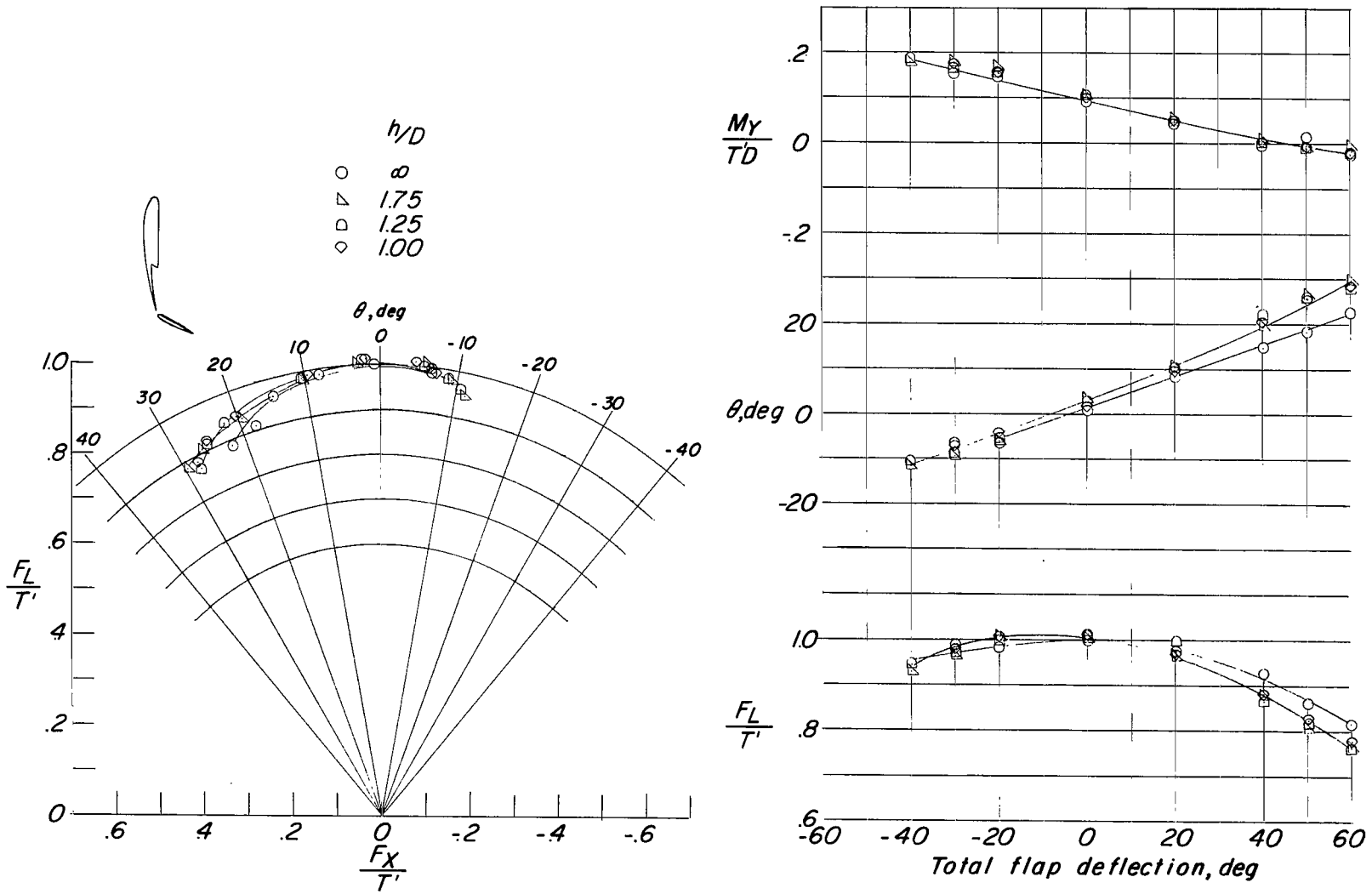

(a) Turning effectiveness, pitching moment, and lift-thrust ratio.

Figure 17.- Ground effect on hovering-flight characteristics for tilt-wing single-slotted 40-percent-chord flap configuration with nacelle cutouts. h/D = ∞ to 1.00.

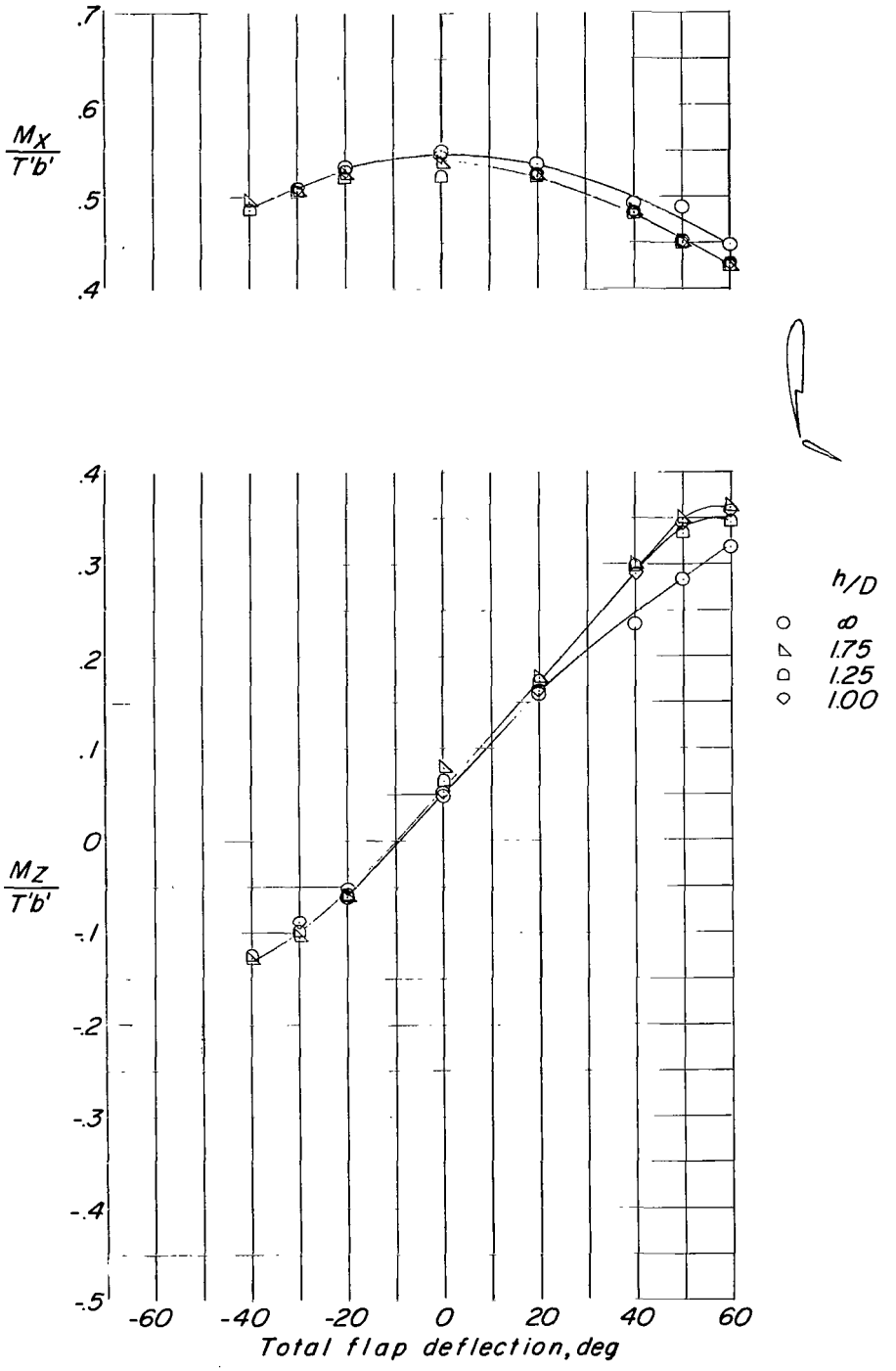

(b) Root bending moments.

Figure 17.- Concluded.

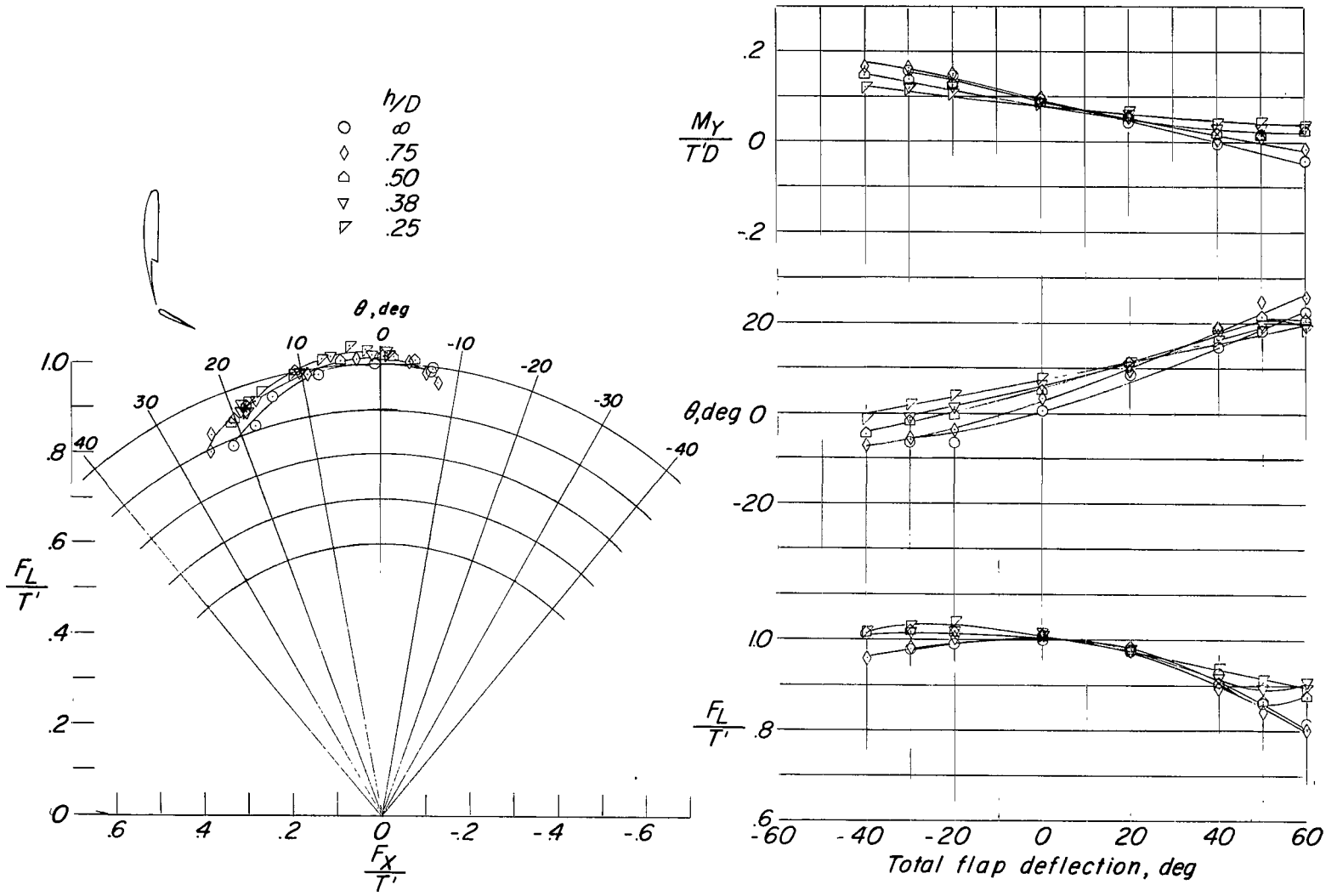

(a) Turning effectiveness, pitching moment, and lift-thrust ratio.

Figure 18.- Ground effect on hovering-flight characteristics for tilt-wing single-slotted 40-percent-chord flap configuration with nacelle cutouts. h/D = 0.75 to 0.25.

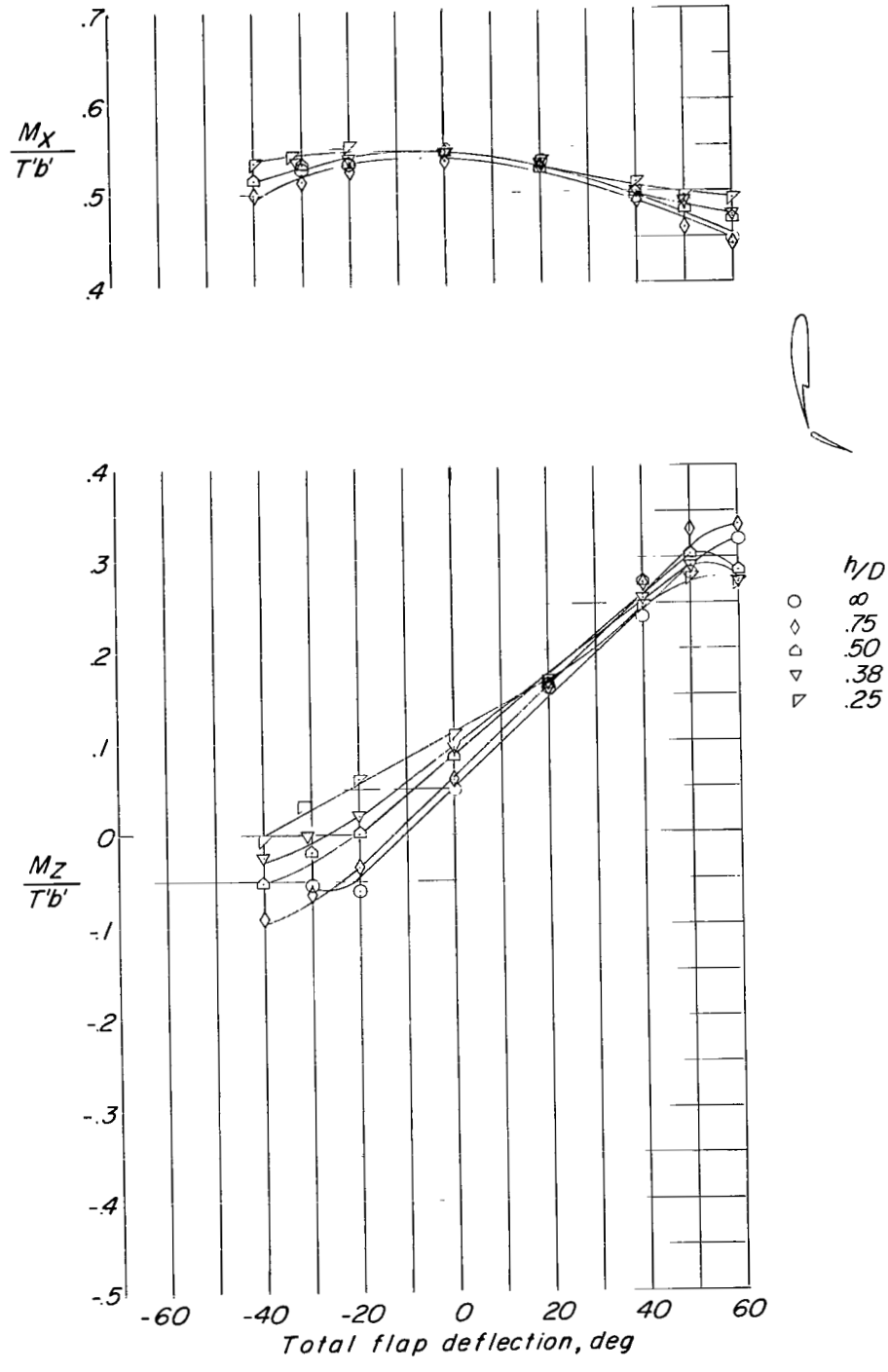

(b) Root bending moments.

Figure 18.- Concluded.

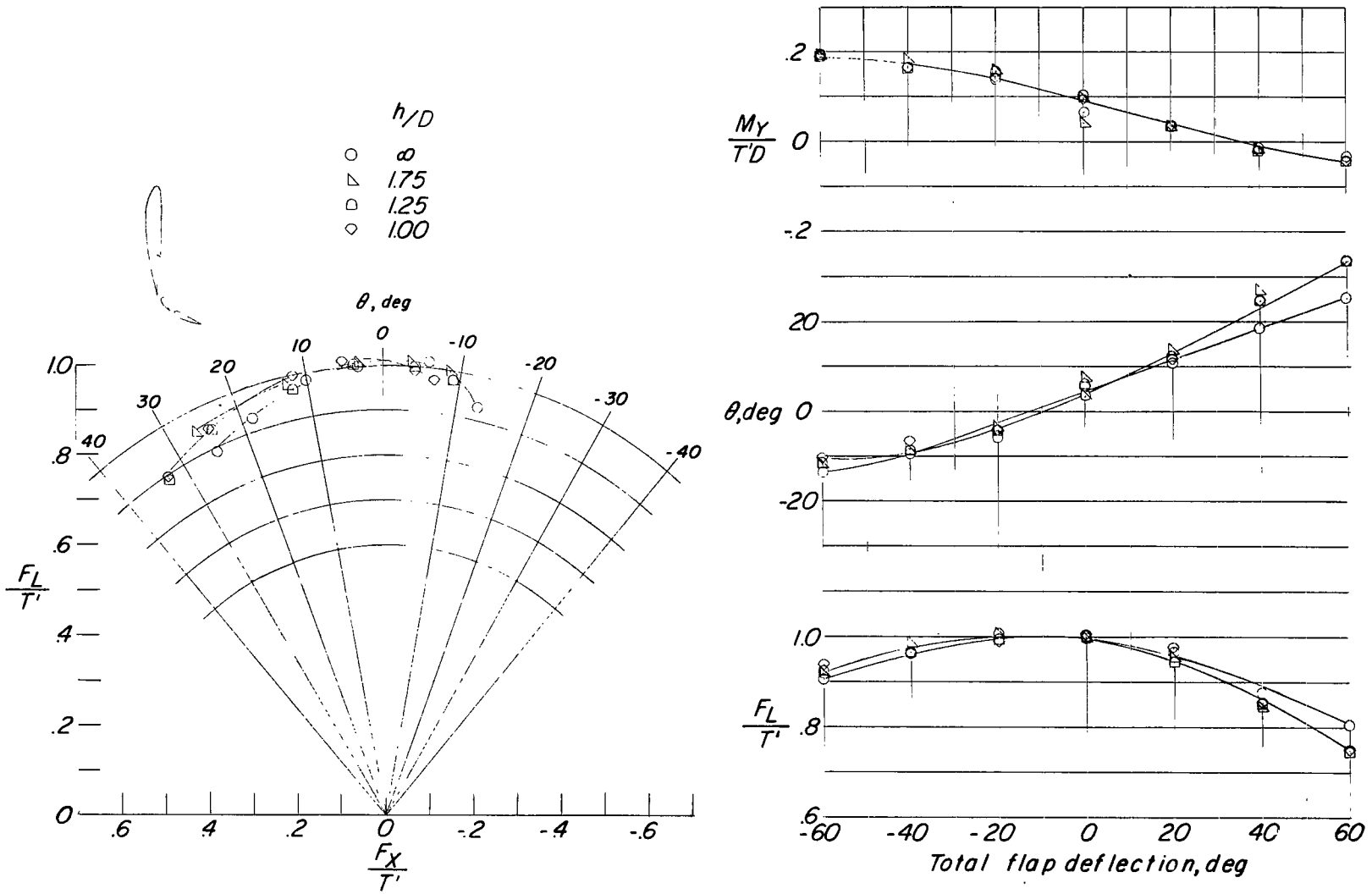

(a) Turning effectiveness, pitching moment, and lift-thrust ratio.

Figure 19.- Ground effect on hovering-flight characteristics for tilt-wing double-slotted 14-percent-chord vane and 22-percent-chord flap configuration. h/D = ∞ to 1.00.

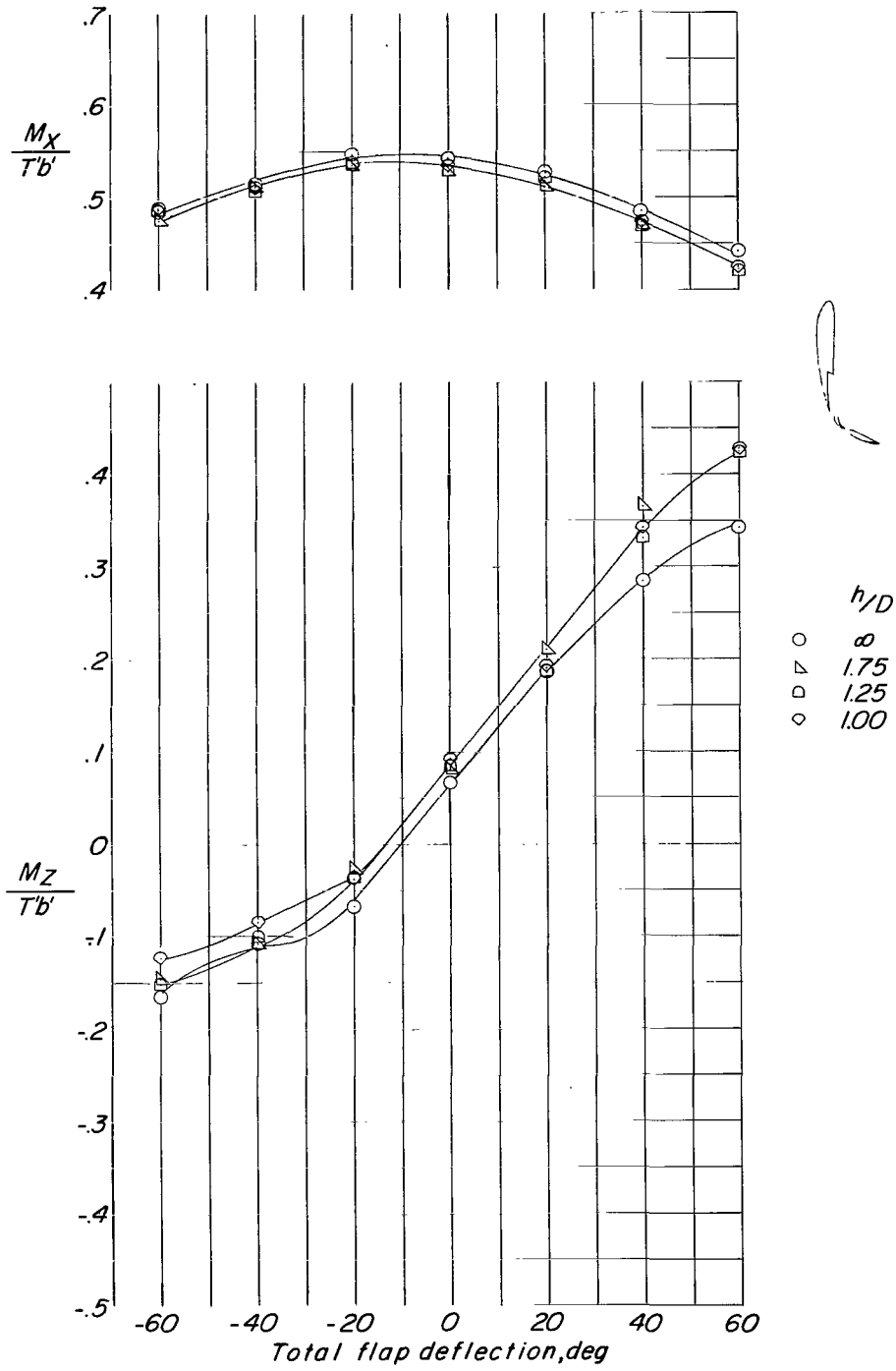

(b) Root bending moments.

Figure 19.- Concluded.

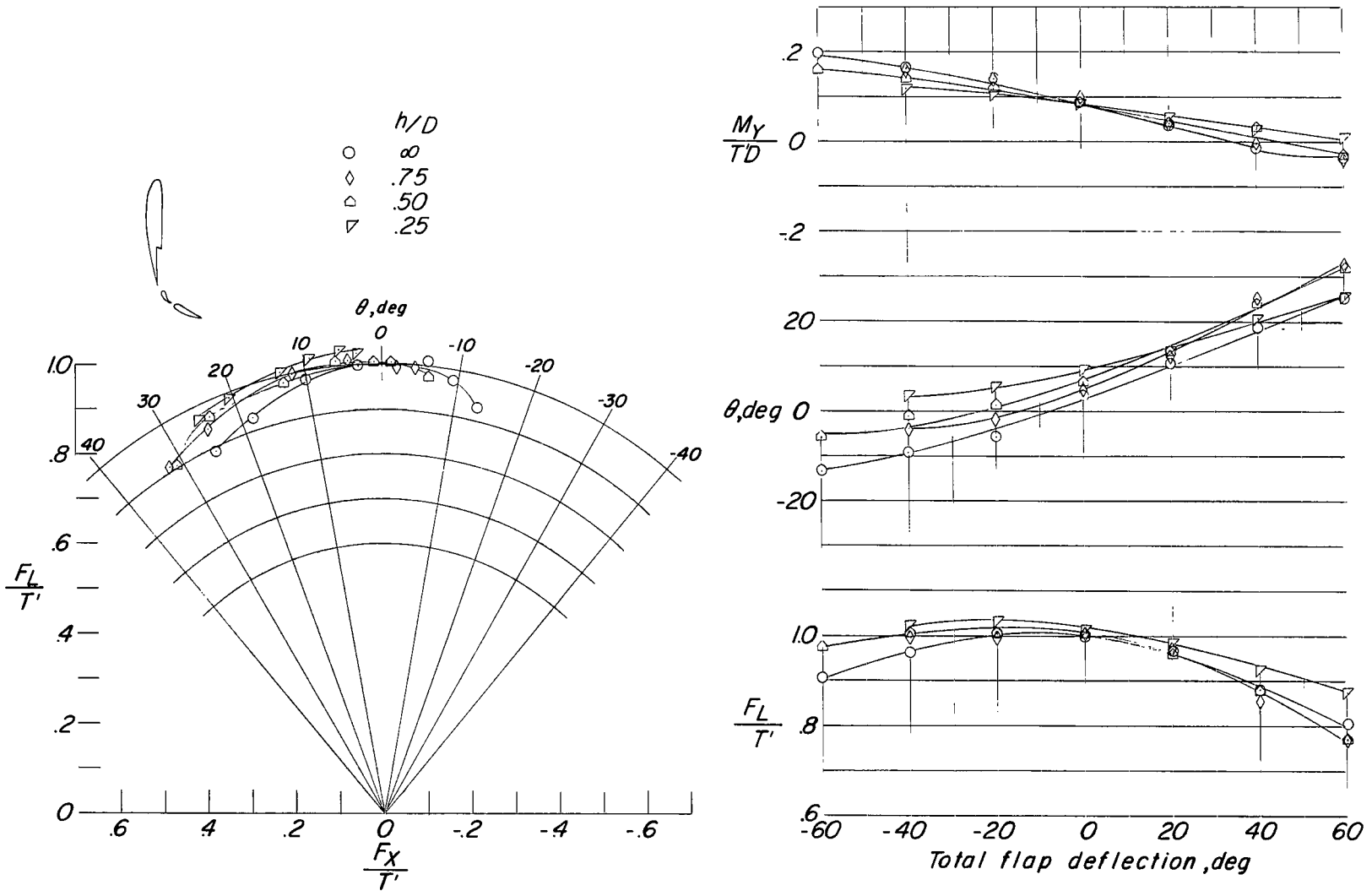

(a) Turning effectiveness, pitching moment, and lift-thrust ratio.

Figure 20.- Ground effect on hovering-flight characteristics for tilt-wing double-slotted 14-percent-chord vane and 22-percent-chord flap configuration. h/D = 0.75 to 0.25.

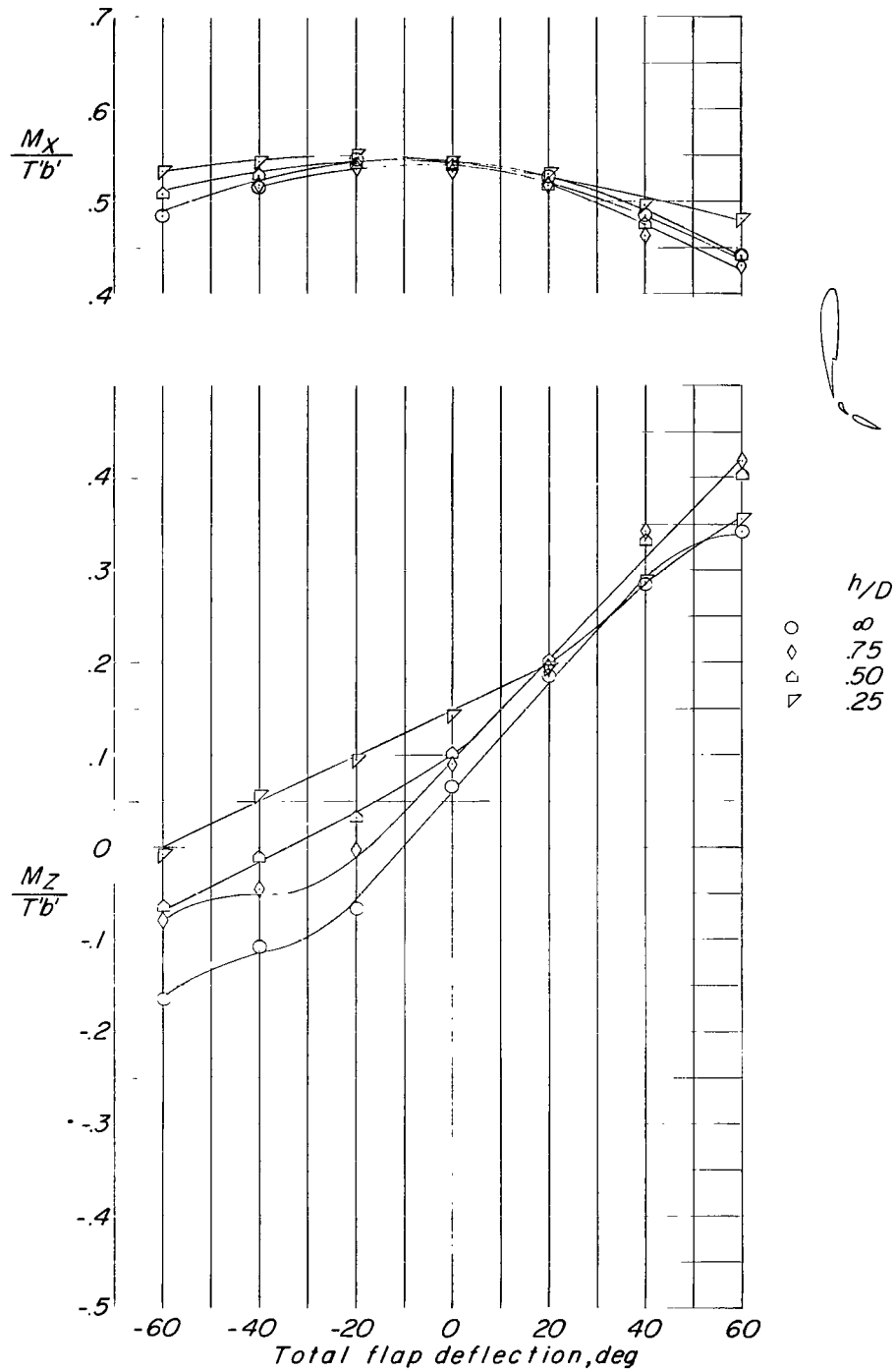

(b) Root bending moments.

Figure 20.- Concluded.

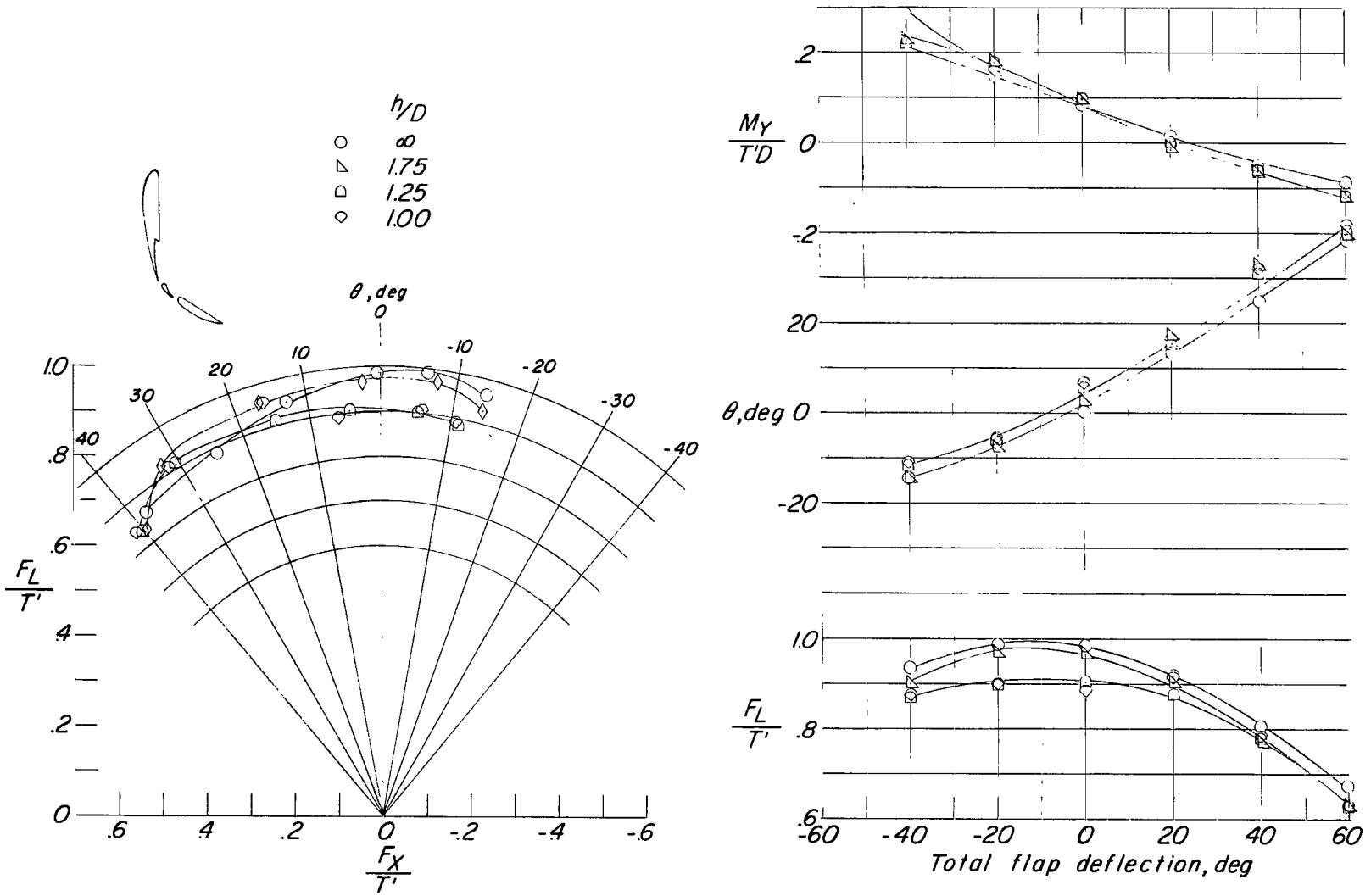

(a) Turning effectiveness, pitching moment, and lift-thrust ratio.

Figure 21.- Ground effect on hovering-flight characteristics for tilt-wing double-slotted 14-percent-chord vane and 44-percent-chord flap configuration. h/D = ∞ to 1.00.

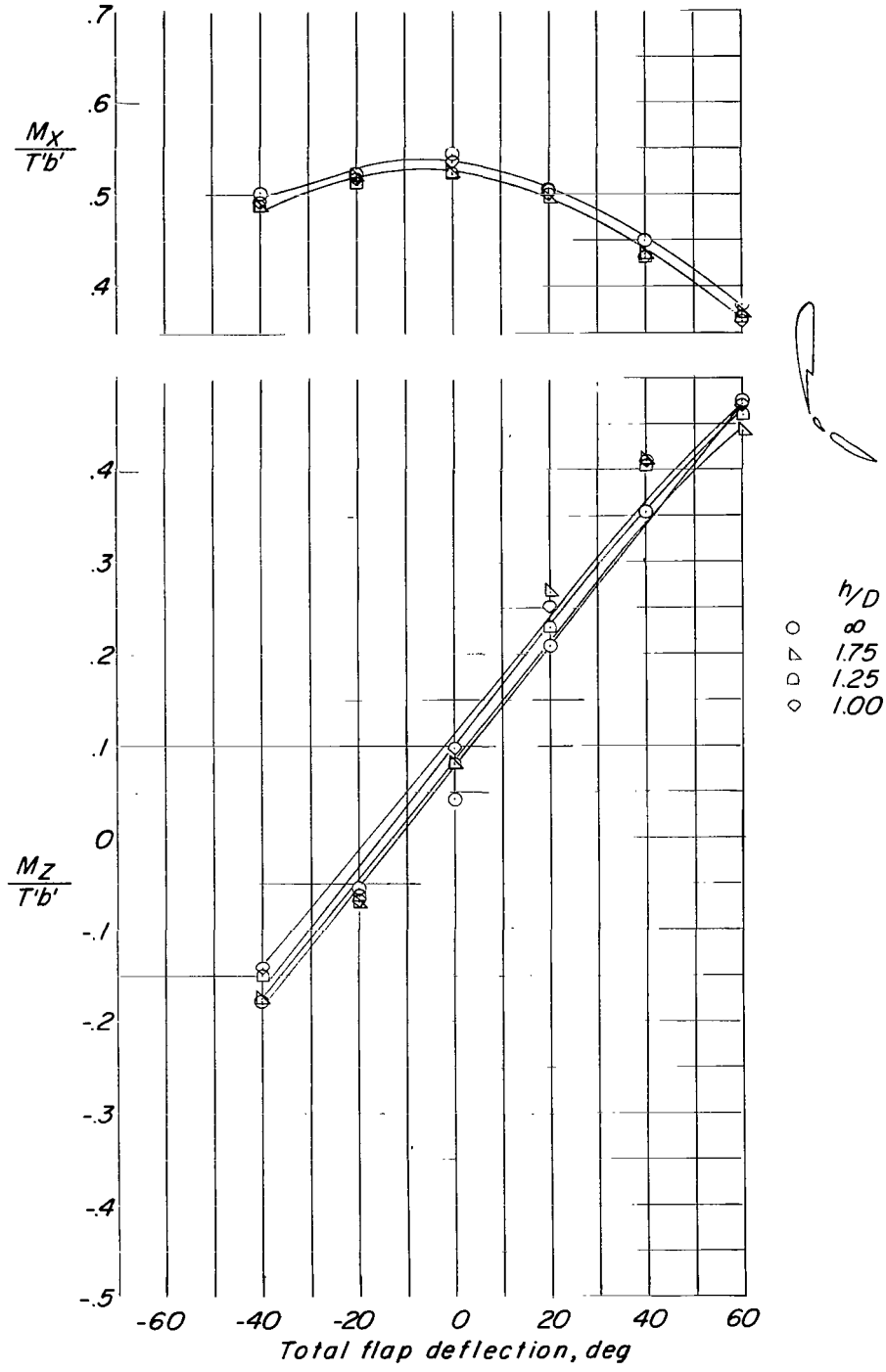

(b) Root bending moments.

Figure 21.- Concluded.

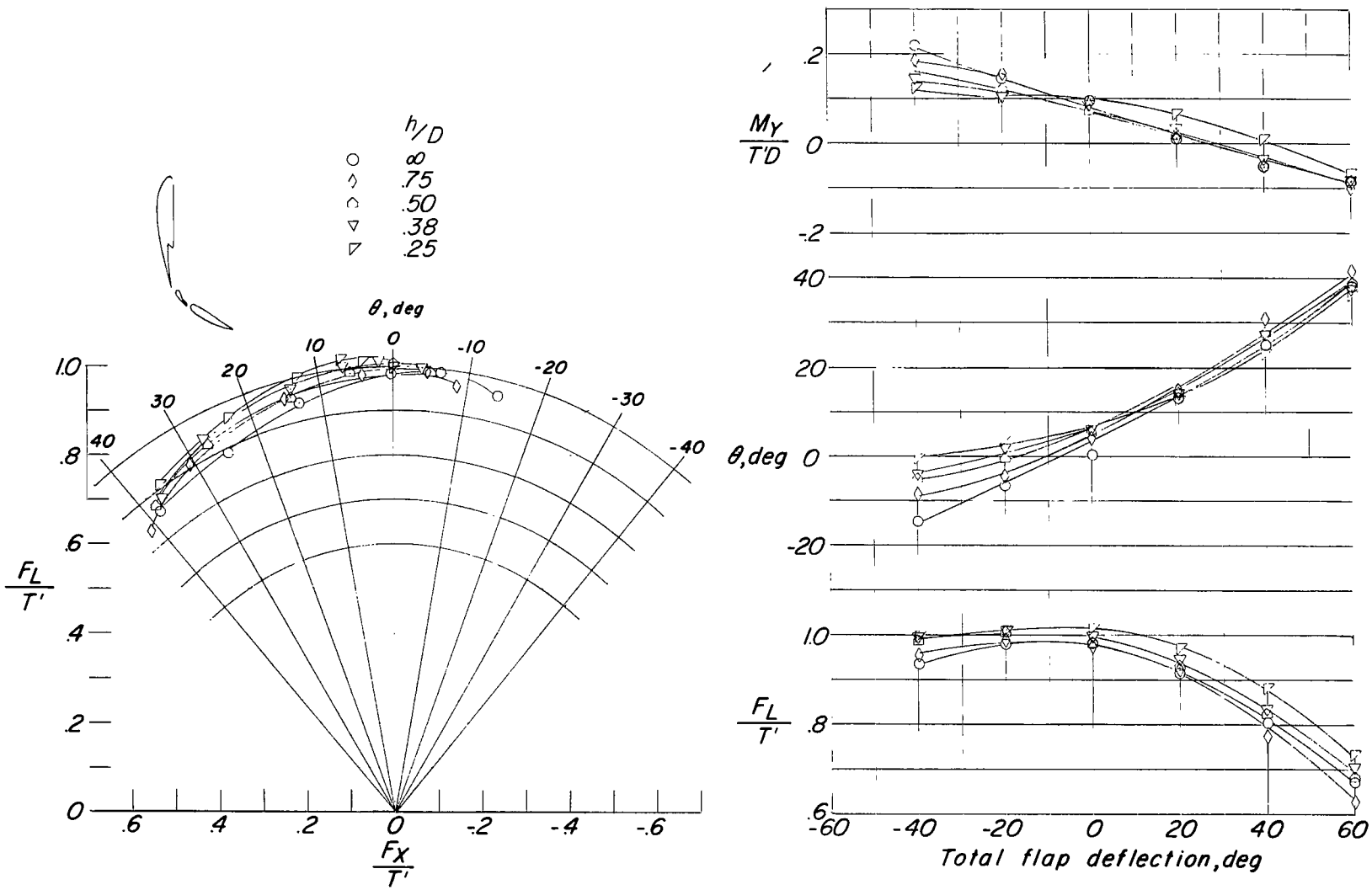

(a) Turning effectiveness, pitching moment, and lift-thrust ratio.

Figure 22.- Ground effect on hovering-flight characteristics for tilt-wing double-slotted 14-percent-chord vane and 44-percent-chord flap configuration. h/D = 0.75 to 0.25.

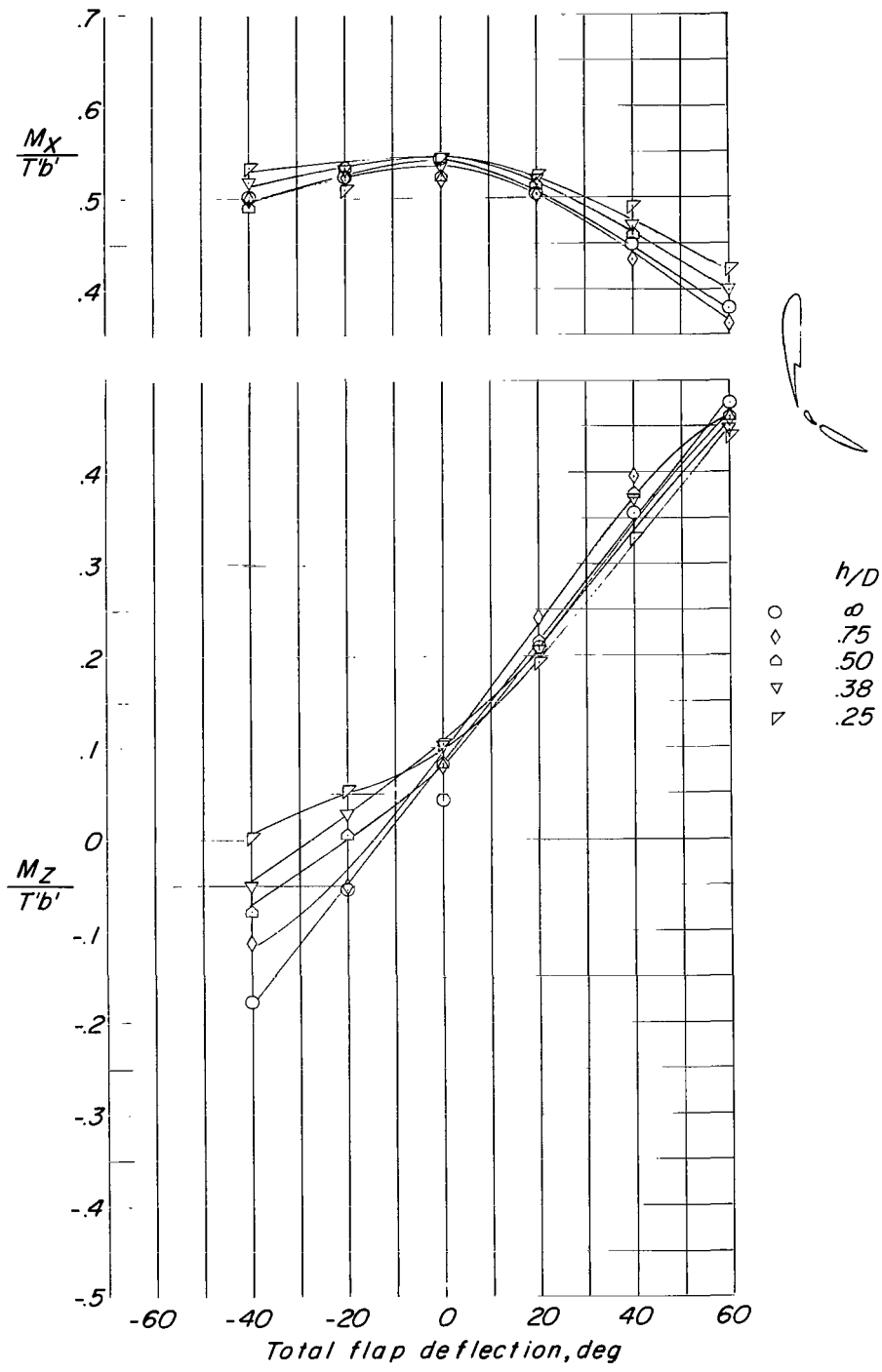

(b) Root bending moments.

Figure 22.- Concluded.

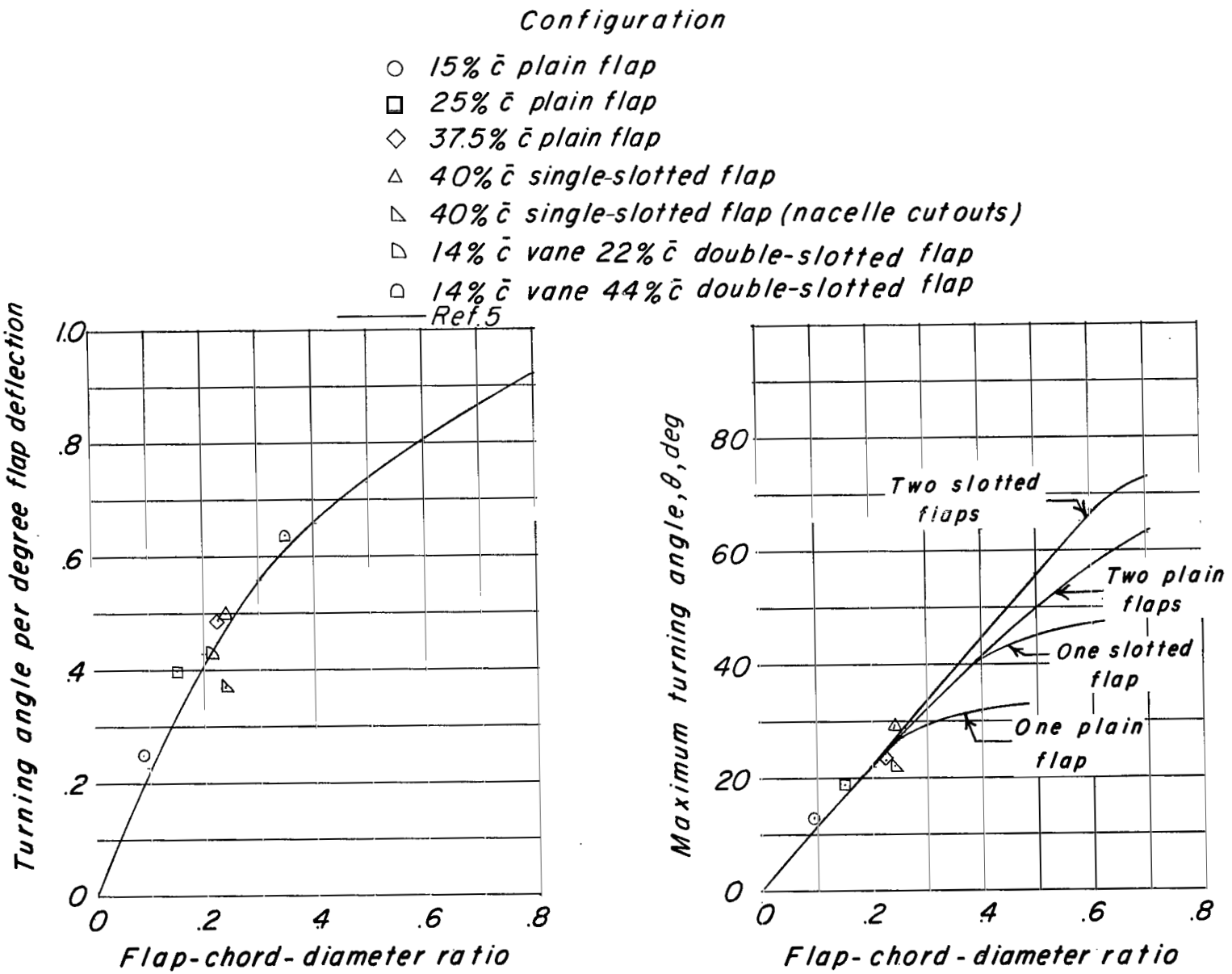

Figure 23.- Variation of turning angle with ratio of total flap chord to propeller diameter for various flap configuration in hovering out of ground effect. (Basic curves from ref. 5.)

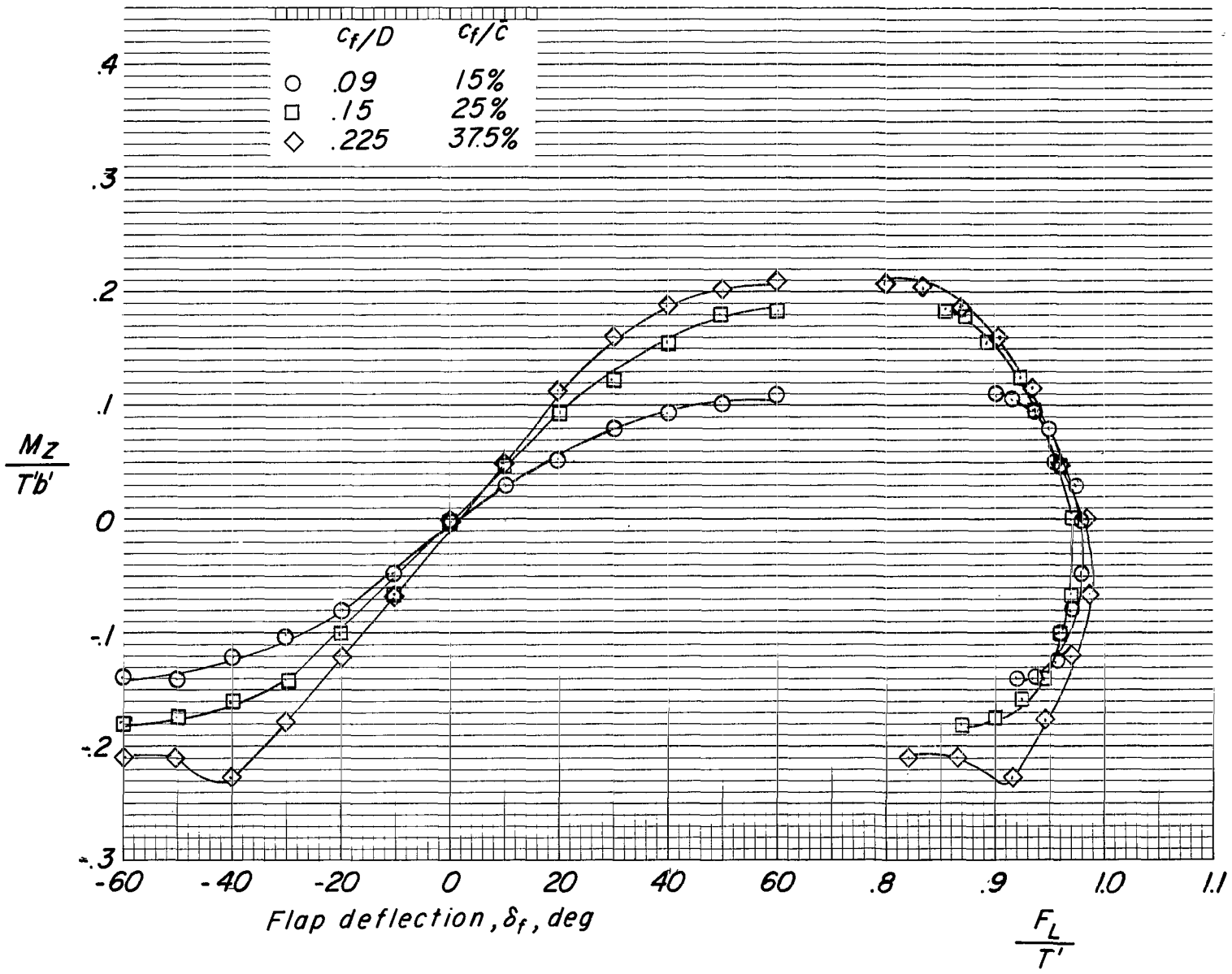

Figure 24.- Effect of flap chord length on hovering control moment and ratio of lift to thrust for plain-flap configurations. $h/D = \infty$.

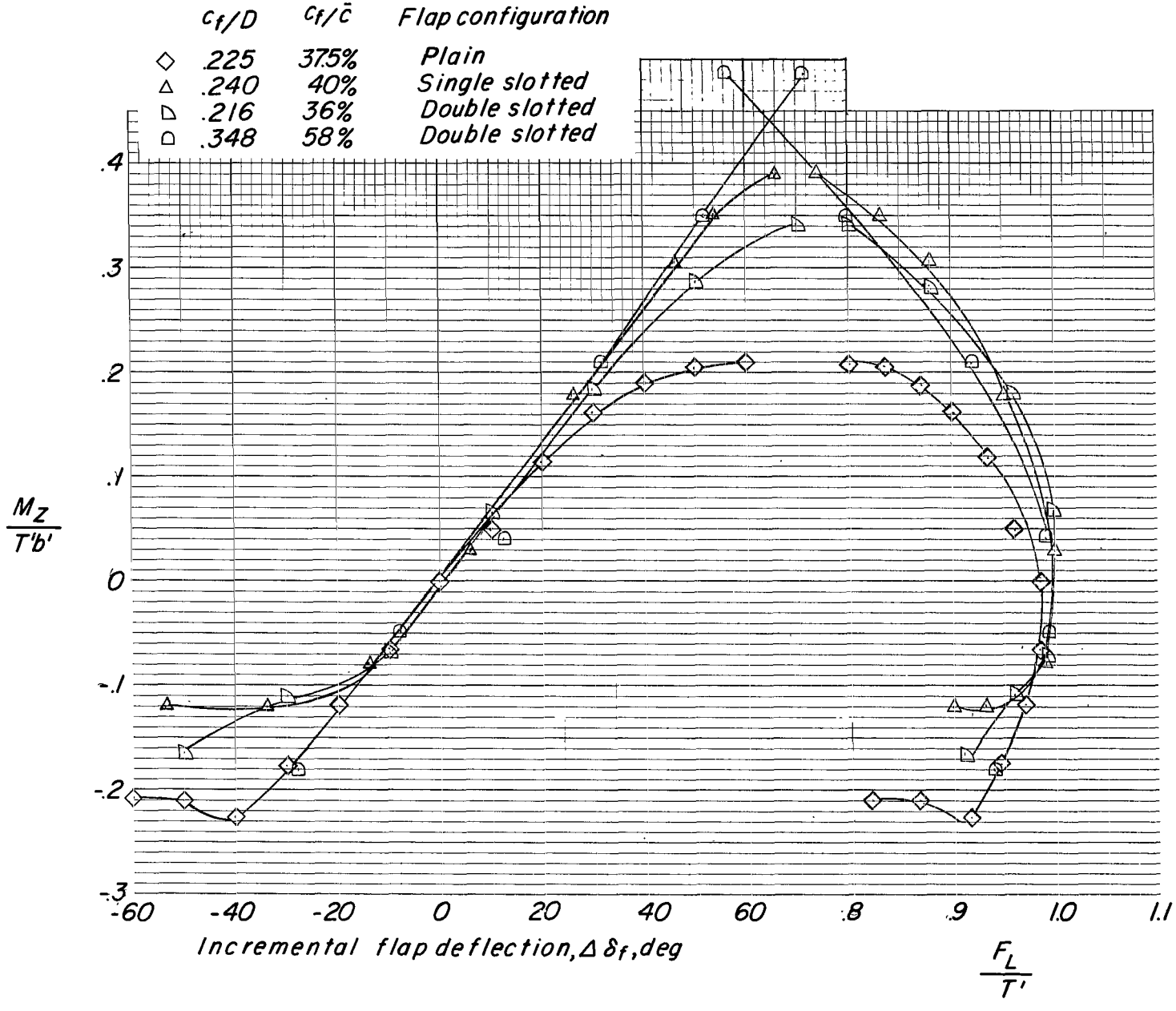

Figure 25.- Effect of change in configuration on hovering control moment and ratio of lift to thrust for configurations presented. h/D = ∞.

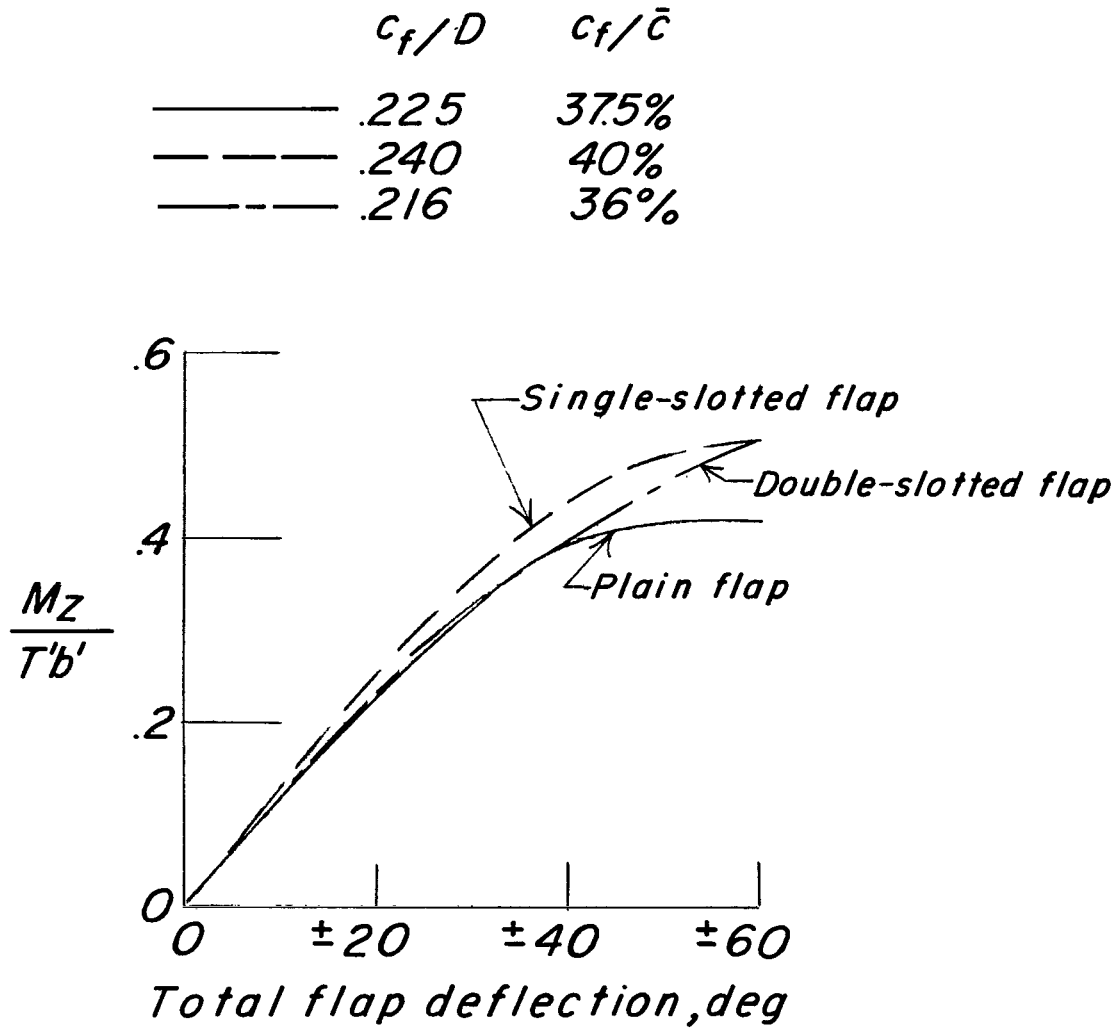

Figure 26.- Comparison of hovering control moment for each configuration where $c_f/D \approx 0.22$ and $h/D = \infty$.

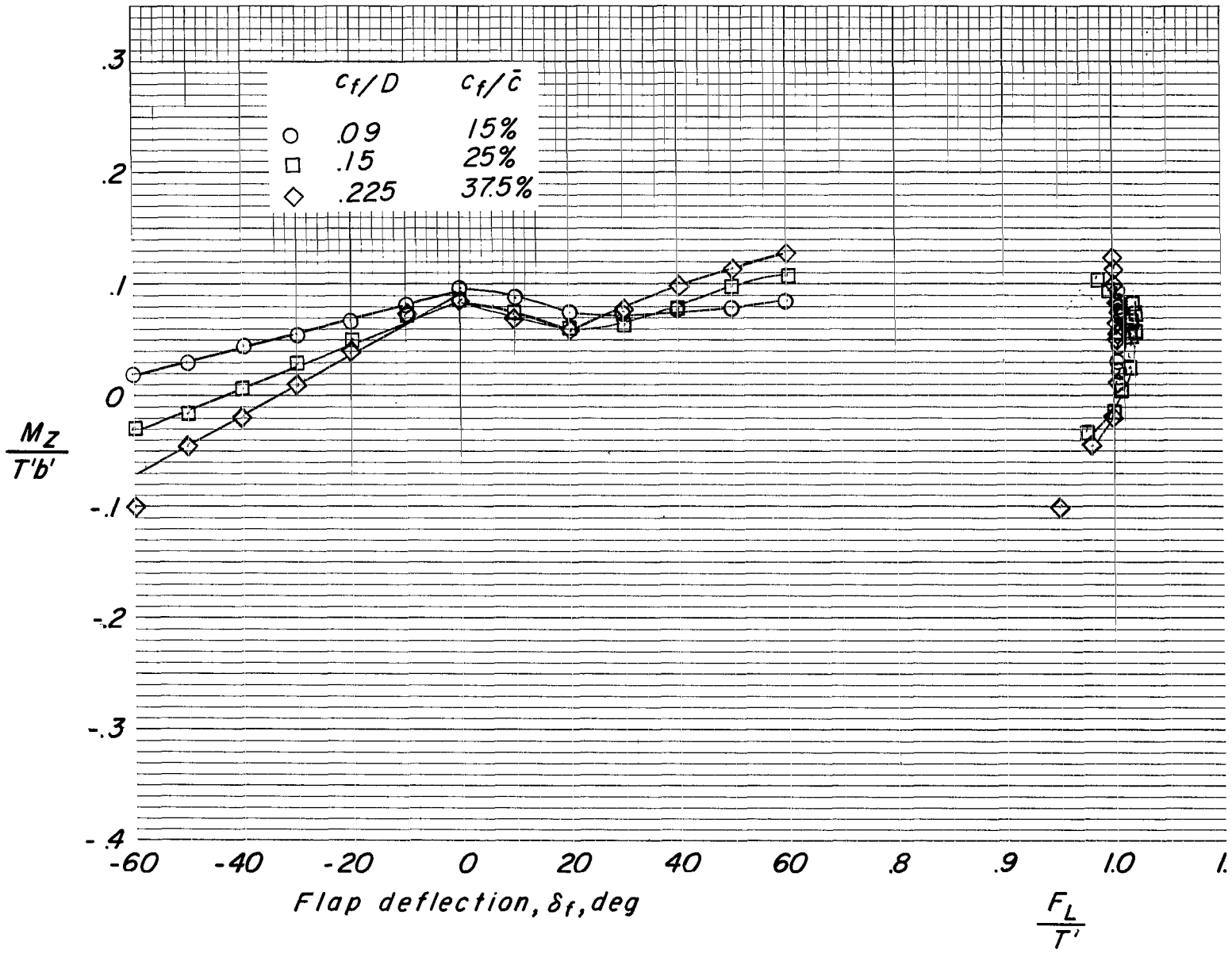

Figure 27.- Effect of flap-chord length on hovering control moment and ratio of lift to thrust for plain-flap configurations. h/D = 0.25.

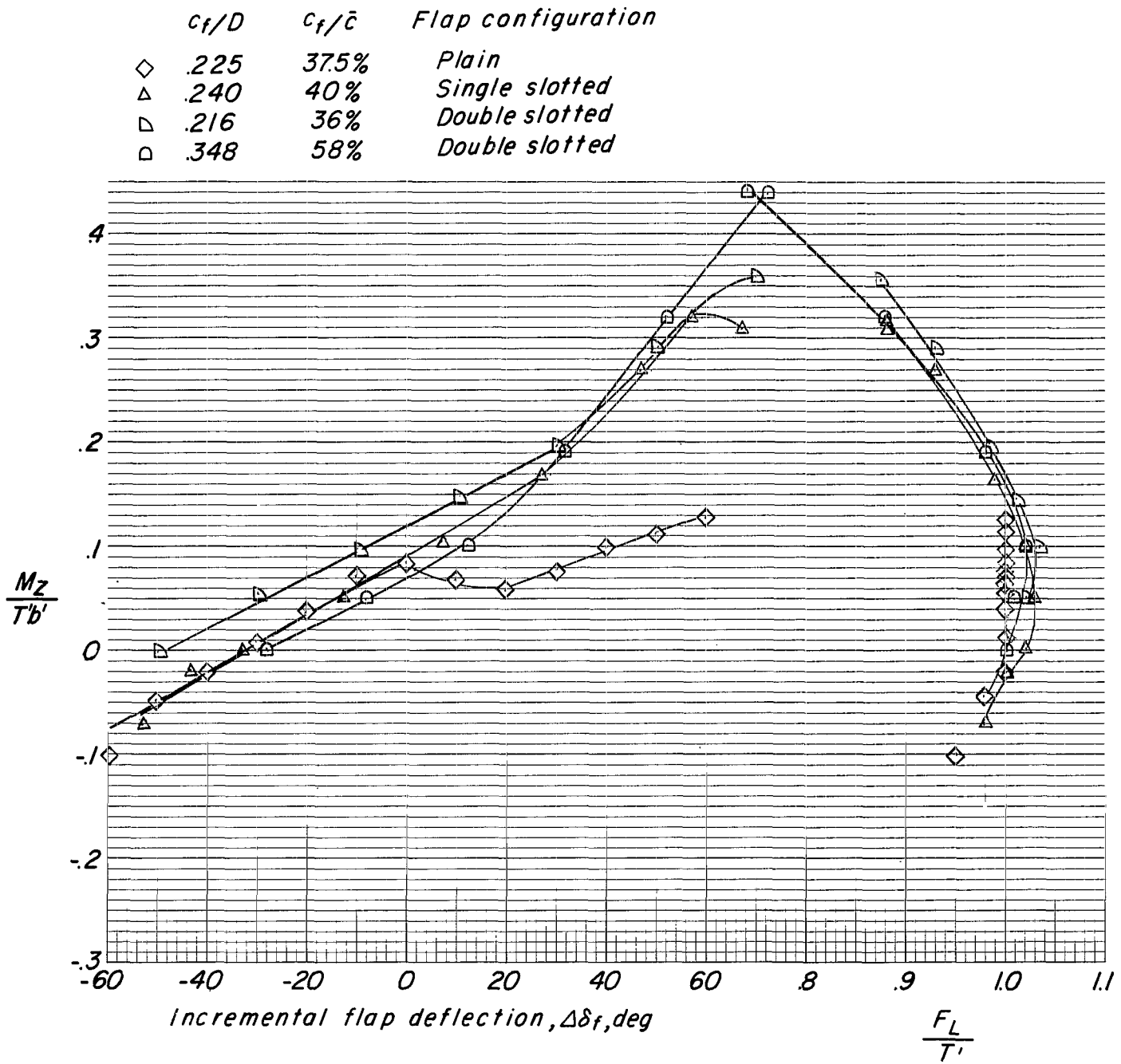

Figure 28.- Effect of change in configuration on hovering control moment and ratio of lift to thrust for all configurations presented. h/D = 0.25.

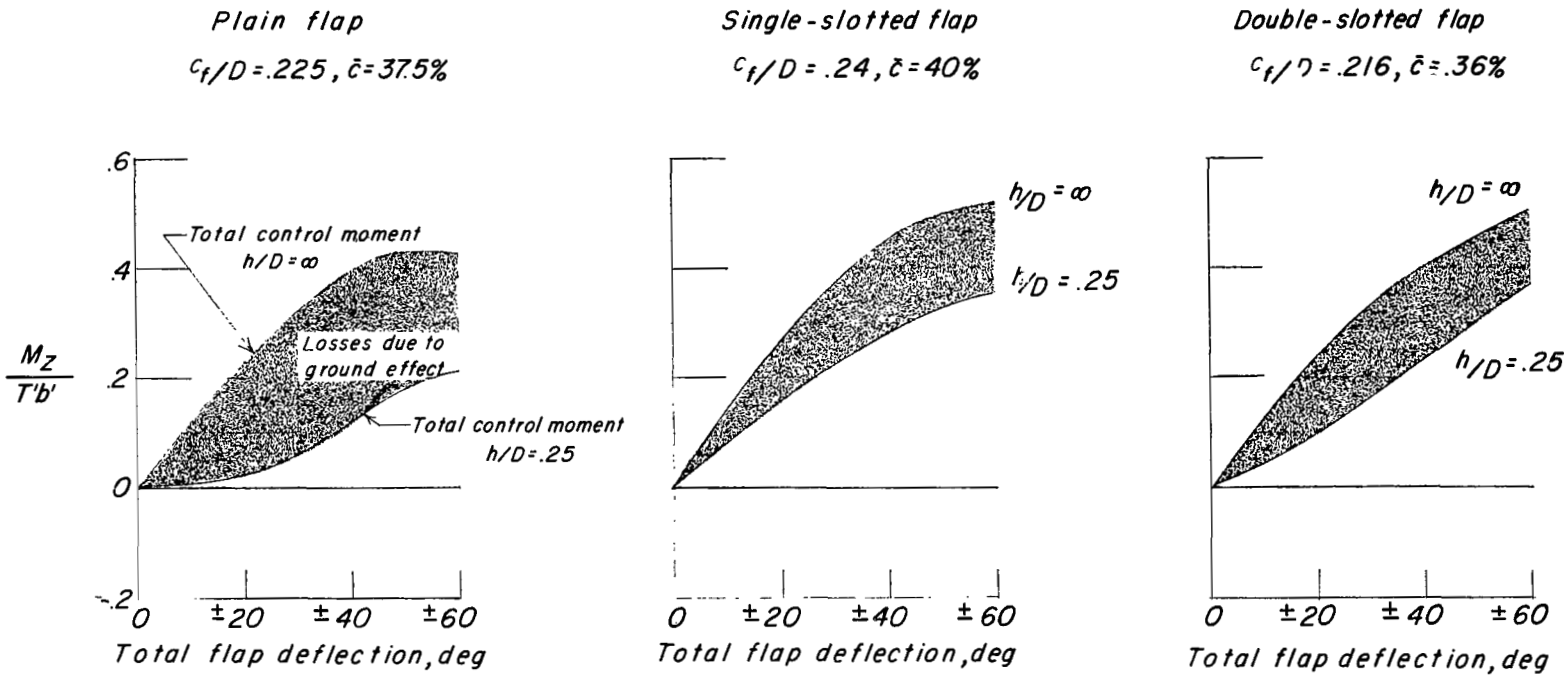

Figure 29.- Ground-effect comparison of different flap configurations (where $c_f/D \approx 0.22$) indicating total hovering control moment available when flaps are used differentially as ailerons. (Positive flap deflection, trailing edge down; negative flap deflection, trailing edge up.)

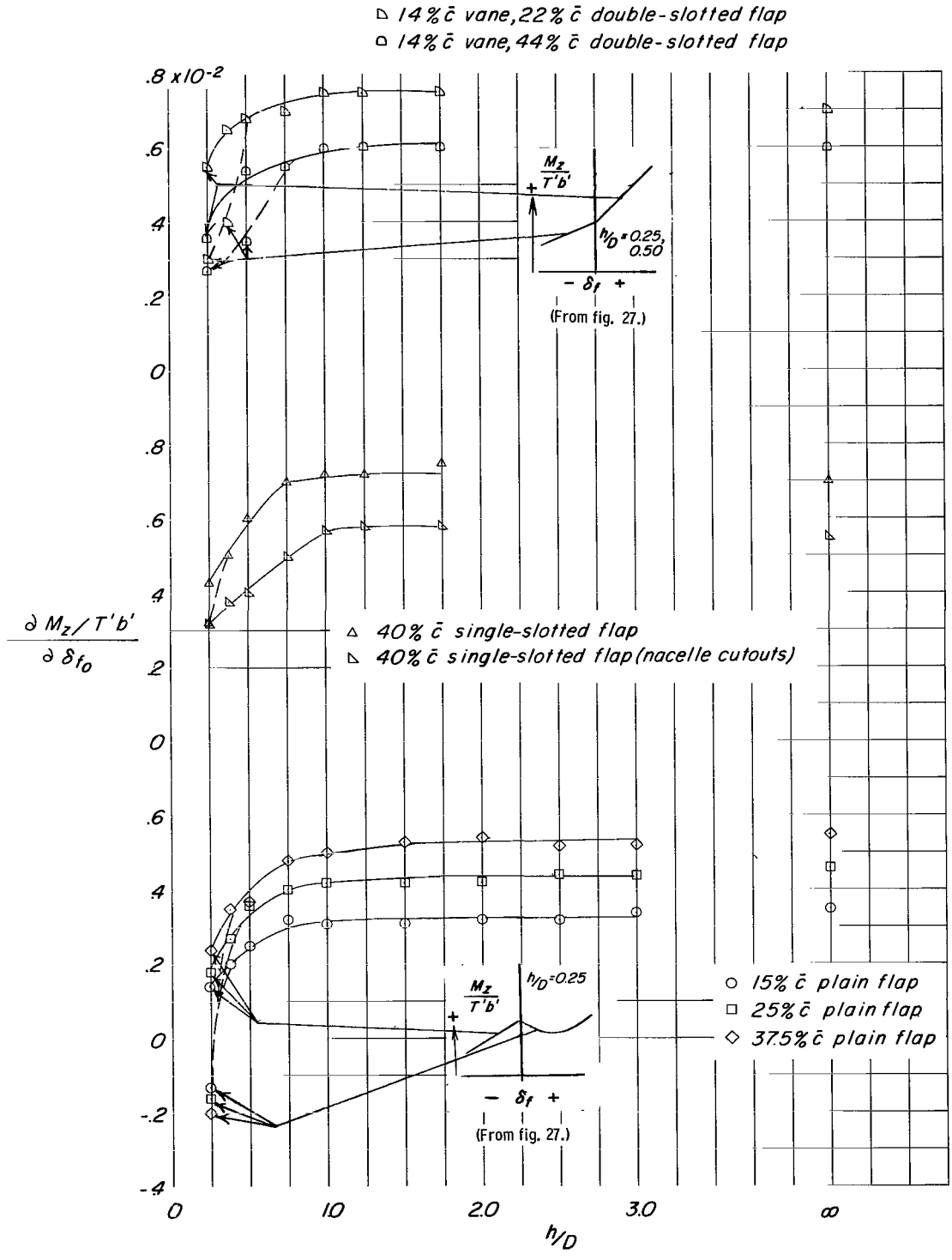

Figure 30.- Hovering control effectiveness for all configurations through a ground height range.

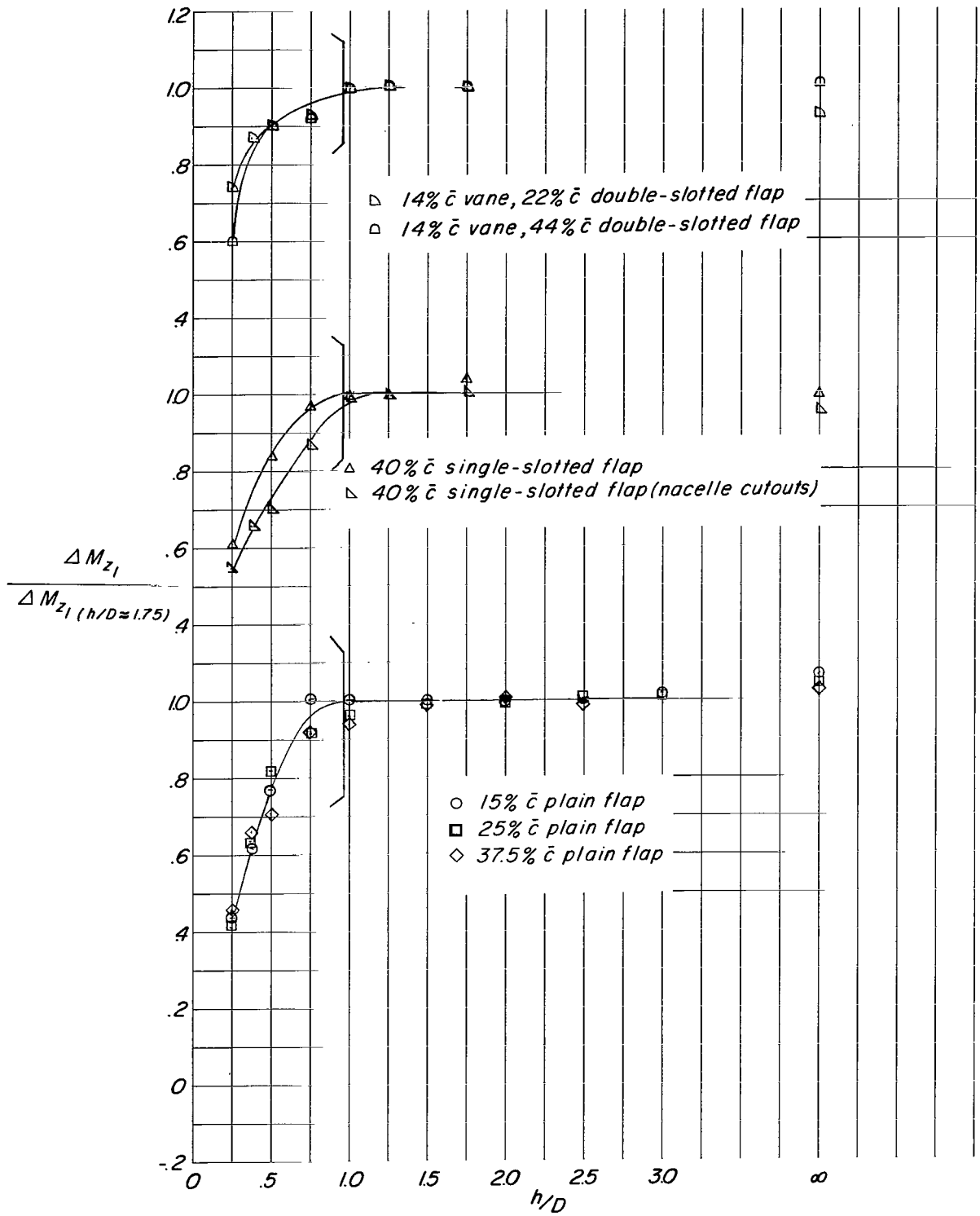

Figure 31.- Ratio of control effectiveness for all ground heights for all configurations.

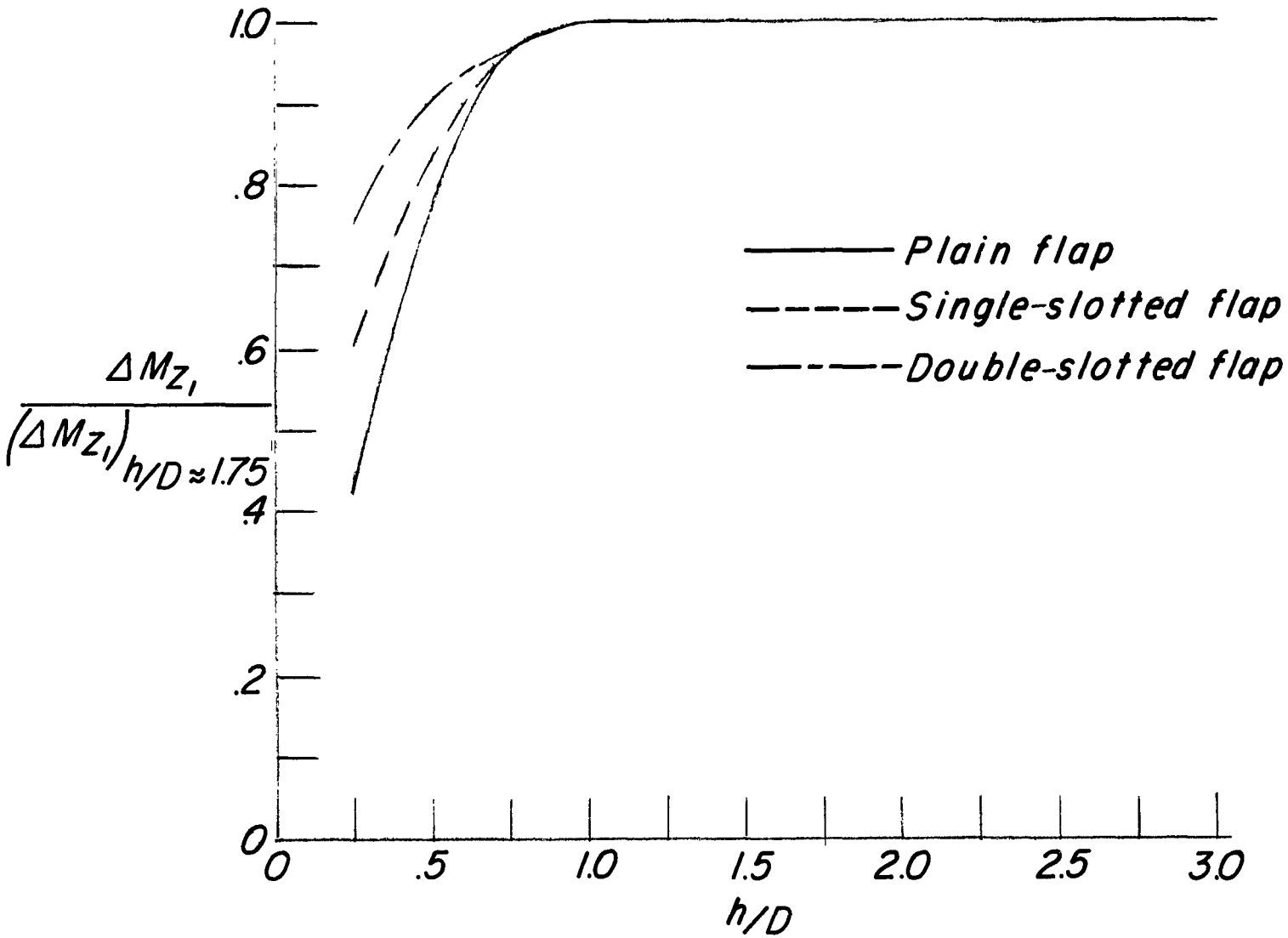

Figure 32.- Comparison of ratio of control effectiveness for each configuration. $c_f/D \approx 0.22$.

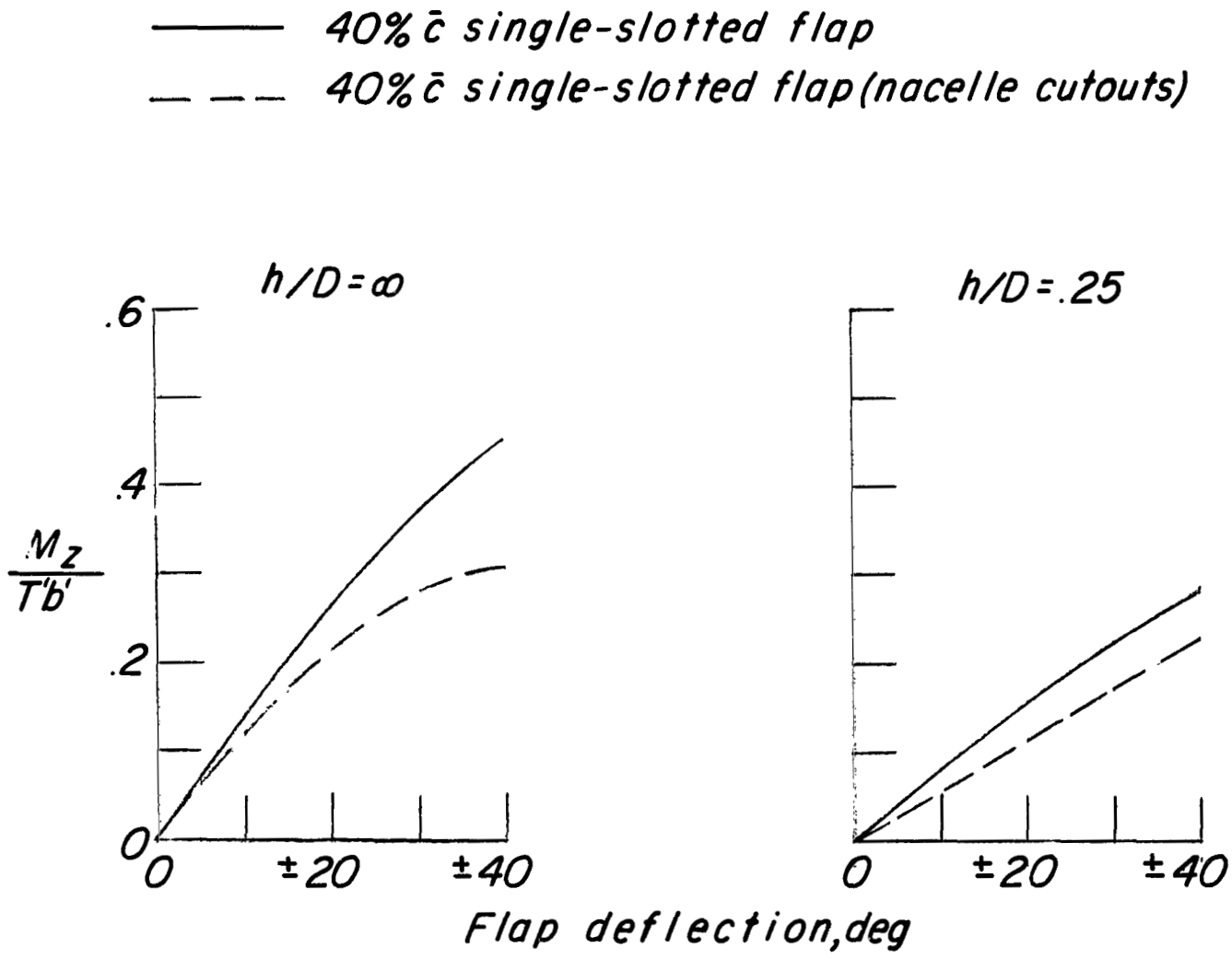

Figure 33.- Effect of nacelle cutouts on total control moment at $h/D = \infty$ and $h/D = 0.25$.

Configuration	$c_f/\bar{c}$	b'_a/b'
Present investigation		
○ Plain flap	15%	100%
□ Plain flap	25%	100%
◇ Plain flap	37.5%	100%
△ Single-slotted flap	40%	100%
◺ Single-slotted flap (Nacelle cut outs)	40%	85%
◺ Double-slotted flap	36%	100%
⌂ Double-slotted flap	58%	100%
Airplane tests		
◇ Plain flap (Ref. 3)	23%	77%
Complete model tests		
⌂ Plain flap(partial span ailerons)	20%	62%
◊ Plain flap(partial span ailerons)	25%	52%

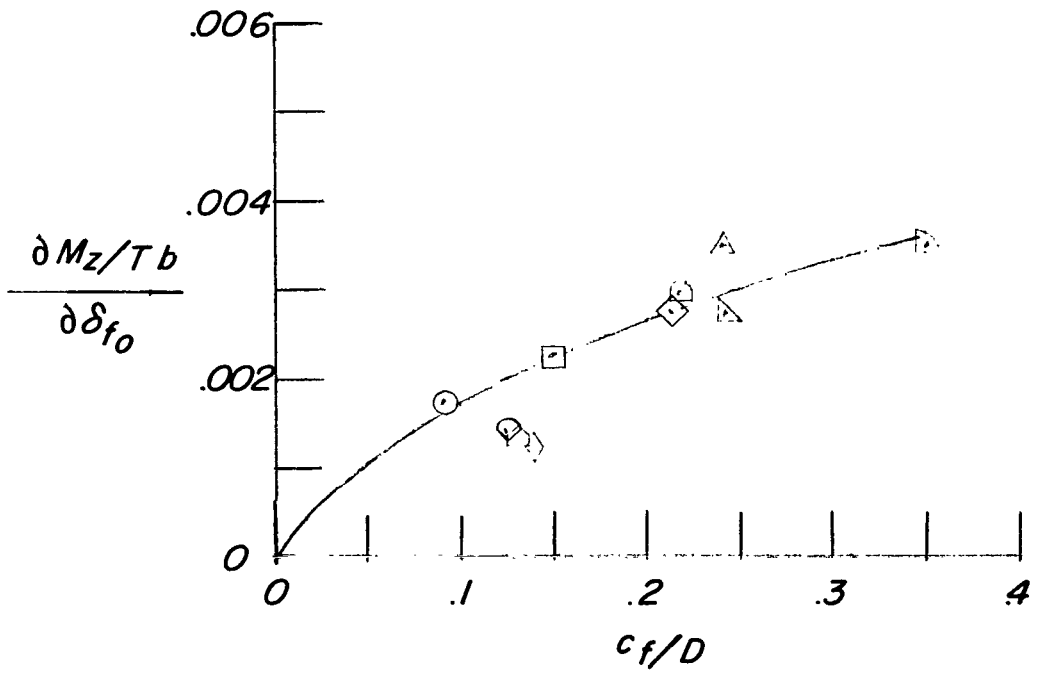

Figure 34.- Comparison of hovering control effectiveness as a function of the ratio of flap chord to propeller diameter from data of present investigation with other tests. $h/D = \infty$.

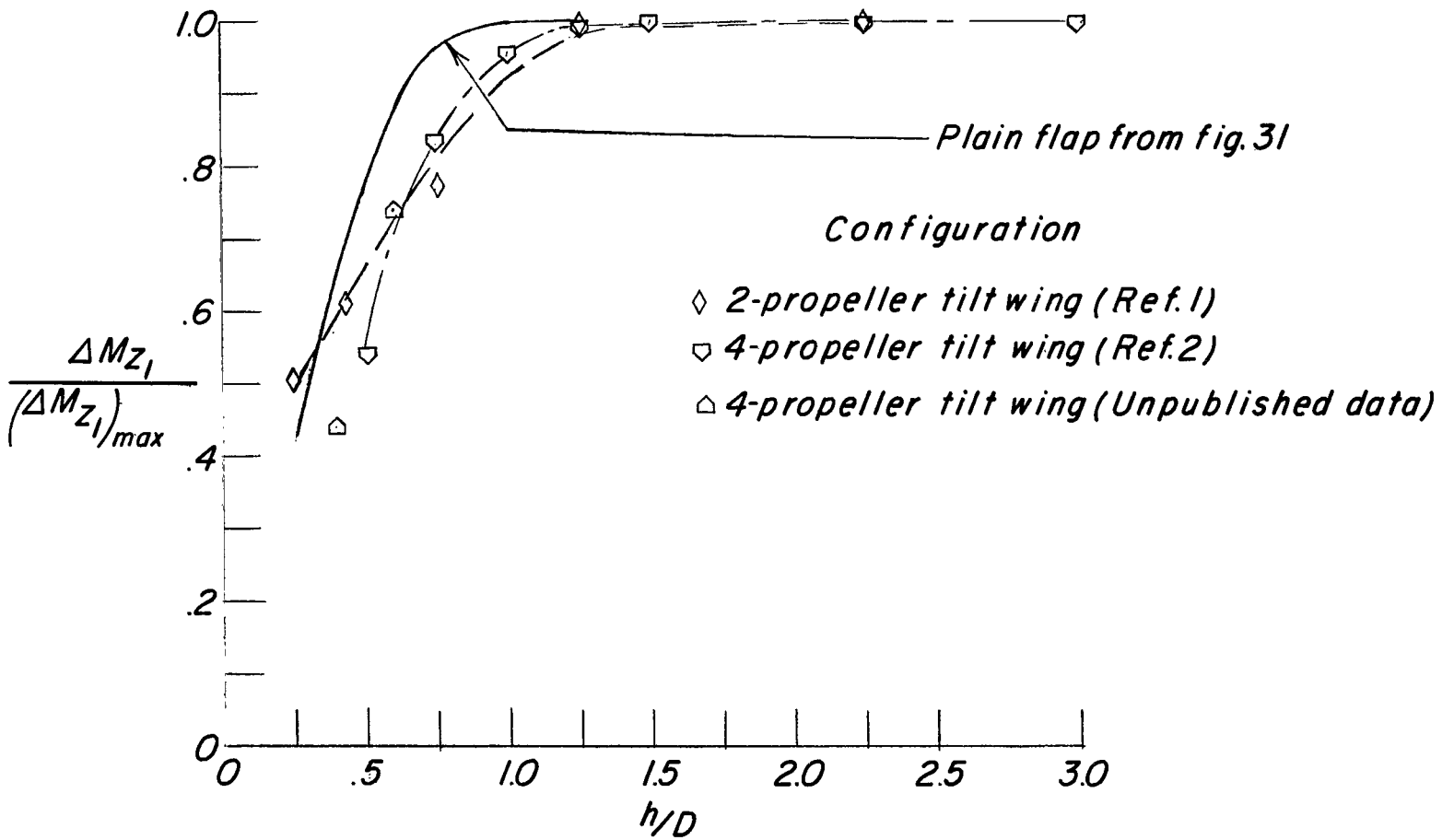

Figure 35.- Comparison of aileron-effectiveness data in ground effect from references and present investigation.

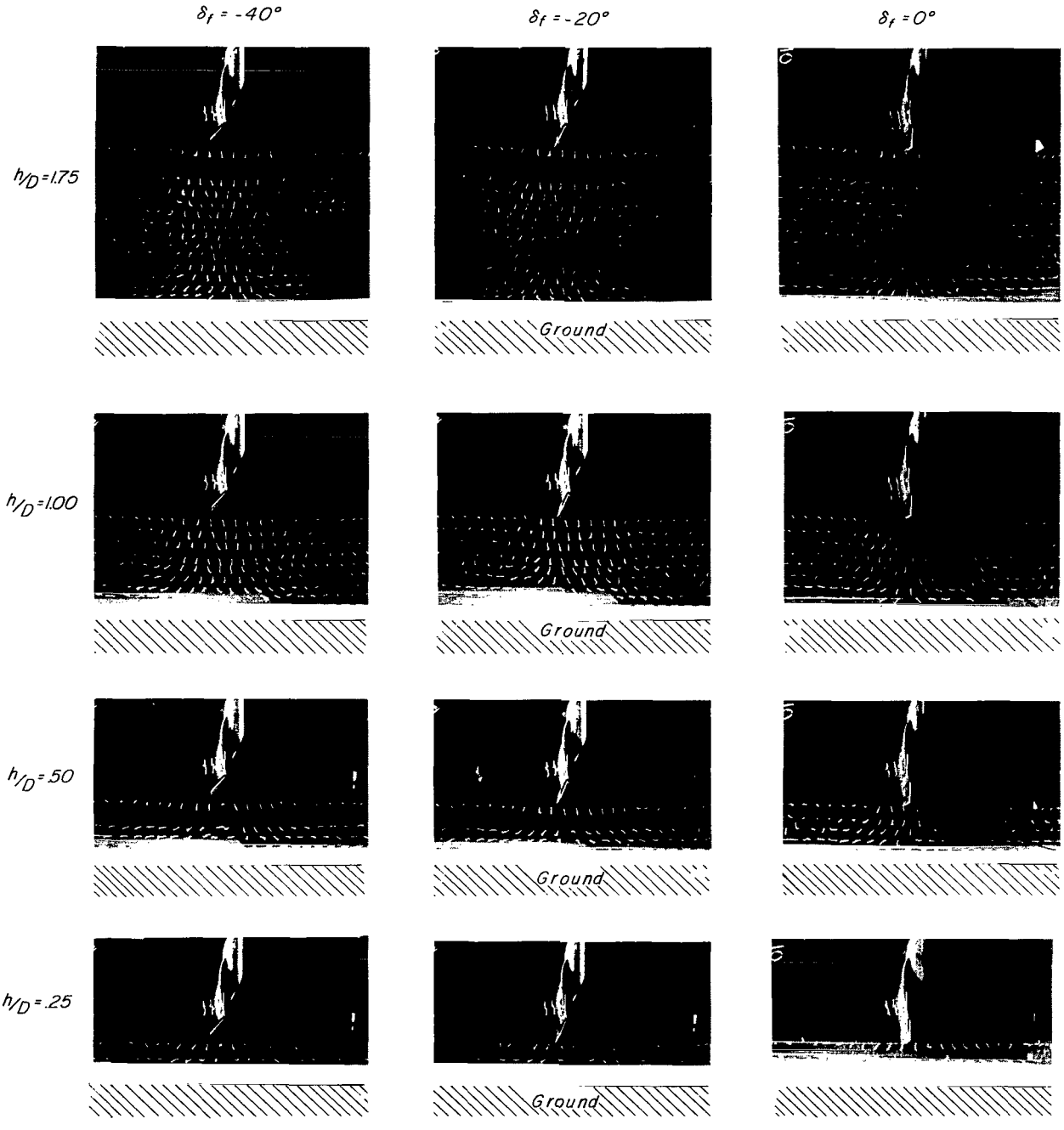

(a) $\delta_f = -40^0$ to 0^0.

L-66-1098

Figure 36.- Tuft-grid surveys of 40-percent-chord single-slotted-flap configuration (with nacelle cutouts) to determine effect of ground height on slipstream. Tuft grid located at center line of outboard propeller. δ_f, variable; h/D, variable.

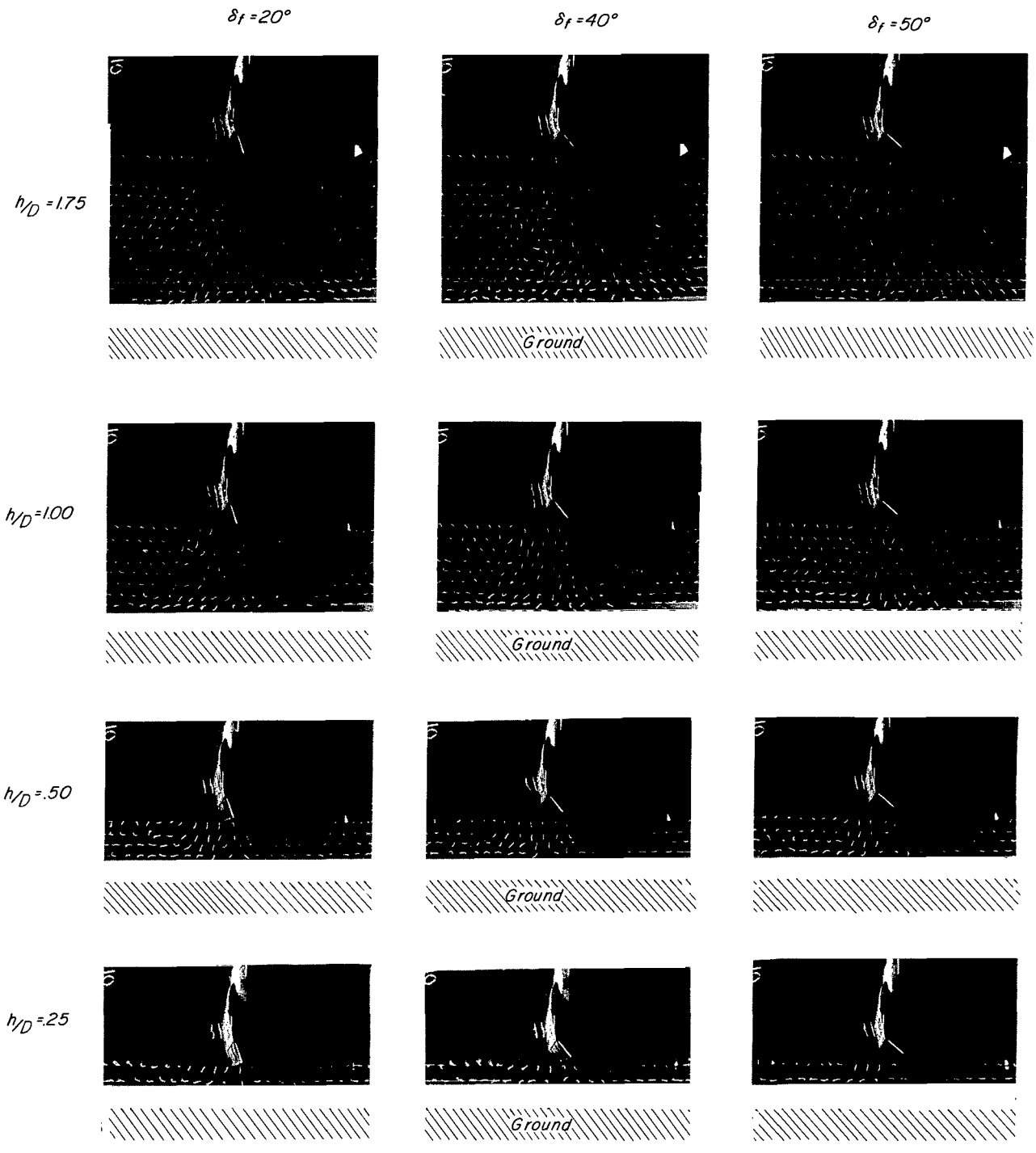

(b) $\delta_f = 20^0$ to 50^0.

L-66-1099

Figure 36.- Concluded.

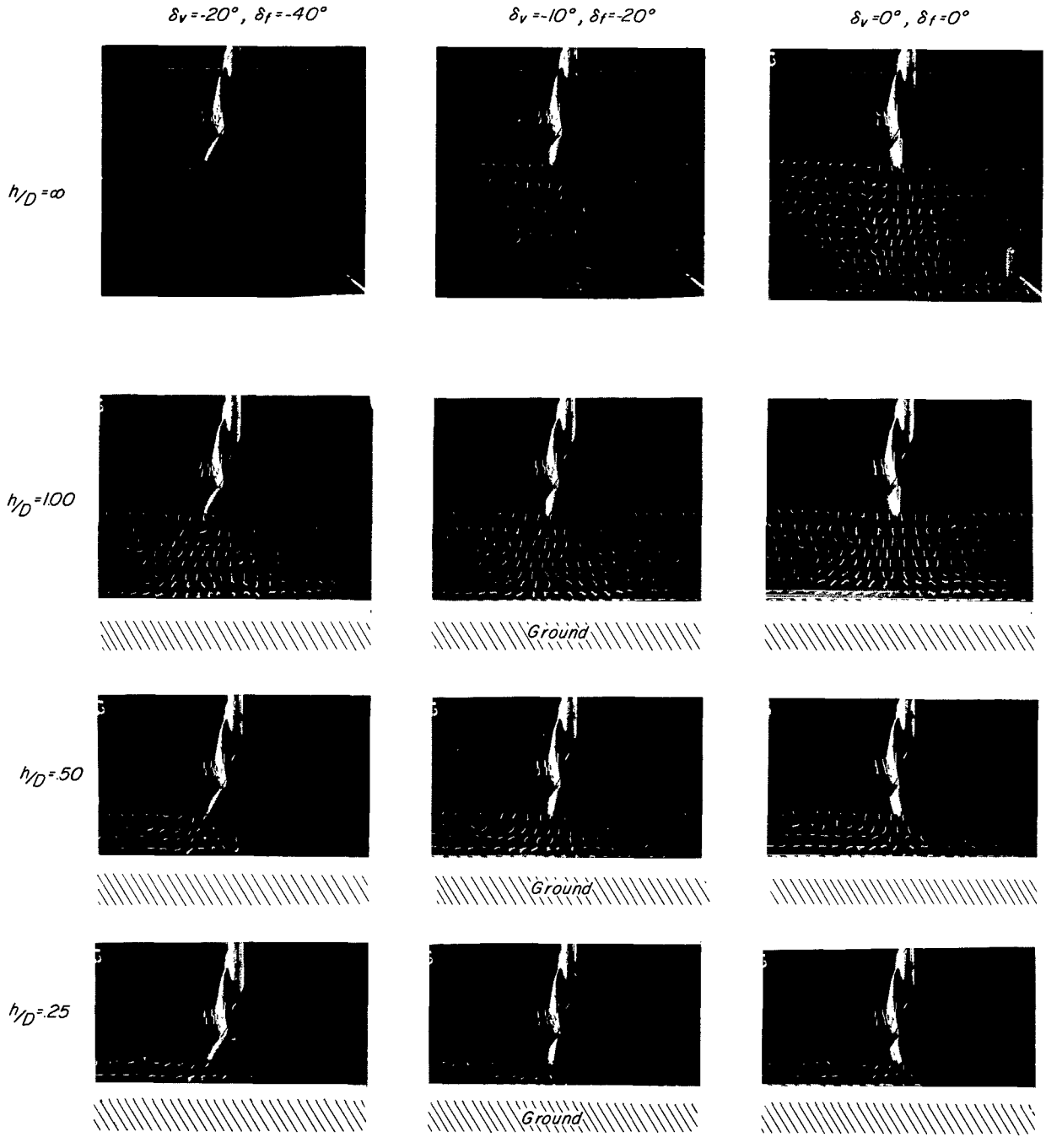

(a) From $\delta_v = -20^0$ and $\delta_f = -40^0$ to $\delta_v = 0^0$ and $\delta_f = 0^0$. L-66-1100

Figure 37.- Tuft-grid surveys of 14-percent-chord vane 44-percent-chord double-slotted-flap configuration to determine effect of ground height on slipstream. Tuft grid located at center line of outboard propeller. δ_f, variable; h/D, variable.

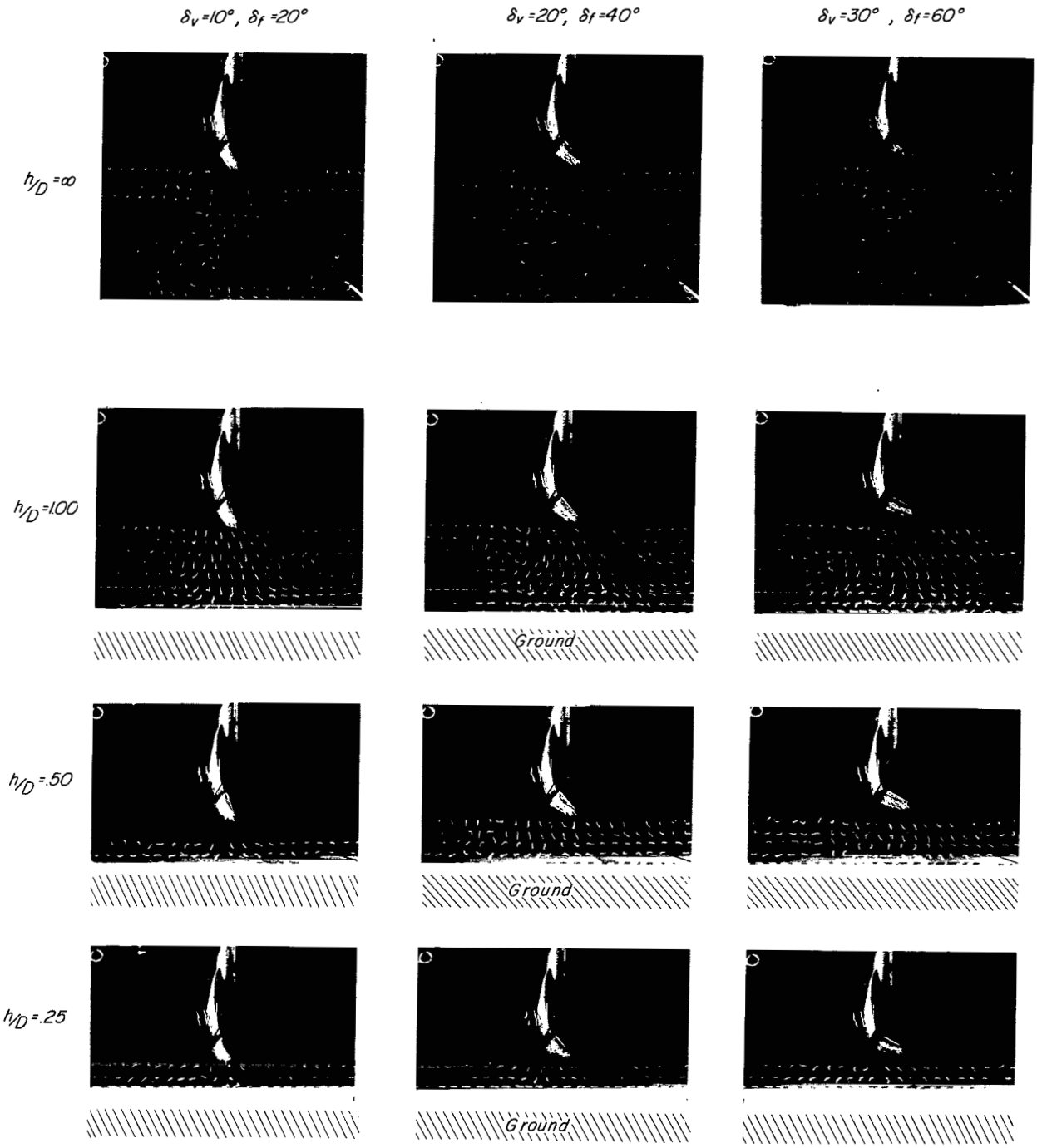

(b) From $\delta_V = 10^0$ and $\delta_f = 20^0$ to $\delta_V = 30^0$ and $\delta_f = 60^0$. L-66-1101

Figure 37.- Concluded.

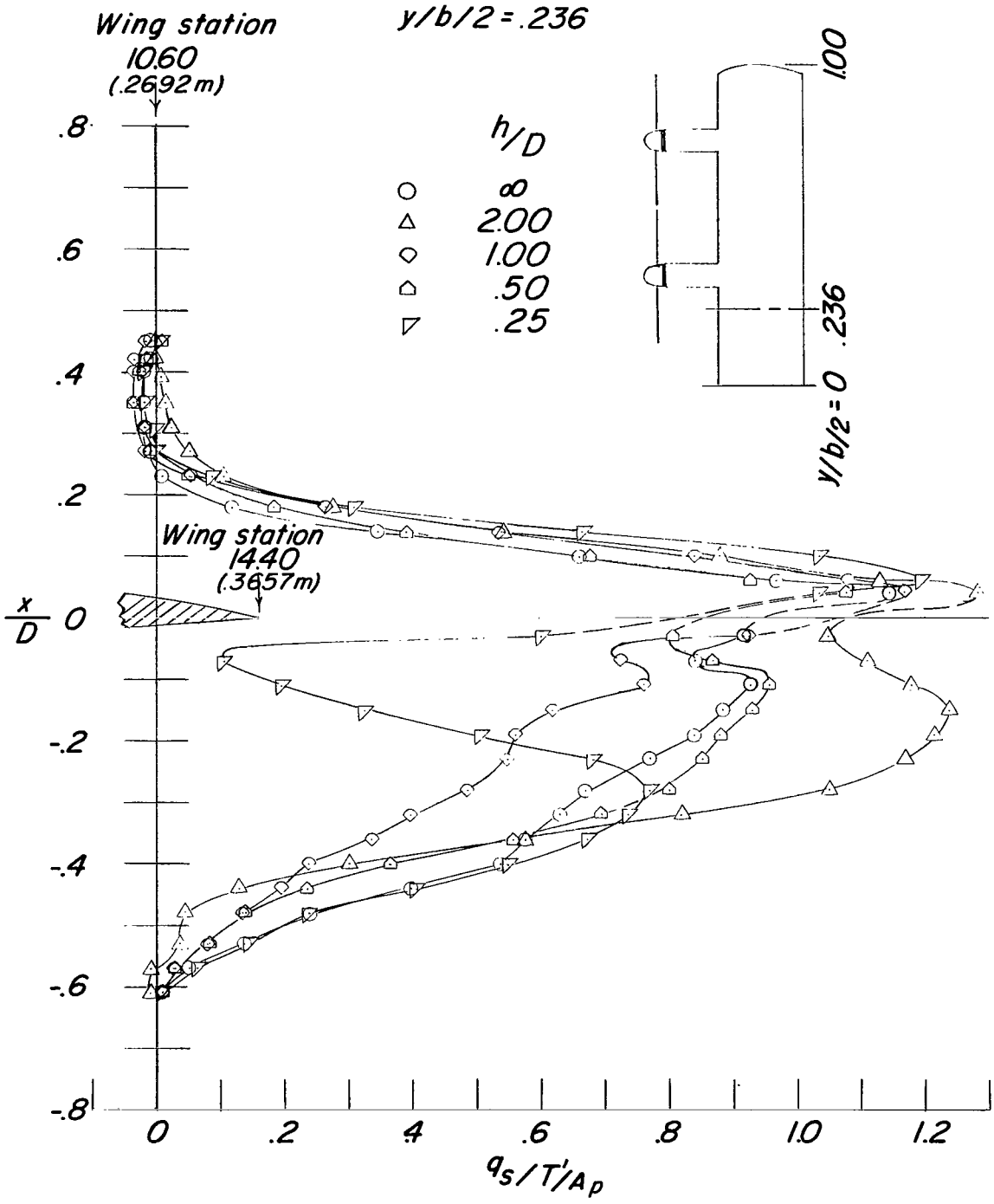

(a) $\frac{y}{b/2} = 0.236$.

Figure 38.- Ground effect on slipstream dynamic pressure measured above and below the wing at a number of spanwise stations.

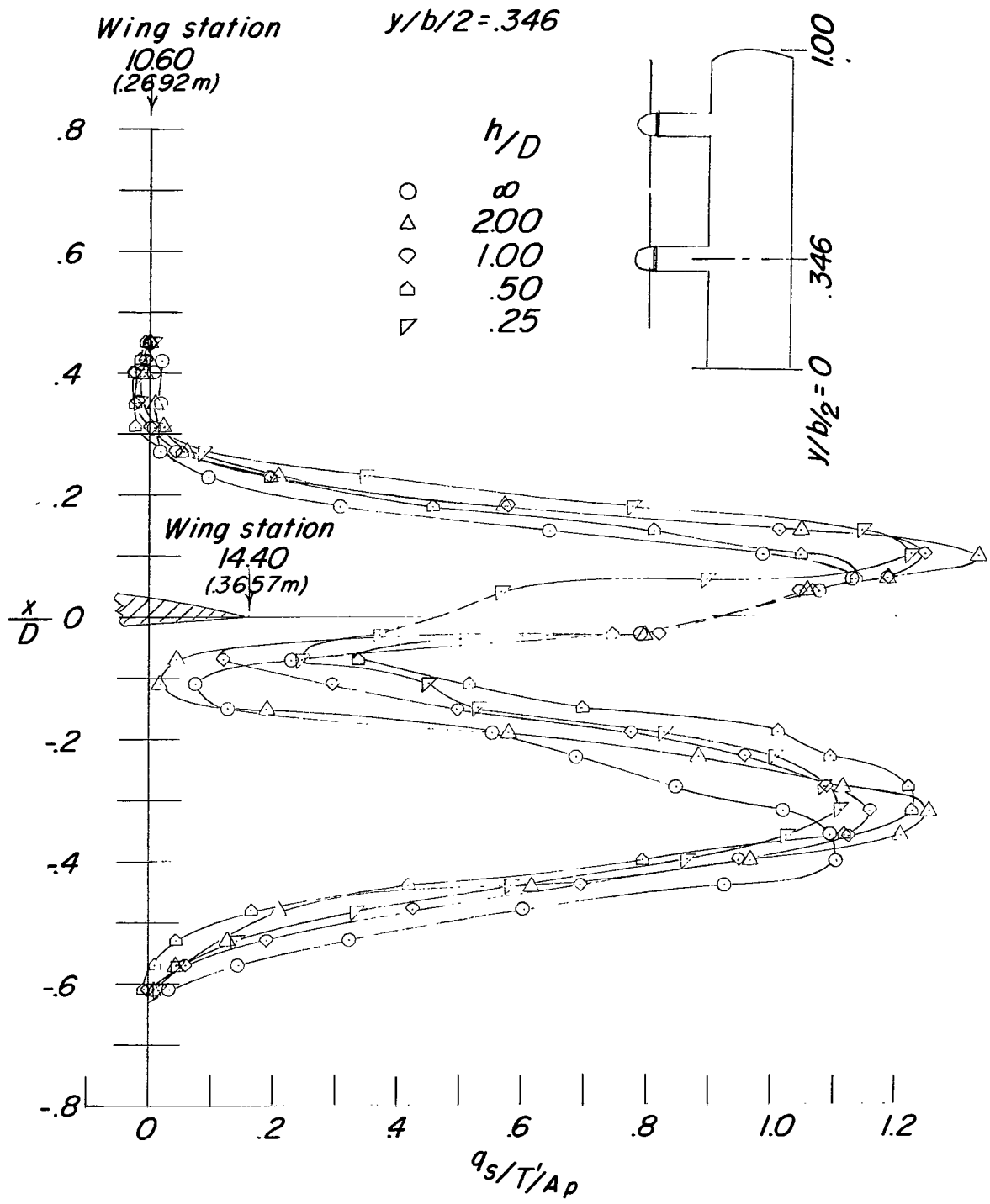

(b) $\frac{y}{b/2} = 0.346$.

Figure 38.- Continued.

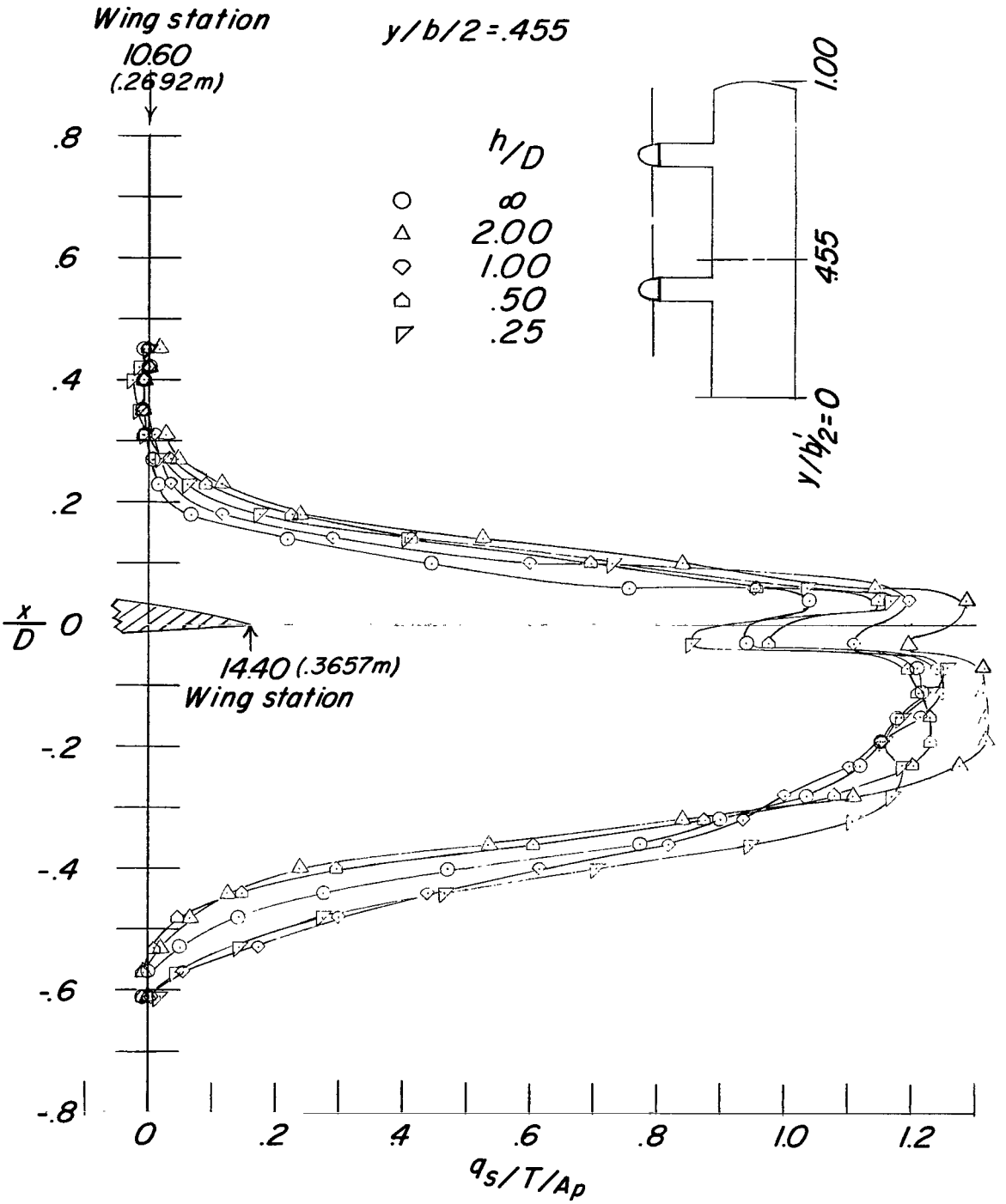

(c) $\frac{y}{b/2} = 0.455$.

Figure 38.- Continued.

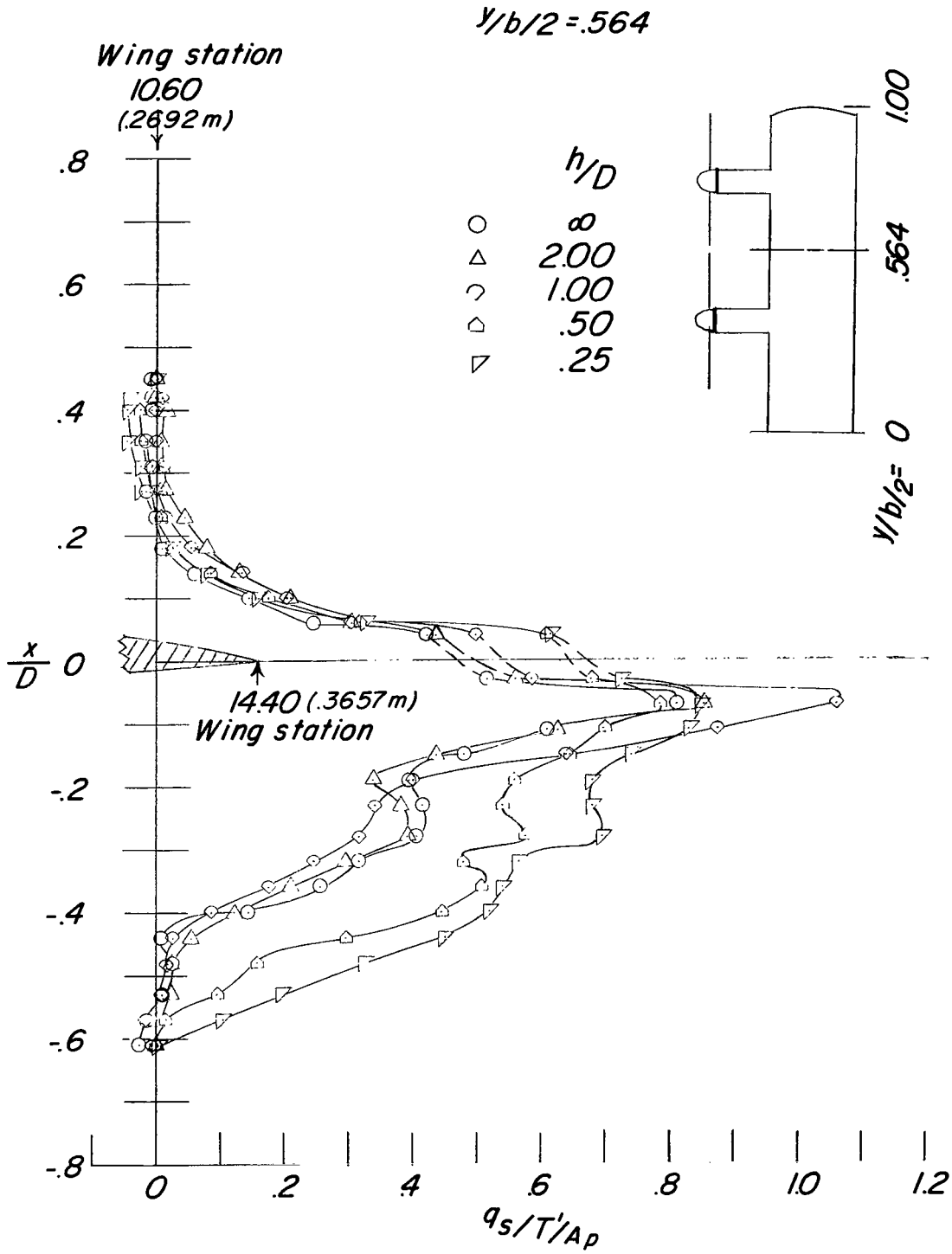

(d) $\frac{y}{b/2} = 0.564$.

Figure 38.- Continued.

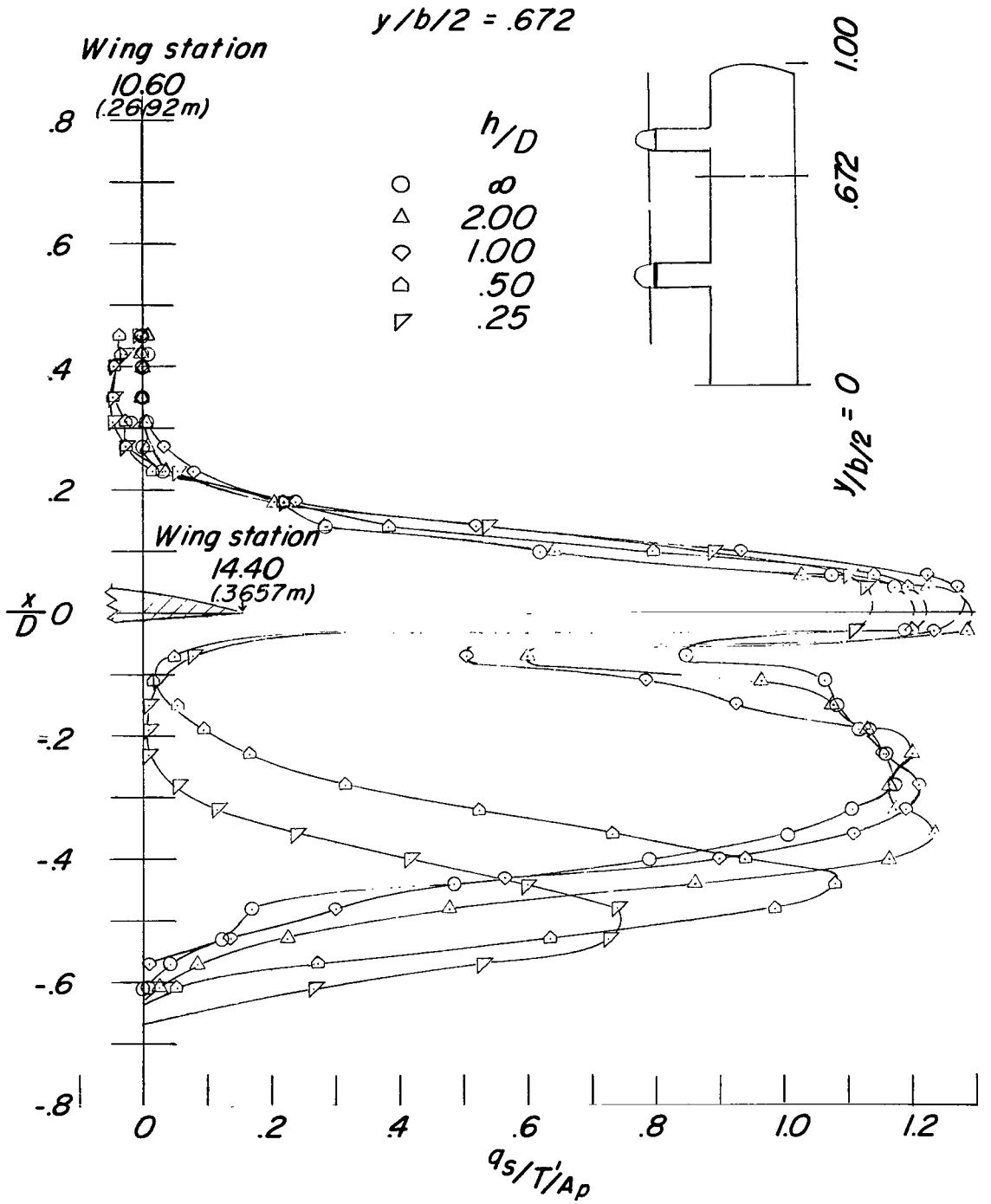

(e) $\frac{y}{b/2} = 0.672$.

Figure 38.- Concluded.

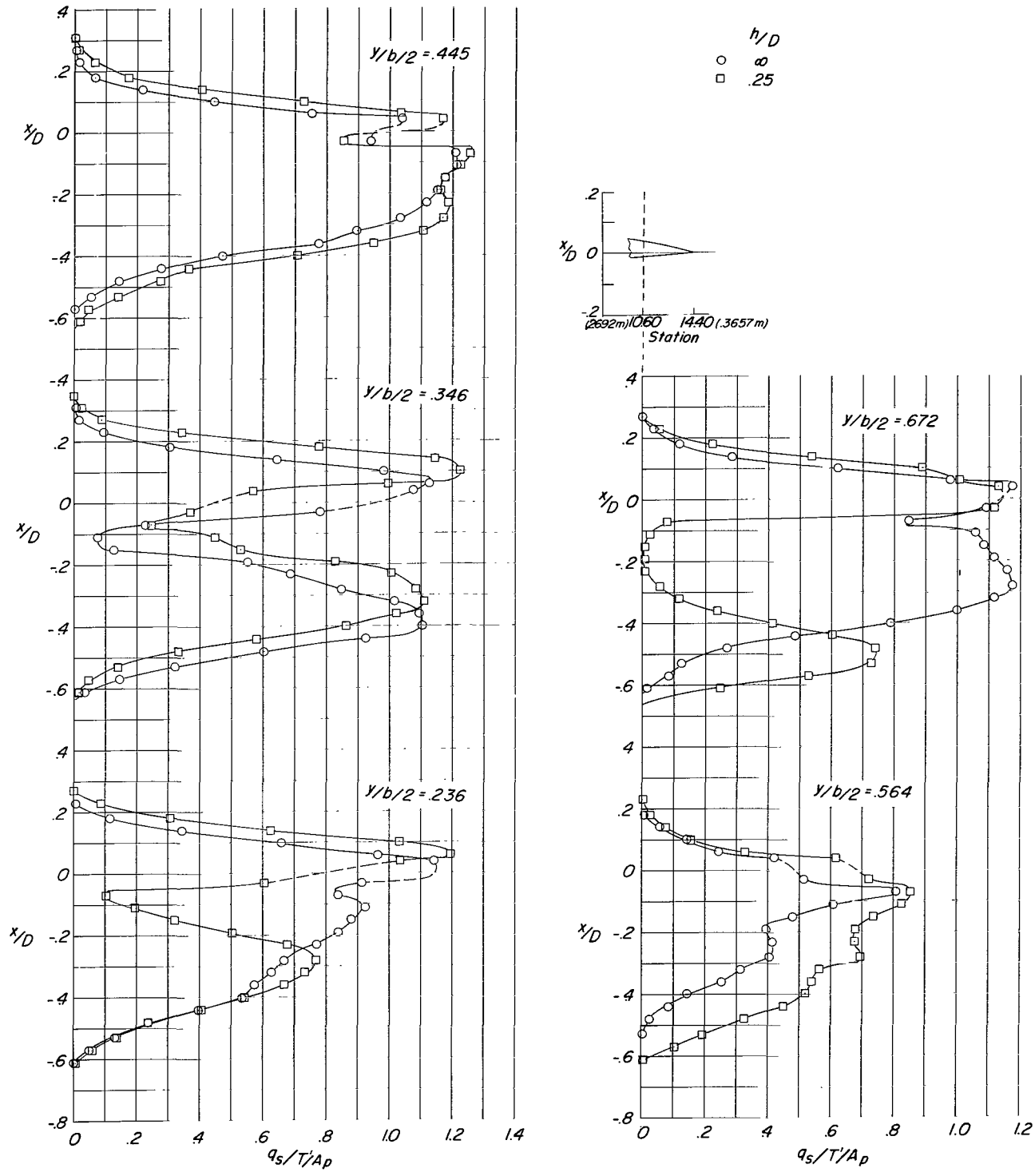

Figure 39.- Ground effect at h/D = 0.25 and ∞ on slipstream dynamic pressure measured above and below the wing at a number of spanwise stations.

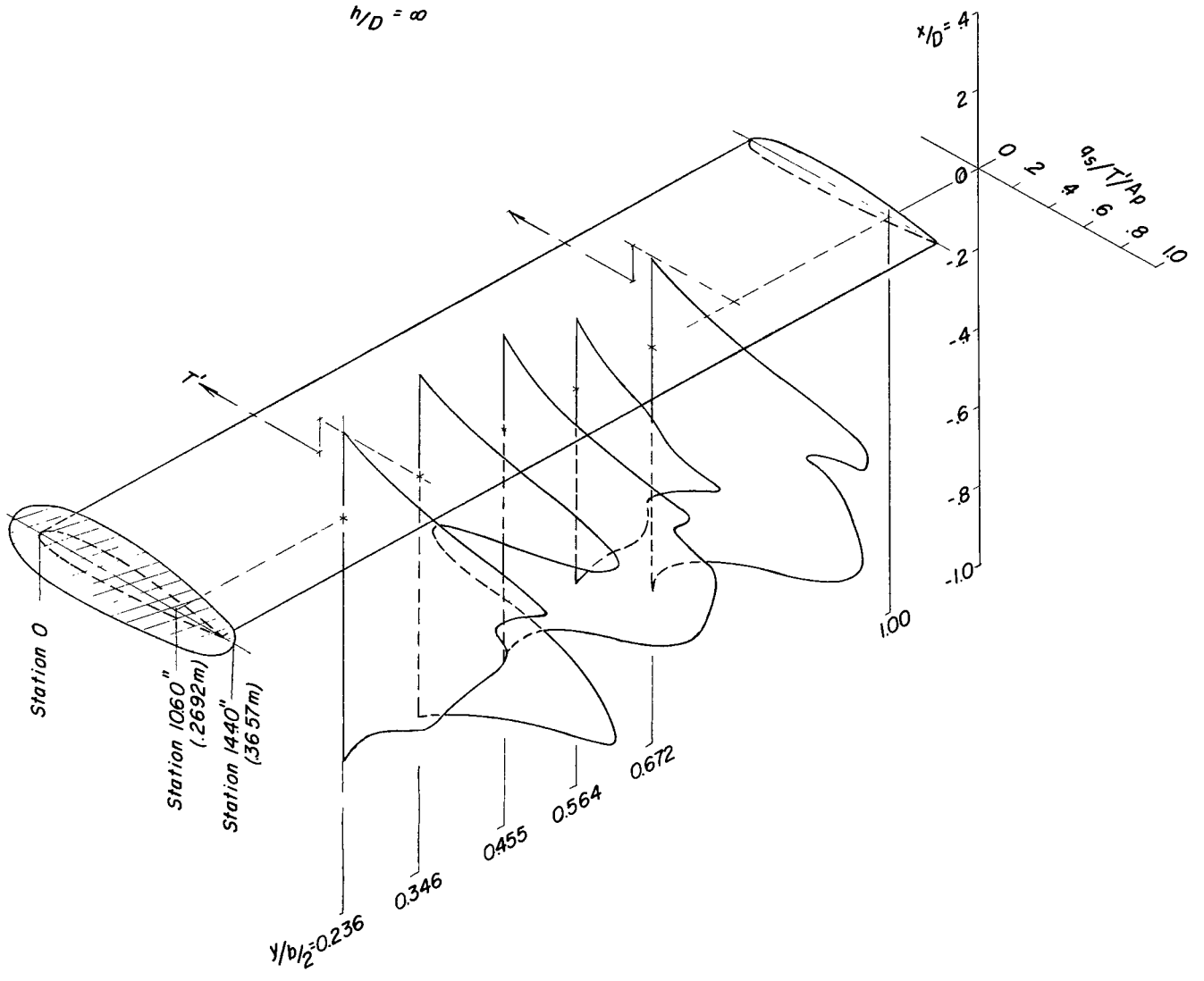

(a) h/D = ∞.

Figure 40.- Isometric projection of slipstream dynamic pressure affected by ground for h/D = 0.25 and ∞ at a number of spanwise stations.

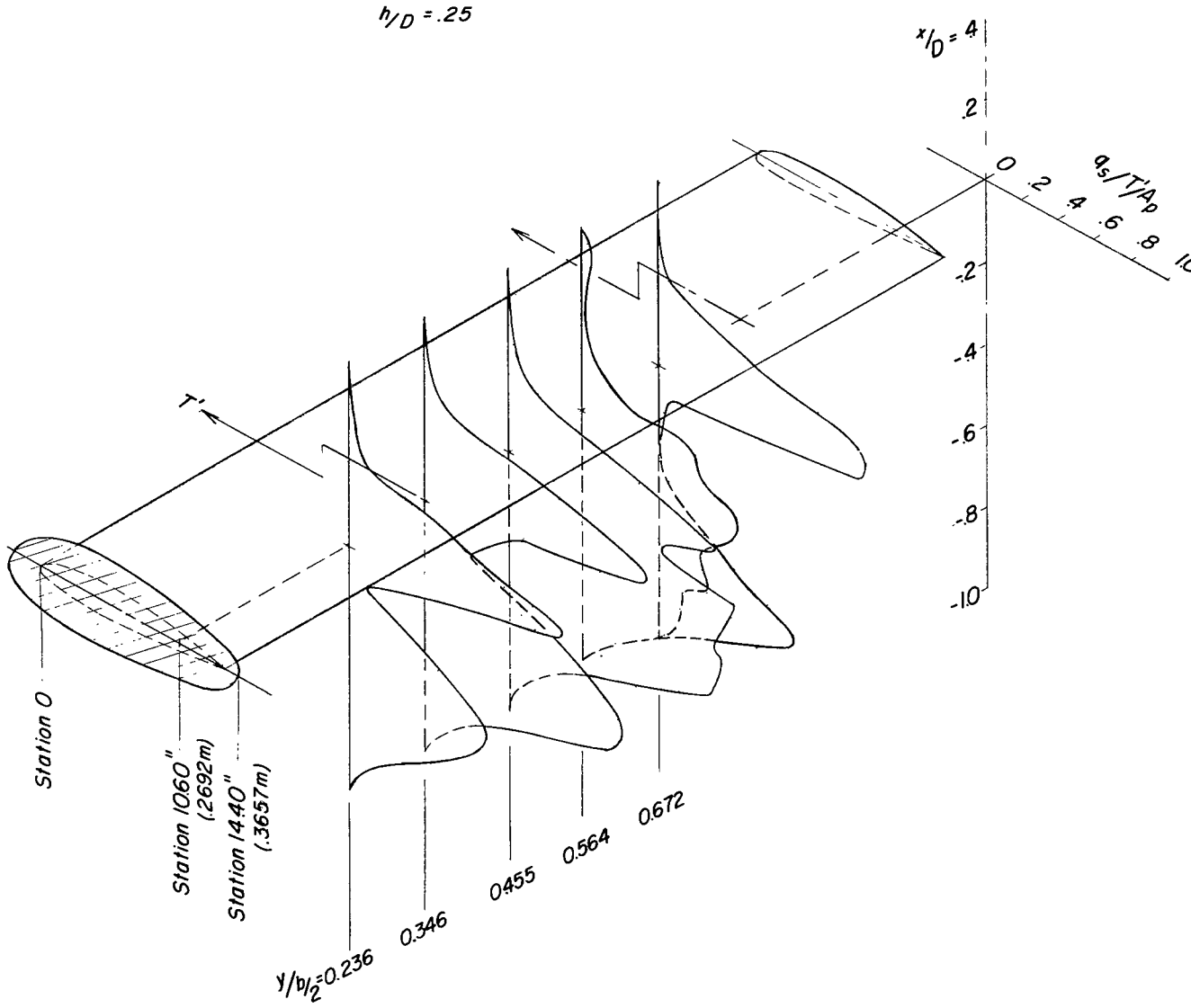

(b) h/D = 0.25.

Figure 40.- Concluded.

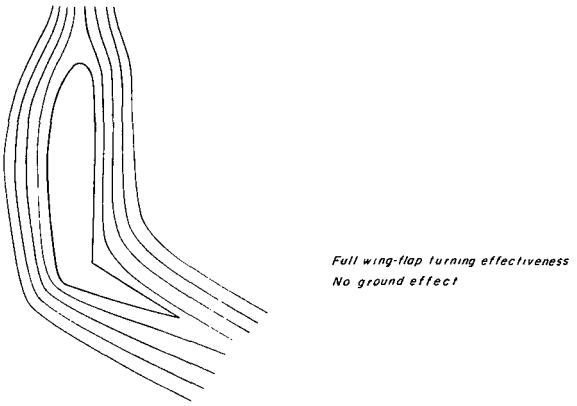

(a) Out of ground.

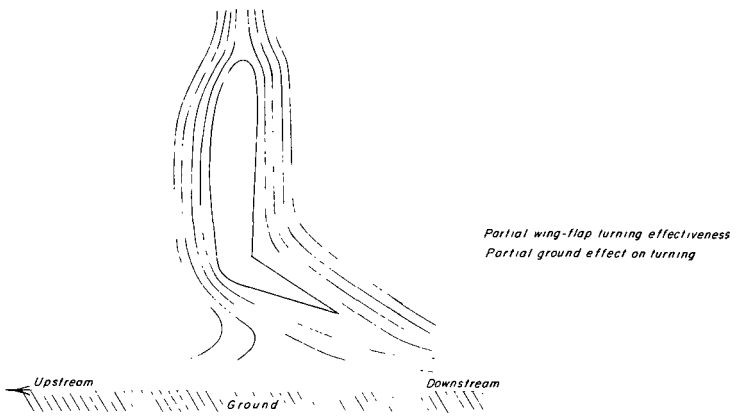

(b) Near ground.

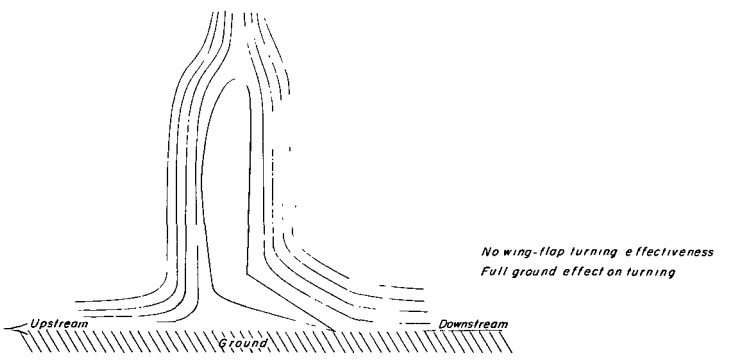

(c) Touching ground.

Figure 41.- Schematic representation of flow from out-of-ground to in-ground effects indicating ground effect on the wing-flap turning effectiveness. (Data based on actual tuft studies (figs. 36 and 37).)

"The aeronautical and space activities of the United States shall be conducted so as to contribute . . . to the expansion of human knowledge of phenomena in the atmosphere and space. The Administration shall provide for the widest practicable and appropriate dissemination of information concerning its activities and the results thereof."

—NATIONAL AERONAUTICS AND SPACE ACT OF 1958

NASA SCIENTIFIC AND TECHNICAL PUBLICATIONS

TECHNICAL REPORTS: Scientific and technical information considered important, complete, and a lasting contribution to existing knowledge.

TECHNICAL NOTES: Information less broad in scope but nevertheless of importance as a contribution to existing knowledge.

TECHNICAL MEMORANDUMS: Information receiving limited distribution because of preliminary data, security classification, or other reasons.

CONTRACTOR REPORTS: Technical information generated in connection with a NASA contract or grant and released under NASA auspices.

TECHNICAL TRANSLATIONS: Information published in a foreign language considered to merit NASA distribution in English.

TECHNICAL REPRINTS: Information derived from NASA activities and initially published in the form of journal articles.

SPECIAL PUBLICATIONS: Information derived from or of value to NASA activities but not necessarily reporting the results of individual NASA-programmed scientific efforts. Publications include conference proceedings, monographs, data compilations, handbooks, sourcebooks, and special bibliographies.

Details on the availability of these publications may be obtained from:

SCIENTIFIC AND TECHNICAL INFORMATION DIVISION

NATIONAL AERONAUTICS AND SPACE ADMINISTRATION

Washington, D.C. 20546